Tesis Doctoral

HIDRÓXIDOS LAMINARES ORGÁNICO-INORGÁNICOS PARA APLICACIONES EN CATÁLISIS Y ADSORCIÓN

ORGANIC-INORGANIC LAYERED HYDROXIDES FOR APPLICATIONS IN CATALYSIS AND ADSORPTION

Daniel Cosano Hidalgo

Directores:
Prof. Dr. José Rafael Ruiz Arrebola
Prof. Dr. César Jiménez Sanchidrián

Universidad de Córdoba
Facultad de Ciencias
Departamento de Química Orgánica

Córdoba, 2019

TITULO: *HIDRÓXIDOS LAMINARES ORGÁNICO-INORGÁNICOS PARA APLICACIONES EN CATÁLISIS Y ADSORCIÓN*

AUTOR: *Daniel Cosano Hidalgo*

Campus de Rabanales
Ctra. Nacional IV, Km. 396 A
14071 Córdoba

https://www.uco.es/ucopress/index.php/es/
ucopress@uco.es

TÍTULO DE LA TESIS: HIDRÓXIDOS LAMINARES ORGÁNICO-INORGÁNICOS PARA APLICACIONES EN CATÁLISIS Y ADSORCIÓN

DOCTORANDO/A: Daniel Cosano Hidalgo

INFORME RAZONADO DEL/DE LOS DIRECTOR/ES DE LA TESIS

(se hará mención a la evolución y desarrollo de la tesis, así como a trabajos y publicaciones derivados de la misma).

D. Daniel Cosano Hidalgo ha realizado un excelente trabajo durante los años en que llevó a cabo la parte experimental de su Tesis, habiendo culminado esta labor con la redacción de esta Memoria de Tesis Doctoral en los últimos meses. Durante todo este tiempo adquirió una gran experiencia en la síntesis, caracterización y aplicación de varios tipos de hidróxidos dobles laminares (HDLs) en procesos de adsorción y de catálisis. Ha aprendido el manejo e interpretación de los datos obtenidos de técnicas tales como la difracción de rayos X, la porosimetría de nitrógeno, la desorción a temperatura programada, la espectroscopia Raman, de infrarrojo y de fluorescencia de rayos X, entre otras. Además, ha utilizado frecuentemente reactores de microondas o ultrasonidos. Algunos de los hidróxidos dobles laminares calcinados se han aplicado en la adsorción de iones cianuro contenidos en disoluciones acuosas o como catalizadores en la reacción de transferencia catalítica de hidrógeno (reacción de Meerwein-Ponndorf-Verley (MPV)). El cianuro es un contaminante muy potente que afecta muy gravemente a la salud de los seres vivos, por lo que su vertido al medio ambiente debe ser controlado y no exceder los límites marcados por la legislación vigente. Por otra

parte, la reacción MPV es un proceso de reducción, por transferencia de hidrógeno, de grupos carbonilo. Esta reducción se realiza en condiciones muy suaves y con una selectividad total hacia el grupo carbonilo, lo que es muy empleada en Química Fina. Como resultado de sus investigaciones se han publicado tres artículos, y un cuarto que se encuentra enviado, que conforman la base de esta Tesis Doctoral y que se detallan a continuación:

- D. Cosano, C. Jimenez-Sanchidrián, J.R. Ruiz, *Vibrational spectroscopic study of sol–gel layered double hydroxides containing different tri- and tetravalent cations,* Journal of Sol-Gel Science and Technology, 76 (2015) 614-620. En este artículo se sintetizaron HDLs de metals di-, tri- y tetravalentes empleando el método sol-gel. Todos los HDLs fueron caracterizados empleando diferentes técnicas instrumentales.

- D. Cosano, C. Esquinas, C. Jimenez-Sanchidrián, J.R. Ruiz, *Use of Raman spectroscopy to assess the efficiency of MgAl mixed oxides in removing cyanide from aqueous solutions*, Applied Surface Science, 364 (2016) 428-433. En este trabajo se realiza la eliminación de aniones cianuro contenidos en disoluciones acuosas. Esta eliminación se realizó aprovechando el efecto memoria que poseen los HDLs.

- D. Cosano, D. Esquivel, F.J. Romero-Salguero, C. Jimenez-Sanchidrián, J.R. Ruiz, *Microwave-assisted synthesis of hybrid organo-layered double hydroxides containing cholate and deoxycholate*, Materials Chemistry and Physics, 225 (2019) 28-33. En este trabajo se describe la síntesis y caracterización de órgano-HDLs, es decir, HDLs conteniendo aniones inorgánicos, tales como colato y desoxicolato. La síntesis se ha realizado empleando un método asistido por microondas.

- D. Cosano, J. Hidalgo-Carrillo, M. D. Esquivel, F. J. Romero, C. Jiménez-Sanchidrián and J. R. Ruiz , Microwave-assisted synthesis of basic mixed oxides from hydrotalcites. En este trabajo, los óxidos mixtos obtenidos por diferentes métodos, se han empleado como catalizadores de la reacción MPV de benzaldehído con 2-butanol.

A parte de los artículos que conforman esta Memoria de Tesis Doctoral, Daniel Cosano Hidalgo ha presentado 30 comunicaciones en congresos, lo que ha permitido desarrollar su capacidad para comunicar los resultados de su investigación. Además, paralelamente ha estas investigaciones, ha participado en cuatro contratos de investigación del grupo FQM-346 relacionados con la Arqueología, que le han permitido publicar 7 trabajos en revistas internacionales y varias comunicaciones congresos.

Su dedicación y su entrega, su formación y evolución en su carrera científica han dado como resultado esta Tesis Doctoral que valoramos de forma muy positiva.

Por todo ello, se autoriza la presentación de la Tesis Doctoral

Córdoba, 18 de junio de 2019

Firma de los directores

Fdo.: José Rafael Ruiz Arrebola

Fdo.: César Jiménez Sanchidrián

D. José Rafael Ruiz Arrebola, Director del departamento de Química Orgánica de la Universidad de Córdoba

CERTIFICA:

Que el presente Trabajo de Investigación, titulado "HIDRÓXIDOS LAMINARES ORGÁNICO-INORGÁNICOS PARA APLICACIONES EN CATÁLISIS Y ADSORCIÓN", que constituye la Memoria presentada por Daniel Cosano Hidalgo para optar al título de Doctor en Química, ha sido realizado en los laboratorios del Departamento de Química Orgánica de la Universidad de Córdoba, bajo la dirección de los profesores D. José Rafael Ruiz Arrebola y D. César Jiménez Sanchidrián, así como en el Departamento de Química Inorgánica y Química Física de la Universidad de Gante (Bélgica), durante la estancia de tres meses que realizó bajo la supervisión del Prof. Pascal Van Der Voort.

Y para que conste, firmo el presente certificado en Córdoba, a 18 de junio de 2019.

Fdo.: D. José Rafael Ruiz Arrebola

Las investigaciones realizadas en la presente Tesis Doctoral forman parte de una Plan de Investigación desarrollado por el grupo FQM-346: “Catálisis Orgánica y Materiales Nanoestructurados”. Este Plan de Investigación ha sido subvencionado con cargo al Proyecto MAT2013-44463-R, del Ministerio de Ciencia e Innovación. Asimismo, estas investigaciones han recibido subvenciones de los Fondos Feder.

Por otra parte, el doctorando ha disfrutado de varios contratos con cargo a proyecto por la Universidad de Córdoba. Además, la Universidad de Córdoba le proporcionó una beca para la realización de una estancia de tres meses en el Departamento de Química Inorgánica y Química Física de la Universidad de Gante (Bélgica).

Mediante la defensa de esta Memoria de Tesis Doctoral se pretende optar a la obtención del **título de Doctor con Mención Internacional**, habida cuenta de que el doctorando reúne los requisitos para tal mención, según el artículo 35 de la Normativa Reguladora de los Estudios de Doctorado de la Universidad de Córdoba:

- ✓ El doctorando ha realizado una estancia de tres meses de duración en el Center of Ordered Materials, Organometallics and Catalysis (COMOC), perteneciente al Departamento de Química Inorgánica y Química Física de la Universidad de Gante.

- ✓ Parte de la Memoria de la Tesis Doctoral se ha redactado en una lengua distinta de las lenguas oficiales de España.

- ✓ Parte de los informes favorables de dos doctores expertos con experiencia acreditada, pertenecientes a una institución no española de Educación Superior:

  - ❖ Dr. Ali Khalilov (Baku State University, Azerbaijan)
  - ❖ Dra. Souad Bouasla (Ecole Normale Supérieure d'Enseignement Technique, ENSET de Skikda, Algiers, Algeria)

- ✓ Un miembro del tribunal que ha de evaluar la Tesis es un doctor experto con experiencia acreditada, perteneciente a una institución no española de Educación Superior, y es distinto del responsable de la estancia mencionada en el primer apartado:

  - ❖ Dr. Carlos Baleizão (Universidad de Lisboa, Portugal)

- ✓ La presentación de esta Tesis Doctoral se realizará en una lengua distinta de las lenguas oficiales de España.

INDICE GENERAL

ÍNDICE GENERAL

HIPÓTESIS Y OBJETIVOS

HIPÓTESIS Y OBJETIVOS.

Las hipótesis y objetivos propuestos para la realización de la siguiente tesis se resumen en los siguientes puntos:

Hipótesis 1

Los hidróxidos dobles laminares (HDLs) naturales y sintéticos han despertado un enorme interés en diversas áreas científicas, entre las que podemos destacar la catálisis y la adsorción. Se han realizado multitud de investigaciones basadas en la síntesis de HDLs utilizando diversos cationes di y trivalentes en combinación con diferentes aniones. La mayoría de estos materiales han sido sintetizados utilizando el método de coprecipitación. También se han utilizado alternativas, como el método sol-gel y el método de precipitación homogénea por hidrólisis de urea, obteniendo materiales con propiedades químico superficiales, texturales y estructurales diferentes.

El uso de metales poco comunes para la síntesis de estos materiales esta menos investigado, por ejemplo, el uso de metales como Ga o In es reducido y aún más raros son los HDLs con Sn o Zr.

Las técnicas de caracterización de HDLs más comunes son la difracción de rayos X (DRX), espectroscopia infrarroja con transformada de Fourier (FT-IR) y la resonancia magnética nuclear de estado sólido (RMN MAS). Por el contrario, la espectroscopia Raman se emplean minoritariamente en esta caracterización.

Objetivo 1

El método sol-gel se emplea habitualmente para sintetizar HDLs conteniendo metales di y trivalentes. Estos HDLs generalmente se caracterizan empleando técnicas como la difracción de rayos X o las espectroscopias de infrarrojo y de resonancia magnética nuclear, entre otras. La espectroscopia Raman, sin embargo, no es muy empleada en estos estudios. El objetivo que nos marcamos en esta tesis Doctoral fue la síntesis de HDLs conteniendo, además de metales divalentes y

trivalentes, metales tetravalentes, empleando el método sol-gel. Este método todavía no había sido descrito en la bibliografía en la síntesis de HDLs con metales tetravalentes. Además, la caracterización de estos nuevos HDLs, junto con la difracción de rayos X, nos planteamos en uso de la espectroscopia Raman, tampoco empleada hasta entonces para caracterizar estos materiales.

Este estudio queda recogido en el artículo ***"Vibrational spectroscopic study of sol-gel layered double hydroxides containing different tri-and tetravalent cations"*.**

Hipótesis 2

La contaminación de las aguas se está convirtiendo en un verdadero problema no solo para las personas, sino también para los seres vivos que habitan en el medio ambiente. Según la Organización mundial de la salud (OMS), el agua contaminada es aquella que no reúne las condiciones necesarias para ser utilizada beneficiosamente en el consumo para el ser humano y el resto de animales. Cada contaminante posee unos valores de concentración límite en el agua, dependiendo de la legislación de cada país. De este modo, planteamos sintetizar un sólido con la capacidad de adsorber contaminantes aniónicos como es el caso del cianuro (CN^-).

El cianuro, como sustancia altamente toxica presente en la naturaleza, puede ser letal en ciertas concentraciones. Según el "Centro de Control y Prevención de Enfermedades de Estados Unidos (CDC)", puede existir en varias formas, como gas incoloro (ej: cianuro de hidrógeno (HCN)) o en forma de sal sódica (cianuro potásico (KCN)). Este último es un anión que se combina fácilmente con metales tales como oro, plata, cobre, cinc y mercurio, formando quelatos solubles en agua. También se utiliza en la industria del plástico, agroquímica, tintes, industria farmacéutica y en la industria minera. Esta última representa la principal fuente de contaminación del agua con cianuro.

Existen diversos métodos de eliminación de cianuro, normalmente este anión es eliminado del agua por cloración alcalina, mediante oxidantes químicos tales como peróxido de hidrógeno, dióxido de azufre, así como técnicas alternativas

tales como ósmosis, acidificación/volatilización o incluso fotólisis, pero consumen mucha energía o utilizan reactivos no aceptados medioambientalmente. Todas estas indicaciones nos han llevado a la opción de plantear la síntesis de un sólido no contaminante y fácil de preparar que tenga la capacidad de adsorber este anión.

Como adsorbentes, los hidróxidos dobles laminares (HDLs) son una buena opción para la eliminación de este tipo de contaminantes aniónicos del agua. Debido a su alta estabilidad y a sus diferentes propiedades, como el efecto memoria o el intercambio aniónico, poseen una alta capacidad de adsorción.

Objetivo 2

Como segundo objetivo se planteó la síntesis de hidróxidos dobles laminares por el método de coprecipitación y posteriormente ser calcinados. De este modo, el material calcinado nos permitió adsorber el anión cianuro contenido en una disolución acuosa. Para la evaluación de esta adsorción nos propusimos emplear la espectroscopia Raman.

El objetivo, por tanto, fue el aprovechamiento del efecto memoria de los HDLs, según el cual cuando un HDL calcinado a una determinada temperatura se pone en contacto con una disolución aniónica, reconstruye su estructura original de HDL tomando los aniones de la disolución. Además, la espectroscopia Raman podría ser una técnica excelente para cuantificar el cianuro de la disolución, pues la señal del enlace C≡N no solapa con ninguna otra.

Todo este estudio queda recogido en el artículo ***"Use of Raman spectroscopy to assess the efficiency of MgAl mixed oxides in removing cyanide from aqueous solutions"*.**

Hipótesis 3

Los hidróxidos dobles laminares han sido utilizados comúnmente para la adsorción de aniones, debido a sus propiedades estructurales. Dichas propiedades solo afectan a compuestos aniónicos, de este modo, se planteó la posibilidad de

sintetizar un HDL capaz de adsorber compuestos no aniónicos mediante interacciones intermoleculares, tales como las fuerzas de Van der Waals.

La naturaleza del anión interlaminar del HDL puede ser muy variada. La intercalación de aniones orgánios en el HDL conduce a la formación de compuestos organo-HDLs, con propiedades específicas para la adsorción de compuestos no aniónicos, tales como fármacos y/o contaminantes. Este nuevo material genera microestructuras únicas controladas.

Estos organo-HDLs pueden ser sintetizados mediante métodos como la coprecipitación en presencia del anión orgánico, el intercambio aniónico o la reconstrucción del HDL a partir de óxidos mixtos obtenidos por la calcinación del material. Estos métodos son lentos y poco reproducibles, por ello planteamos la opción de utilizar un método de intercambio asistido por microondas permitiéndonos generar un órgano-HDL cuyo anión orgánico interlaminar posee la capacidad de adsorber compuestos de interés no aniónicos.

Estos nuevos HDLs poseen interesantes aplicaciones para la adsorción de compuestos en disoluciones acuosas debido a la alto hidrofobicidad de los HDLs, haciendo de este un material idóneo para la adsorción de compuestos orgánicos en agua. Por este motivo, en las dos últimas décadas se están realizando múltiples estudios en la síntesis de organo-HDLs con tamaño de partícula pequeño, uniforme y alta superficie específica. Uno de los métodos más exitoso en la síntesis de dichos materiales consiste en un método asistido por microondas, el cual proporciona una rápida intercalación de moléculas aniónicas de diferente naturaleza. Sin embargo, no existe un elevado número de materiales sintetizados empleando técnicas de microondas.

Objetivo 3

Como tercer objetivo se planteó la síntesis de órgano-HDLs de colato/Mg,Al-HDL y desoxicolato/Mg,Al-HDL empleando un método de intercambio iónico asistido por microondas, partiendo de un HDL conteniendo nitrato como anión interlaminar. El material sintetizado poseerá propiedades imprescindibles para la

adsorción de compuestos orgánicos de interés, tales como fármacos y contaminantes.

El empleo de microondas puede suponer un recorte importante de los tiempos de síntesis, por lo que nos planteamos la utilización de esta forma de energía para obtener los órgano-HDLs. Estos órgano-HDLs serán empleados, en estudios futuros, como adsorbentes de moléculas de interés en farmacología, pues la presencia de varios centros quirales en los aniones orgánicos podría ayudar a una discriminación enantiomérica.

Todo este estudio queda recogido en el artículo ***"Microwave-assisted synthesis of hybrid organo-layered double hydroxides containing cholate and deoxycholate"*.**

Hipótesis 4

Los hidróxidos dobles laminares constituyen una familia de materiales cuya estructura es similar a la brucita, $Mg(OH)_2$. En los HDLs un metal trivalente sustituye a un determinado número de átomos de magnesio, provocando que las láminas hidroxílicas se carguen positivamente, esto le proporciona ciertas propiedades de gran interés para la adsorción de compuestos y catálisis.

El método de síntesis comúnmente empleado es la coprecipitación a pH constante. En este procedimiento, el sólido obtenido es sometido a una etapa de envejecimiento, mejorando su cristalinidad. Esta etapa es lenta, de modo que la realización de un proceso de envejecimiento asistido por microondas, nos proporciona una buena cristalinidad a tiempos cortos. Otro método de síntesis, que nos permite obtener una elevada cristalinidad es el método de coprecipitación homogénea con urea, asistido por microondas, el cual nos proporciona una mejora sensible en sus propiedades texturales.

Una vez sintetizados los HDLs, son sometidos a un proceso de calcinación, transformándolos en un óxido mixto de composición $MgAlO_x$ con propiedades básico-superficiales características, que los hacen catalizadores potenciales para

procesos orgánicos catalizados por bases. Uno de estos procesos es la reacción de Meerwein-Ponndorf-Verley (MPV).

La reacción de MPV consiste en la transferencia de un hidruro desde un alcohol hasta un compuesto carbonílico, produciendo así un nuevo compuesto carbonílico y un nuevo alcohol. En la última década se han desarrollado múltiples investigaciones basadas en el uso de catalizadores heterogéneos, tanto ácidos como básicos, con la capacidad de producir la transferencia de dicho hidruro.

Objetivo 4

Como cuarto objetivo de esta Tesis, se planteó la síntesis de HDLs utilizando diversos métodos asistidos por microondas, para obtener una gama de sólidos con diferentes propiedades texturales. La calcinación de estos HDLs podría conducir a obtener óxidos mixtos con diferentes propiedades texturales y químico-superficiales. Los métodos principales de síntesis a emplear serán el de coprecipitación a pH constante y el de coprecipitación homogénea, en ambos casos con urea asistidos con microondas. También se empleará el método de coprecipitación utilizando un agente director de estructura como el Pluronic 123 (P123), utilizando una técnica de envejecimiento de nuevo asistida con microondas.

La calcinación de estos sólidos nos permitirá obtener una serie de óxidos que serán empleados en la reacción MPV de compuestos carbonílicos empleando 2-butanol.

Todo este estudio queda recogido en el artículo ***"Microwave-assisted synthesis of basic mixed oxides from hydrotalcites".***

RESUMEN/
SUMMARY

RESUMEN DE LA TESIS DOCTORAL, "HIDRÓXIDOS LAMINARES ORGÁNICO-INORGÁNICOS PARA APLICACIONES EN CATÁLISIS Y ADSORCIÓN"

1. Introducción o motivación de la Tesis Doctoral

La síntesis de materiales inorgánicos o híbridos orgánico-inorgánicos con diferentes texturas y sistemas porosos es un campo de investigación muy atractivo, debido a la multitud de aplicaciones que pueden encontrar estos materiales en distintos ámbitos científicos y/o industriales. La solución a muchos problemas medioambientales o industriales de la sociedad actual puede estar en la utilización de materiales que posean unas propiedades singulares. Entre estos materiales podemos destacar los hidróxidos dobles laminares (HDLs) [1]. De hecho, hoy en día estos HDLs están siendo utilizados en diferentes campos como la catálisis, el control de la polución, o el intercambio aniónico, entre otras [2]. Estas aplicaciones tienen que ver con la periodicidad estructural a nivel nanométrico que poseen los HDLs, así como a la separación de cargas existentes entre las láminas de tipo brucita y los aniones situados en la región interlaminar [3].

Generalmente, Los HDLs están formados por aniones divalentes y trivalente, destacándose sobre todos la hidrotalcita, un mineral natural de fórmula $Mg_6Al_2(OH)_{16}CO_3{\cdot}H_2O$, que puede ser sintetizado con suma facilidad en el laboratorio y a gran escala[4]. No obstante, HDLs conteniendo metales tetravalentes y también Li+ han sido descritos. La fórmula general que podemos establecer para un HDL es $[M(II)_{1-x}M(III)_x(OH)_2]^{x+}(A^{n-})_{x/n}{\cdot}m{\cdot}H_2O$ [5,6] donde M(II) y M(III) son metales di y trivalentes, respectivamente; A^{n-} es un anión y x es la relación metálica dada por M(II)/[(M(II)+M(III)]. El anión A^{n-} compensa el defecto de carga de las láminas de tipo brucita y su naturaleza puede ser muy variada [7], tanto inorgánica como orgánica. Cuando introducimos aniones orgánicos obtenemos materiales híbridos orgánico-inorgánicos que abren un enorme abanico de aplicaciones para los mismo.

Por otra parte, muchos de los HDLs poseen una elevada capacidad de intercambio iónico. Otros muchos, cuando se calcina, se transforman en óxidos mixtos con unas extraordinarias propiedades químico-superficiales y texturales que los hacen atractivos para ser empleados como catalizadores[8].

2. Contenido de la investigación

La presente Tesis Doctoral abarca la síntesis, caracterización y aplicaciones de HDLs. Como resultado de esta investigación se han obtenido diferentes materiales laminares utilizando diferentes métodos de síntesis con aplicaciones en adsorción y catálisis.

- En el trabajo ***"Vibrational spectroscopic study of sol-gel layered double hydroxides containing different tri-and tetravalent cations"*** se sintetizaron cinco materiales tipo HDL a partir de etóxido de magnesio en presencia de acetilacetonato de aluminio, galio, indio, estaño y circonio utilizando la técnica sol-gel. Las suspensiones coloidales obtenidas inicialmente fueron gelificadas y finalmente separadas por centrifugación. La caracterización mediante XRD confirmó la estructura tipo hidróxido doble laminar de los materiales y los espectros IR y Raman nos proporcionaron información sobre las diferencias entre los sólidos.

- En el trabajo ***"Use of Raman spectroscopy to assess the efficiency of MgAl mixed oxides in removing cyanide from aqueous solutions"*** se estudió la capacidad de actuación de los HDLs como remediadores ambientales, concretamente en la purificación de agua conteniendo cianuro. El proceso se basa en el "efecto memoria" de los HDL. La cinética del proceso se siguió por espectroscopia Raman. Se demostró que la relación metálica del HDL tiene una influencia crucial en la capacidad de adsorción del óxido mixto resultante tras la calcinación. La caracterización mediante XRD confirmó la estructura laminar de los HDLs y la estructura de tipo periclasa de los óxidos mixtos obtenidos tras calcinación. En este trabajo se utilizó por primera vez la espectroscopia Raman para monitorizar el proceso de adsorción, obtenido como resultado un proceso

eficaz y expeditivo para el propósito previsto, permitiendo la monitorización in situ del proceso de adsorción

- En el trabajo ***"Microwave-assisted synthesis of hybrid organo-layered double hydroxides containing cholate and deoxycholate"*** se sintetizaron materiales hidróxidos dobles laminares (HDLs) orgánico-inorgánicos mediante intercalación de los aniones colato y desoxicolato. Se empleó un método de síntesis asistido por microondas. La caracterización mediante difracción de rayos X y espectroscopia Raman muestra que la intercalación de los aniones orgánicos se produce después de un tratamiento de 1h bajo microondas, lo que supone acortar los tiempos de síntesis frente a otros métodos más convencionales de obtener este tipo de sólidos. En ambos órgano-HDLs el espaciado basal nos indica que los aniones orgánicos se sitúan en la región interlaminar sin entrecruzamiento. Esta distancia interlaminar ha podido ser confirmada con las micrografías de HR-TEM. Asimismo, se ha comprobado que la temperatura de descomposición del anión orgánico aumenta sensiblemente al ser intercalado en el HDL. Esta observación se ha realizado por medidas termogravimétricas y se ha confirmado por espectroscopia Raman, a través de una monitorización de la señal del anión orgánico durante el período de calefacción.

- En el trabajo ***"Microwave-assisted synthesis of basic mixed from hydrotalcites"*** se sintetizaron tres hidróxidos dobles laminares (HDLs) empleando diferentes métodos de irradiación con microondas: un procedimiento de coprecipitación, este mismo procedimiento, pero en presencia de un agente director de estructura como es el Pluronic P123 y un procedimiento de precipitación homogénea con urea. Estos tres HDLs, tras ser calcinadas a 450 °C formaban de fases de óxidos mixtos de composición $MgAlO_x$, cuyas propiedades texturales y químico-texturales dependían directamente del método de síntesis empleado. El óxido mixto obtenido a partir del HDL sintetizado por el método de coprecipitación homogénea es el que presentaba los valores más elevados de superficie específica y de basicidad. Asimismo, presentaba una elevada microporosidad. Los tres óxidos mixtos han sido utilizados como catalizadores

en la reacción de Meerwein-Ponndorf-Verley de benzaldehído y 2-butanol, pudiéndose certificar que la actividad catalítica es directamente proporcional a la población de centros básicos superficiales.

3. Conclusiones

Como conclusión general se puede decir que se han sintetizado con éxito diferentes hidróxidos dobles laminares, los cuales presentaban una estructura de tipo brucita. Algunos de estos HDLs y óxidos mixtos obtenidos por calcinación fueron utilizados en procesos de adsorción y catálisis, mostrando buenas propiedades adsortivas y catalíticas.

A continuación, se detallará las conclusiones específicas obtenidas en cada uno de los trabajos que han dado como resultado la presente Memoria de Tesis Doctoral.

- En el trabajo ***"Vibrational spectroscopic study of sol-gel layered double hydroxides containing different tri-and tetravalent cations"*** se sintetizaron HDLs de Mg/Al, Mg/Ga, Mg/In, Mg/Al/Sn y Mg/Al/Zr en una relación metálica de 3 [(Mg/M(III) + M(IV)] utilizando el método de sol-gel.

  - Los patrones de DRX revelaron que los cinco sólidos poseen una estructura de HDL y el análisis elemental mostró una relación metálica muy cercana a la teórica.

  - El entorno de los grupos hidroxilos fue estudiado en detalle utilizando la espectroscopia IR. La región IR de 2800-3900 cm^{-1} dio señales similares para los cinco sólidos, confirmando la presencia de unidades Mg_3OH y Mg_2Al-OH en los HDLs.

  - La presencia de un catión trivalente distinto del aluminio o la incorporación de un metal tetravalente en la red cristalina del HDL generó variaciones poco significativas en los espectros de FT-IR de los sólidos.

  - La espectroscopia Raman fue utilizada para examinar los aniones de la región interlaminar y los enlaces metal-oxigeno de los HDLs sintetizados.

- Los espectros Raman se registraron en dos zonas diferentes. La región entre 1000-1100 cm^{-1} del espectro contenía señales asignadas a la vibración del anión carbonato, cuya posición varía al variar el tamaño del catión trivalente; sin embargo, la inserción de un catión tetravalente no provocó ningún efecto. La segunda región entre 135-700 cm^{-1}, presentó grandes diferencias entre los HDLs sintetizados. En esta región aparecen las vibraciones de los enlaces M(III)-O.

➢ En el trabajo ***"Use of Raman spectroscopy to assess the efficiency of MgAl mixed oxides in removing cyanide from aqueous solutions"*** se estudió la capacidad de eliminación de CN^- en disolución acuosa de un HDL de Mg/Al calcinado a 450 °C.

- La espectroscopía Raman demostró ser una técnica eficaz, precia y expedita para monitorizar y cuantificar la adsorción del ion cianuro en el óxido mixto obtenido tras la calcinación de un HDL.

- El cianuro se adsorbe mediante un proceso de rehidratación basado en el "efecto memoria" que restaura la estructura inicial del HDL. La adsorción decrecía con el aumento de la relación metálica de Mg/Al del HDL utilizado como precursor para el óxido mixto empleado, siendo el mejor el óxido mixto con relación Mg/Al=2.

- La cinética del proceso se ajustó a un modelo de Lagergren de primer orden. La adsorción de cianuro aumentaba al aumentar la temperatura, lo que sugiere que el proceso era endotérmico. Basándonos en la energía de activación del proceso, la adsorción del cianuro se rige por una reacción con el óxido mixto y no por difusión.

- Finalmente, se observó como la calcinación del HDL después de la adsorción del cianuro restaura el óxido mixto original haciendo posible la reutilización del material.

➢ En el trabajo ***"Microwave-assisted synthesis of hybrid organo-layered double hydroxides containing cholate and deoxycholate"*** se sintetizaron órgano-HDLs mediante un método asistido por microondas suponiendo un considerable ahorro de tiempo en la obtención de estos compuestos al ser comparados con los sintetizados por otros métodos de síntesis.

- La cristalinidad que se obtiene para los mismos es elevada, produciéndose una sustitución total del anión nitrato del HDL de partida por los aniones orgánicos.

- El aumento de tiempo del tratamiento con microondas más allá de una hora redunda negativamente en la cristalinidad del HDL sintetizado. Por primera vez se describe en la literatura el HDL intercalado con colato, cuyas características son similares a las del HDL conteniendo desoxicolato.

- En ambos casos, la distancia interlaminar, determinada experimentalmente por difracción de rayos X y confirmada por HR-TEM, tiene un valor cercano al doble de la longitud de las cadenas de colato o desoxicolato, lo que determina que las cadenas orgánicas se sitúan en el interior del HDL sin entrecruzamiento.

- Finalmente, se ha aplicado, también por primera vez, la espectroscopia Raman al seguimiento de la descomposición térmica del órgano-HDL. Monitorizando las bandas de tensión de los enlaces C-H de las moléculas de colato o desoxicolato se puede establecer la temperatura a la cual se produce la descomposición del mismo, produciéndose el colapso de la estructura del HDL, para transformarse en un óxido mixto de magnesio y aluminio. Este seguimiento nos ha permitido establecer que al intercalar el anión orgánico en el HDL se produce un aumento considerable de su temperatura de descomposición.

➢ En el trabajo ***"Microwave-assisted synthesis of basic mixed from hydrotalcites"*** los óxidos mixtos obtenidos por calcinación de hidróxidos dobles laminares sintetizados empleando distintos métodos de irradiación con microondas se han empleado como catalizadores en la reacción de Meerwein-Ponndorf-Verley de benzaldehído con 2-butanol.

- De los tres óxidos mixtos, el obtenido empleando un método de precipitación homogénea con urea presenta un elevado carácter microporoso y una basicidad superficial casi el doble de la de los dos óxidos mixtos obtenidos por el método coprecipitación (uno de ellos en presencia de Pluronic P-123).

- Todos los óxidos mixtos presentan tres tipos de centros básicos: débiles, medios y fuertes.

- El más activo en la reacción MPV estudiada es el que posee una mayor población de centros básicos de fortaleza moderada a media, como se ha puede justificar por el mecanismo propuesto para la reacción.

- También se realizó la reacción de MPV de ciclohexanonas y algunos derivados, obteniendo excelentes valores de conversión. En la metilciclohexanona, cuando el sustituyente metilo cambia de posición 4 a 3 y 2, se produjo una disminución significativa de la conversión, la cual pudo ser explicada por el impedimento estérico generado por el grupo metilo en el complejo adsorbido.

- Finalmente, se realizaron varias reutilizaciones del catalizador en la reacción de MPV entre ciclohexanona y 2-butanol obteniendo valores de conversión y selectividad similares a la reacción inicial.

4. Bibliografía

[1] D. Evans, R. Slade, Structural Aspects of Layered Double Hydroxides, in: Struct. Bond., Springer-Verlag, Berlin/Heidelberg, 2005: pp. 1–87.

[2] F. Li, X. Duan, Applications of Layered Double Hydroxides, Struct. Bond. 119 (2006) 193–223.

[3] C. Taviot-guého, V. Prévot, C. Forano, G. Renaudin, C. Mousty, F. Leroux, Tailoring Hybrid Layered Double Hydroxides for the Development of Innovative Applications, Adv. Funct. Mater. 28 (2017) 1703868.

[4] J. He, M. Wei, B. Li, D. Evans, X. Duan, Preparation of Layered Double Hydroxides, Struct. Bond. 119 (2006) 89–119.

[5] R. Allmann, The crustal structure of pyroaurite, Acta Crystallogr. B24 (1968) 972–977.

[6] M. Mora, Utilización de soportes de Pd soportado sobre hidrotalcita en la reacción de acoplamiento cruzado de Suzuki, Tesis Doctoral, Universidad de Córdoba, 2008.

[7] T. Hibino, Anion Selectivity of Layered Double Hydroxides: Effects of Crystallinity and Charge Density, Eur. J. Inorg. Chem. 2018 (2018) 722–730.

[8] M. Xu, M. Wei, Layered Double Hydroxide-Based Catalysts: Recent Advances in Preparation, Structure, and Applications, Adv. Funct. Mater. 28 (2018) 1–20.

SUMMARY OF THE DOCTORAL THESIS, "ORGANIC-INORGANIC LAYERED HYDROXIDES FOR APPLICATIONS IN CATALYSIS AND ADSORPTION"

1. Introduction or motivation of the Doctoral Thesis

The synthesis of inorganic and organic-inorganic hybrid materials with different textures and porous systems is a very attractive research field, due to the multiple applications that these materials can find in different scientific and/or industrial areas. The solution to many environmental or industrial problems from the current society can be in the use of materials that own some unique properties. Among these materials we can stand out the layered double hydroxides (LDHs) [1]. In fact, nowadays LDHs are being used in different fields like catalysis, pollution control, or anionic exchange, among others [2]. These applications have to do with the structural regularity at nanometer level that own LDHs, as well as the separation between existent charges between the brucite-type layers and the anions situated in the interlayered region [3].

Generally, LDHs are set up of divalent and trivalent anions, standing out over all the hydrotalcite, a natural mineral formulated as $Mg_6Al_2(OH)_{16}CO_3{\cdot}H_2O$, that can easily be synthesised in large scale [4]. Nevertheless, LDHs containing tetravalent metals and also Li^+ have been described. The general formula that we can establish for a LDH is $[M(II)_{1-x}M(III)_x(OH)_2]^{x+}(A^{n-})_{x/n}{\cdot}m{\cdot}H_2O$ [5,6] where M(II) and M(III) are di and trivalent metals, respectively; A^n is an anion and x is the metallic ratio given by M(II)/[(M(II)+M(III)]. The A^{n-} anion compensates the defect in the brucite-type layer's charge and can have a very different inorganic and organic nature [7]. When we introduce organic anions, we obtain hybrid organic-inorganic materials that open up an enormous range of applications.

On the other hand, many of the LDHs own an enhanced capacity of ionic exchange. Many others, when they are calcined, they turn into mixed oxides with extraordinary surface chemical and textural properties making them attractive to be employed as catalysts [8].

2. Content of the research

This Doctoral Thesis covers the synthesis, characterization and applications of LDHs. As a result of this research, different layered materials using different synthesis methods with applications in adsorption and catalysis have been obtained.

In the paper ***"Vibrational spectroscopic study of sol-gel layered double hydroxides containing different tri-and tetravalent cations",***ffive different layered double hydroxides were synthesized from magnesium ethoxide in the presence of aluminium, gallium, indium, tin and zirconium acetylacetonates by using the sol–gel technique. The colloid suspensions initially obtained were gelled and separated by centrifugation. XRD diffraction patterns confirmed that the five solids thus obtained possessed a layered double hydroxide structure. Also, IR and Raman spectra revealed differences between the solids.

In the paper **"Use of Raman spectroscopy to assess the efficiency of MgAl mixed oxides in removing cyanide from aqueous solutions"** the ability of LDHs as environmental remediators was studied, specifically in the purification of water containing cyanide. The process is based on the "memory effect" of LDHs. The kinetics of the process was examined by Raman spectroscopy. The metal ratio of the LDH was found to have a crucial influence on the adsorption capacity of the resulting mixed oxide. The characterization by XRD confirmed the layered structure of the LDHs and the periclase-like structure of the mixed oxides obtained by calcination. In this work, Raman spectroscopy was for the first time used to monitor the adsorption process. Based on the results, this technique is an effective, expeditious choice for the intended purpose and affords in situ monitoring of the adsorption process.

- In the paper ***"Microwave-assisted synthesis of hybrid organo-layered double hydroxides containing cholate and deoxycholate"*** Organic–inorganic layered double hydroxides (LDHs) were synthesized by intercalation of the cholate and deoxycholate ion. A microwave-assisted synthesis method was used. The characterization by X-ray diffraction and Raman spectroscopy for the resulting

LDHs showed that a treatment time of only 1 h sufficed to ensure complete intercalation of the organic anions. This makes the proposed synthetic method more expeditious than existing alternatives for the same purpose. Based on the baseline spacing for the organo-LDHs, the organic anions were intercalated with no cross-over between their molecular chains. The interlayer distance of the solids was confirmed by high-resolution transmission electron micrographs (HR-TEM). As revealed by thermogravimetric monitoring measurements, and confirmed by Raman spectra, the decomposition temperature for the LDHs increased considerably upon intercalation of the organic anion.

- In the paper ***"Microwave-assisted synthesis of basic mixed from hydrotalcites"*** three layered double hydroxides (LDHs) were prepared by using three different microwave irradiation methods, namely: coprecipitation in the absence and presence of Pluronic P123 as template, and homogeneous precipitation in the presence of urea. Calcination at 450 ºC of the three hydrotalcites gave $MgAlO_x$ mixed oxides. Their textural and surface chemical properties were found to depend on the particular synthetic method used. The mixed oxide obtained from the hydrotalcite prepared by homogeneous coprecipitation exhibited the highest specific surface area and basicity, in addition to a high microporosity. The three mixed oxides were used as catalysts in the Meerwein–Ponndorf–Verley reaction of benzaldehyde with 2-butanol, where the activity was found to be directly proportional to the population of basic surface sites.

3. Conclusions

As a general conclusion, it can be said that several layered double hydroxides (LDHs) have been synthesized successfully, exhibiting a brucite-type structure. Some of these LDHs and mixed oxides obtained by calcination were used in adsorption processes and catalysis, most of them showing good adsorptive and catalytic properties.

Coming up next, the specific conclusions of each of the articles published that have resulted from this Doctoral Thesis are detailed.

- In the paper ***"Vibrational spectroscopic study of sol-gel layered double hydroxides containing different tri-and tetravalent cations"*** we prepared Mg/Al, Mg/Ga, Mg/In, Mg/Al/Sn and Mg/Al/Zr LDHs in a metal ratio of 3 [(Mg/*M*(III) + *M*(IV)] by using the sol–gel method.

- XRD patterns revealed that the five solids possess a layered double hydroxide structure and a metal ratio very close to the theoretical one.

- The environment of hydroxyl groups was studied in detail by using IR spectroscopy. The IR zone from 2800 to 3900 cm^{-1} was quite similar for the five solids and seemingly confirms the presence of Mg_3OH and Mg_2Al-OH environments in the LDHs.

- The presence of a trivalent cation other than aluminium or the insertion of a small amount of a tetravalent ion in the LDH crystal network had little effect on the FT-IR spectra for the solids in this zone.

- Raman spectra were recorded in two different zones. One spanned the wavenumber range 1000–1100 cm^{-1} and contained the signal for stretching vibrations in carbonate, its position changing with the size of the trivalent cation — inserting a tetravalent cation had no effect on it, however. The other zone, 135–700 cm^{-1}, was that exhibiting the greatest differences between LDHs. In this region, the stretching vibration of *M*(III)–OH bonds was also present.

- In the paper ***"Use of Raman spectroscopy to assess the efficiency of MgAl mixed oxides in removing cyanide from aqueous solutions"*** the removal capacity of CN^- in aqueous solution of an LDH of Mg / Al calcined at 450 ° C was studied.

- Raman spectroscopy is an effective, accurate, expeditious technique for monitoring and quantifying the adsorption of cyanide ion on a mixed oxide obtained by calcining a layered double hydroxide (LDH).

- Cyanide is adsorbed by a rehydration process based on a "memory effect" that restores the initial structure of the LDH. The adsorption rate was found to

decrease with increase in metal (Mg/Al) ratio of the LDH used as precursor for the mixed oxide, being optimum for the oxide with Mg/Al = 2.

- The kinetics of the process conformed to a first-order Lagergren model. The fact that the cyanide adsorption rate increased with increasing temperature suggests that the process is endothermic. Based on the activation energy for the process, the adsorption of cyanide is governed by its reaction with the mixed oxide rather than by diffusion.

- Finally, calcination of the LDH after adsorption of cyanide restores the original mixed oxide, which can thus be reused as a cyanide sorbent

➢ In the paper ***"Microwave-assisted synthesis of hybrid organo-layered double hydroxides containing cholate and deoxycholate"*** microwave-assisted anion-exchange provides substantial time savings in synthesizing organo-LDHs when compared with those synthesized by other methods of synthesis.

- The resulting solids possess a high crystallinity by effect of the starting nitrate anion being completely substituted by the organic anions.

- More than 1 h of microwave treatment was found to have an adverse impact on crystallinity, however. A cholate-containing LDH was for the first time prepared here whose properties were similar to those of the deoxycholate-containing solid.

- In both, the interlayer distance as determined by XRD spectroscopy and confirmed by HR-TEM measurements was almost twice the length of a cholate or deoxycholate chain; there was thus no cross-over of organic chains in the LDHs.

- Finally, Raman spectroscopy was also for the first time used to monitor the thermal decomposition of the organo-LDHs through the stretching vibrations of C–H bonds in cholate and deoxycholate. This allowed the temperature at which the LDHs collapsed by decomposition into an Mg/Al mixed oxide to be precisely established. As shown by the results, intercalating an organic anion into an inorganic LDH considerably raises its decomposition temperature.

➢ In the paper ***"Microwave-assisted synthesis of basic mixed oxides from hydrotalcites"*** mixed oxides obtained by calcining hydrotalcites prepared under

microwave irradiation were used as catalysts in the Meerwein–Ponndorf–Verley (MPV) reaction between benzaldehyde and 2-butanol.

- Out of the three mixed oxides, the oxide obtained by homogeneous coprecipitation with urea possessed a high microporosity and a surface basicity almost doubling that of the two oxides obtained by coprecipitation both in the absence or presence of Pluronic P123 as template.

- All oxides contained three types of basic sites, namely: weak, medium and strong.

- The most active oxide in the target MPV reaction was that possessing the largest population of moderate to strong basic sites, which is consistent with the proposed reaction mechanism.

- Also, the MPV reaction of cyclohexanones and some compounds related to it were carried out, obtaining excellent conversion values. In the case of methylcyclohexanone, when the methyl substituent changes from position 4 to 3 and 2, there was a significant decrease in conversion. This decrease can be explained by the steric hindrance of the methyl group on the proposed adsorbed complex.

- Finally, several reuses of the catalyst were carried out in the reaction of MPV between cyclohexanone and 2-butanol, obtaining similar conversion and selectivity values to the initial reaction.

4. Bibliography

[1] D. Evans, R. Slade, Structural Aspects of Layered Double Hydroxides, in: Struct. Bond., Springer-Verlag, Berlin/Heidelberg, 2005: pp. 1–87.

[2] F. Li, X. Duan, Applications of Layered Double Hydroxides, Struct. Bond. 119 (2006) 193–223.

[3] C. Taviot-guého, V. Prévot, C. Forano, G. Renaudin, C. Mousty, F. Leroux, Tailoring Hybrid Layered Double Hydroxides for the Development of Innovative Applications, Adv. Funct. Mater. 28 (2017) 1703868.

[4] J. He, M. Wei, B. Li, D. Evans, X. Duan, Preparation of Layered Double Hydroxides, Struct. Bond. 119 (2006) 89–119.

[5] R. Allmann, The crustal structure of pyroaurite, Acta Crystallogr. B24 (1968) 972–977.

[6] M. Mora, Utilización de soportes de Pd soportado sobre hidrotalcita en la reacción de acoplamiento cruzado de Suzuki, Tesis Doctoral, Universidad de Córdoba, 2008.

[7] T. Hibino, Anion Selectivity of Layered Double Hydroxides: Effects of Crystallinity and Charge Density, Eur. J. Inorg. Chem. 2018 (2018) 722–730.

[8] M. Xu, M. Wei, Layered Double Hydroxide-Based Catalysts: Recent Advances in Preparation, Structure, and Applications, Adv. Funct. Mater. 28 (2018) 1–20.

CAPÍTULO I.

INTRODUCCIÓN

I. HIDRÓXIDOS DOBLES LAMINARES

I.1. INTRODUCCIÓN

Los hidróxidos dobles laminares (HDLs), naturales o sintéticos, también denominados hidrotalcitas (HT) son compuestos pertenecientes a la familia de las arcillas aniónicas. Fueron descubiertos en Suecia (1842) y forman un conjunto natural de hidróxidos de metales divalentes y trivalentes. En 1942, Feitknecht [1] sintetizó varios compuestos que presentaban una estructura parecida a los HDLs, siendo denominados "doppleschichstrukturen" (estructura doble laminar). Los HDLs se organizan en el espacio en estructuras laminares, compuestas por dos o más cationes diferentes. La fórmula general de estos hidróxidos es:

$$[M(II)_{1-x}M(III)_x(OH)_2^{x+}[A_{x/n}]^{n-}\cdot mH_2O \text{ [2,3]}$$

donde M(II) y M(III) representan a un metal divalente y trivalente, respectivamente, ocupando posiciones octaédricas en las láminas hidroxílicas; A^{n-} es el anión interlaminar; m es el número de moléculas de agua interlaminar; y x es la relación metálica, dada por M (III)/ [M (II)+M (III)].

I.2. ESTRUCTURA DE LA BRUCITA

Para comprender la estructura de los hidróxidos dobles laminares, es fundamental conocer la estructura de la brucita [4], $Mg(OH)_2$. En la figura 1 se muestra la estructura tridimensional de una lámina de brucita. Esta estructura consta de átomos de Mg^{2+} coordinados octaédricamente a grupos hidroxilos (OH^-) cuyos octaedros comparten sus aristas formando láminas. La estructura de la brucita se denomina trioctaédrica, debido a que cada grupo OH^- está rodeado por tres posiciones ocupadas octaédricamente.

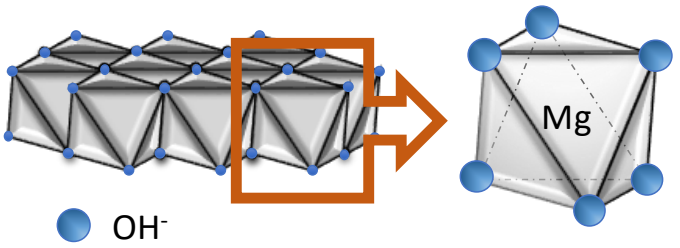

Figura 1. Estructura tridimensional de una lámina de brucita

La figura 2 muestra el apilamiento de láminas de $Mg(OH)_2$ formando la estructura de la brucita. El gran espaciado a lo largo del eje c es ocasionado mediante enlaces débiles entre láminas adyacentes por puentes de hidrógeno.

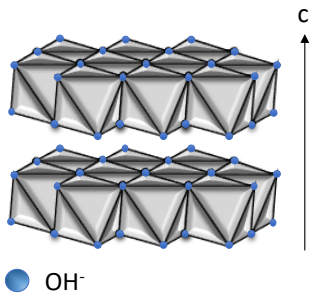

Figura 2. Estructura tridimensional de la brucita

La unidad básica de la brucita consiste en láminas de cationes Mg^{2+} localizados en el centro de octaedros. Estos cationes Mg^{2+} se encuentran coordinados octaédricamente por seis grupos OH^-. De este modo, si los vértices y los centros de los octaedros son grupos hidroxilos y cationes, respectivamente, la lámina es

eléctricamente neutra. Según Pauling [5], cada catión de Mg^{2+} comparte su carga con seis grupos hidroxilos, aportando $+^2/_6 = +^1/_3$ de carga; mientras que cada hidroxilo (OH^-) se encuentra coordinado con tres centros de magnesio, aportando $-^1/_3 = -^1/_3$, generando por tanto una carga electrostática total neutra ($+^1/_3 - ^1/_3 = 0$)[6].

I.3. ESTRUCTURA Y COMPOSICIÓN DE LAS LÁMINAS TIPO BRUCITA

La estructura de los hidróxidos dobles laminares se comprende fácilmente relacionándola con la estructura de la brucita. Consiste en láminas hidroxílicas cargadas positivamente, con un espaciado interlaminar con aniones, encargados de compensar la carga positiva de estas, junto a moléculas de agua. Como se muestra en la figura 3, la carga positiva de las láminas procede de la sustitución isomórfica, del metal divalente (Mg^{2+}) por un metal trivalente (Al^{3+}), el cual genera una carga residual positiva a lo largo del hidróxido doble laminar.

A la cohesión entre láminas contribuyen los grupos OH^- de los vértices del octaedro, los cuales interaccionan por puentes de hidrógeno. Las moléculas de agua y los aniones se sitúan en el espacio interlaminar.

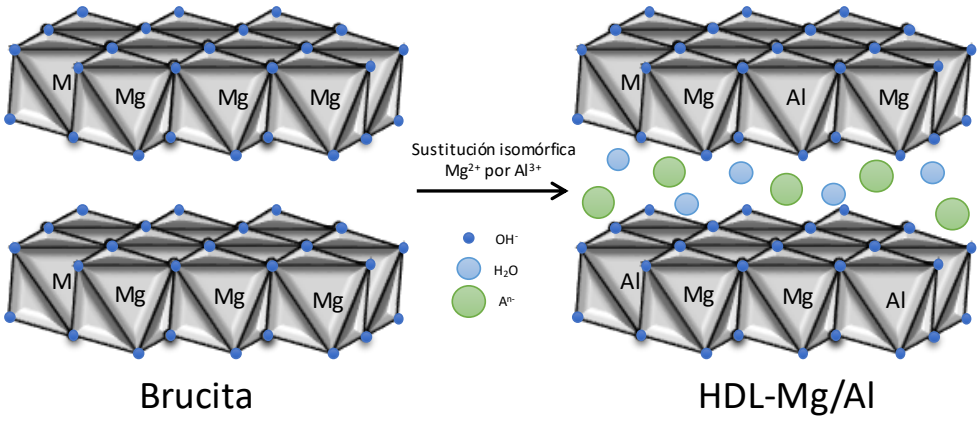

Figura 3. Sustitución isomórfica de una lámina de brucita

Este conjunto de láminas apiladas posee una secuencia de empaquetamiento AbCbA…, donde A y C, se refieren a las láminas formadas por cationes y los grupos hidroxilo, mientras que b hace referencia al espacio interlaminar formado por las

moléculas de agua y los aniones que conforman el HDL[7], como se muestra en la figura 4.

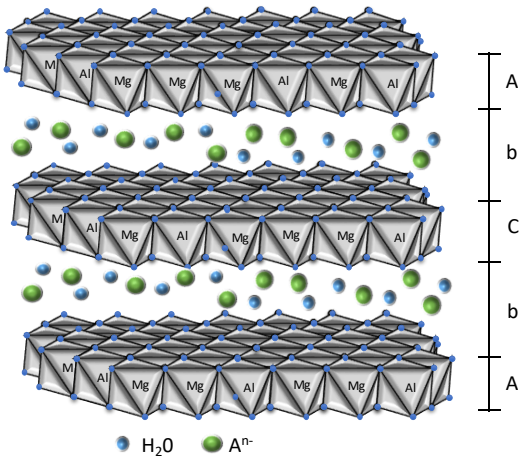

Figura 4. Estructura laminar de un HDL

La carga neta de las láminas estará determinada por el número de cationes metálicos trivalentes que sustituyen a los divalentes. De este modo, la cantidad de aniones interlaminares será proporcional a la densidad de carga residual generada. La fracción x, que indica la relación metálica M(III)/[M(II)+M(III)], es un parámetro que puede variar dentro de un intervalo. En el caso de HDLs de Mg/Al naturales, el límite superior de x es 0.35, correspondiente a una relación Mg/Al=2 [8]. En los HDLs sintéticos, el valor de x puede ser mayor, afectando así a la cristalinidad del sólido [9]. En general se obtienen materiales con buena cristalinidad para relaciones $2 < {}^{Mg}/_{Al} < 4$.

El tamaño de los radios catiónicos, con respecto a la sustitución isomórfica del metal trivalente por el divalente, es un parámetro a tener en cuenta. Las sustituciones isomórficas son producidas por metales cuyos radios catiónicos son semejantes [10]. La sustitución del metal provoca una leve deformación en los octaedros de las láminas de tipo brucita. Cuando se realiza la sustitución de un metal cuyo radio catiónico sea muy superior al Mg^{2+} puede provocar la ruptura del octaedro, llevando a la destrucción de la estructura tipo brucita del HDL, mientras que la sustitución de un metal de radio muy inferior puede provocar el cambio de

estructura octaédrica por tetraédrica, generando defectos en la estructura del sólido.

La única condición para realizar la sustitución isomórfica es que las unidades constituyentes de la lámina sean octaedros, para que se puedan disponer de forma planar, compartiendo sus aristas. Así, podría pensarse en sólidos con múltiples cationes diferentes que cumplan esta condición.

Se han realizado diversas investigaciones sobre la sustitución parcial del Mg^{2+} por cationes de radio catiónico diferente, como es el caso del In^{3+} (0.93 Å). Este posee un radio catiónico considerablemente mayor al Al^{3+} (0.67 Å) [11]. Cuando se realiza la sustitución completa del ion Mg^{2+} por metales de diferente radio iónico, se produce una sustitución más inestable [12].

La característica principal de las láminas de HDL es la existencia de cationes heterovalentes en su composición, provocando un defecto de carga en las mismas. La composición metálica de las láminas se representa principalmente por pares catiónicos, tales como M^{2+}/M^{3+}, M^{+}/M^{3+}, M^{2+}/M^{4+}, donde los cationes divalentes [13–15] pueden ser Mg^{2+}, Zn^{2+}, Co^{2+}, Ni^{2+}, Cu^{2+}, Mn^{2+}, etc., los trivalentes [14,16,17] Al^{3+}, Cr^{3+}, Fe^{3+}, Co^{3+}, Ni^{3+}, Mn^{3+}, Ga^{3+} ,In^{3+},etc., los monovalentes [18] pueden ser únicamente Li^{+} y los tetravalentes [19–21] Ti^{4+}, Zr^{4+}, Sn^{4+},etc. La coexistencia de tres o más tipos de cationes en las láminas supone una mayor variedad en las propiedades de los HDLs [22–24]. Estos últimos HDLs serán explicados con mayor detenimiento en el capítulo II de esta tesis doctoral.

El orden-desorden con respecto a la distribución catiónica en las láminas octaédricas de los HDLs es aleatorio. La elevada pseudometría, microcristalinidad y desorden en el apilamiento de las láminas dificultan su análisis. Hofmeister y von Platen [25], postularon que la mayoría de las estructuras de un HDL, posee una distribución catiónica que sigue un orden complejo, donde la ordenación de cationes divalentes y trivalentes dependerá de la relación metálica M(II)/M(III). Brindley y Kikkawa [26] demostraron que los centros metálicos trivalentes se posicionan lo más lejos posible entre sí, con el objetivo de minimizar las posibles

repulsiones catiónicas generadas y bajo ningún concepto encontrarse dos centros trivalentes unidos por sus aristas, formando M(III)-M(III).

I.4. EL ESPACIADO INTERLAMINAR

Los HDLs contienen en su región interlaminar tanto moléculas de agua como aniones inorgánicos y/o orgánicos gracias a la elevada densidad de carga de las láminas.

Las moléculas de agua presentes en la región interlaminar están unidas a través de puentes de hidrógeno con los grupos OH^- de los octaedros de las láminas de tipo brucita, y en algunas ocasiones también con los aniones situados en esta región interlaminar. Debido a la continua ruptura y formación de estos puentes de hidrógeno, las moléculas de agua se mueven con cierta libertad en la región interlaminar sin destruir la estructura del HDL [27].

La naturaleza de los aniones puede ser diferente. Podemos encontrar aniones monovalentes (Cl^-, Br^-, I^-, NO_3^-) [28], divalentes ($CO_3^=$,$SO_4^=$,$CrO_4^=$) [29,30], trivalentes (PO_4^{3-}) [31] y tetravalentes ($Fe(CN)_6^{4-}$) [32]. A su vez, la geometría molecular de los aniones puede ser sencilla, plana-triangular, tetraédrica, octaédrica o incluso láminas tetraédricas bidimensionales.

Los HDLs conteniendo aniones orgánicos son muy abundantes. Se han descrito HDLs conteniendo aniones orgánicos de cadena larga (oleato [33], sulfatos orgánicos [34]), aniones de fármacos (ibuprofeno [35], diclofenaco [36]) o aniones derivados de ciclodextrinas [37], entre otros. Debido a la capacidad que poseen los HDLs de aumentar su espaciado interlaminar, es posible la incorporación de estos aniones tan voluminosos [38]. La incorporación de aniones de naturaleza orgánica crea un nuevo grupo de HDLs híbridos, denominado órgano-HDLs, cuyas propiedades serán discutidas en capítulos posteriores.

I.5. PROPIEDADES DE LOS HIDRÓXIDOS DOBLES LAMINARES

En este apartado se mostrarán algunas de las propiedades más importantes de los HDLs, las cuales influyen enormemente en su aplicación como adsorbentes y/o catalizadores.

I.5.1 Intercambio aniónico

Una de las propiedades más importantes de los hidróxidos dobles laminares, es su capacidad para intercambiar aniones en su región interlaminar. Gracias a la particular estructura de los HDLs, el intercambio iónico realizado es de tipo topotáctico, es decir, la estructura laminar se mantiene invariable con respecto al intercambio realizado, mientras los enlaces más débiles entre los aniones y las láminas se rompen [39]. De este modo, el intercambio aniónico está relacionado únicamente con la carga y el tamaño del anión entrante, no afectándose la estructura tipo brucita del HDL [40].

La cantidad de aniones intercambiados es proporcional a su afinidad por las láminas del HDL. Miyata [41] estableció una escala de afinidad hacia la intercalación de los aniones, superior para aniones divalentes respecto a los monovalentes, siguiendo el orden:

$$NO_3^- < Br^- < Cl^- < F^- < OH^- < MoO_4^{2-} < SO_4^{2-} < CrO_4^{2-} < HAsO_4^{2-} < HPO_4^{2-} < CO_3^{2-}$$

Por ello, un HDL con nitrato como anión interlaminar obtendrá mejores resultados en un intercambio aniónico debido a la baja afinidad de este anión por las láminas. Además, la gran afinidad del carbonato exige el uso de atmósferas inertes y disolventes descarbonatados que eviten la contaminación por CO_2.

El intercambio iónico se realiza habitualmente dispersando el hidróxido doble laminar en una disolución acuosa que contiene el anión a intercalar, en condiciones de agitación constante y pH adecuado. El uso de métodos de intercambio asistidos por microondas [42] disminuye sustancialmente el tiempo necesario para el intercambio.

Este proceso de intercambio aniónico permite sintetizar innumerables materiales de tipo HDL conteniendo aniones como por ejemplo, oleato [43], colato [44], polímeros aniónicos [45] o derivados de la ciclodextrina [46]. La figura 5 muestra el proceso de intercambio del anión sulfato de β-ciclodextrina, en un HDL de Mg y Al con nitrato como anión precursor. Existen técnicas de caracterización,

como la difracción de rayos X, que permiten el seguimiento de la intercalación de dichos aniones [47], tal y como se comentará en posteriores apartados.

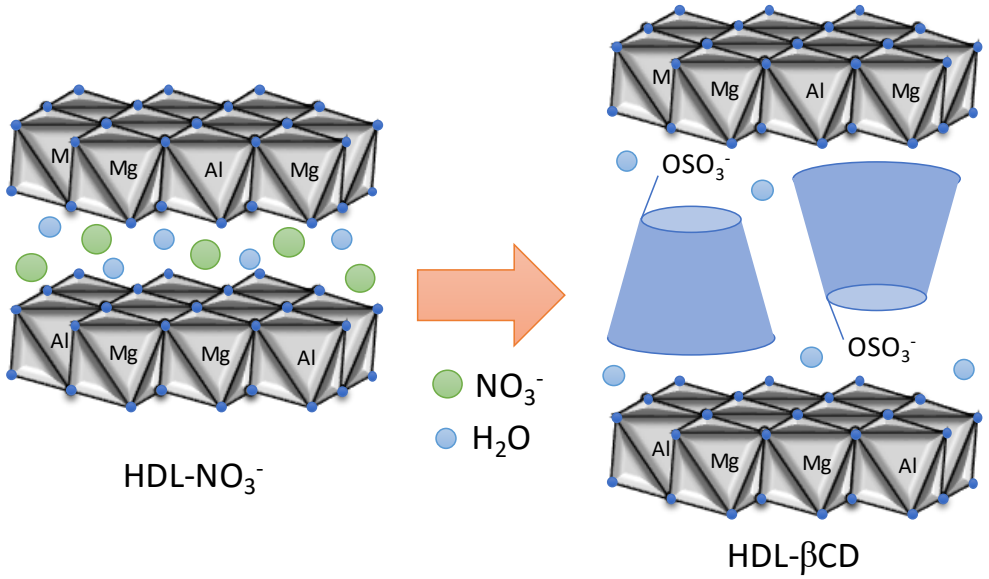

Figura 5. Sulfato de β-Ciclodextrina en un HDL de Mg/Al

I.5.2 Tratamiento térmico de los HDLs

Cuando un HDL se somete a un tratamiento térmico sufre un proceso que puede ser descrito en tres etapas [48]. La primera de ellas, hasta los 250°C aproximadamente, supone la pérdida de las moléculas de agua interlaminar persistiendo su estructura. En la segunda etapa (hasta los 450-500 °C), se produce la deshidroxilación de las láminas de tipo brucita, junto con la pérdida de los aniones interlaminares produciéndose la formación de un óxido mixto ($MgAlO_x$) [49]. Esta etapa supone colapso de la estructura laminar [50]. Cuando sometemos el HDL a temperaturas superiores se produce la transformación del óxido mixto en una espinela [51]. Para el caso de un HDL de Mg/Al tendríamos el siguiente proceso de descomposición térmica:

$$Mg_6Al_2(OH)_{16}CO_3 \cdot nH_2O \xrightarrow[H_2O]{200\text{-}250\,^{\circ}C} Mg_6Al_2(OH)_{16}CO_3 \xrightarrow[H_2O + CO_2]{450\text{-}500\,^{\circ}C} Mg(Al)O_x \xrightarrow{>550\,^{\circ}C} MgAl_2O_4$$

Los óxidos mixtos calcinados a una temperatura de 450 °C, obtenidos a partir de estos HDLs de Mg/Al, presentan pares ácidos-base, centros ácidos de Lewis (debido a la presencia de cationes Al^{3+}) y distintos tipos de centros básicos de fortaleza variable [52]. Estos últimos pueden ser de naturaleza:

- Fuerte, (centros O^{2-} directamente unidos a los metales).
- Media, (centros O^{2-} enlazados a átomos adyacentes a los centros metálicos).
- Débil, (grupos OH^- superficiales).

I.5.3 Efecto memoria

Como acabamos de comentar, cuando se calcina un HDL a temperaturas en el intervalo de 300-600 °C se produce el colapso de la estructura laminar, obteniéndose un óxido mixto [53]. Este nuevo óxido mixto posee la capacidad de rehidratarse al ser tratado con una disolución acuosa que contenga el anión a intercalar, restableciéndose la estructura de HDL. A este fenómeno se le denomina "efecto memoria". En la figura 6 se esquematiza el efecto de la rehidratación para la intercalación de un nuevo anión.

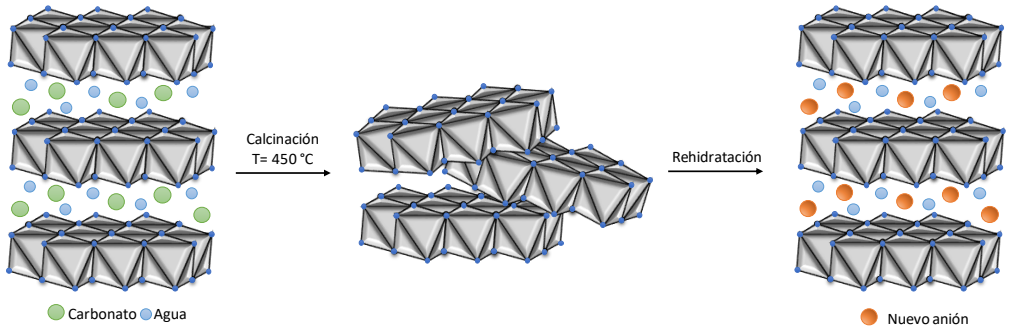

Figura 6. Aplicación del efecto memoria de los HDLs.

Si la temperatura de calcinación es superior a los 700 °C se produce la segregación de fases, formándose una fase espinela. Esta fase espinela es termodinámicamente más estable, haciendo que el proceso de reconstrucción deje de ser reversible [54].

I.6. SÍNTESIS DE HIDRÓXIDOS DOBLES LAMINARES

Las síntesis de hidróxidos dobles laminares, tanto a nivel de laboratorio como industrial, son relativamente sencillas y de bajo costo. Existen diversos métodos de síntesis de estos sólidos. Después de la síntesis se suelen aplicar tratamientos de envejecimiento para mejorar las propiedades estructurales y texturales. A continuación, algunos métodos de síntesis serán brevemente comentados.

- Coprecipitación: es el método más comúnmente utilizado para la síntesis de HDLs en grandes cantidades. Se puede llevar a cabo en dos condiciones:
  - *Precipitación a baja supersaturación:* consiste en la adición lenta de una disolución, que contiene los cationes metálicos, a un reactor que contiene una disolución acusa con el anión interlaminar deseado. Una segunda disolución alcalina es añadida al reactor simultáneamente a una velocidad controlada, para mantener el valor de pH constante que conduce a la coprecipitación del HDL.
  - *Precipitación a alta supersaturación:* este método requiere de la adición de una disolución que contiene los cationes metálicos a un reactor que contiene una disolución alcalina con el anión interlaminar deseado. Generalmente esta síntesis da como resultado materiales menos cristalinos, debido al elevado número de núcleos de cristalización [55].
- Método de precipitación homogénea: consiste en la adición de una disolución de las sales metálicas a un reactor con una disolución acuosa con urea a una temperatura determinada. La hidrólisis de la urea produce su descomposición en amonio y bicarbonato generando un pH básico en el medio que favorece la precipitación del HDL [56].
- Reconstrucción: este método está basado en el "efecto memoria" que poseen los óxidos mixtos obtenidos tras la calcinación de un HDL. Para ello se dispersan los óxidos mixtos en una disolución acuosa con el anión deseado a intercalar. El agua es absorbida por el óxido mixto recobrando la estructura tipo brucita. Los aniones, junto con el agua, son incorporados en la región interlaminar del nuevo HDL [57]. Este proceso está favorecido en disoluciones básicas [58]. En un tiempo prolongado, el contacto con la atmósfera puede también provocar la reconstrucción del material [59].

- Hidrólisis inducida: este método consiste en la adición, gota a gota, de una disolución ácida de sales metálicas trivalentes sobre óxidos metálicos divalentes. Los óxidos son disueltos progresivamente, precipitando el HDL siempre que el pH se encuentre tamponado por el óxido o hidróxido en suspensión [60].
- Técnica sol-gel: Este método está basado en una previa obtención del sol, es decir una suspensión coloidal de partículas de tamaño conocido (1-100 nm de diámetro). Dicho sol se forma por la dispersión de un óxido o hidróxido metálico insoluble en un disolvente apropiado, o por la adición de un alcóxido metálico que reacciona con el disolvente formando dicha suspensión coloidal. Finalmente, el sol es envejecido y tratado a cierta temperatura formándose un gel, que consiste en un sólido semirrígido en cuya matriz coloidal está inmerso el disolvente [61].
- Hidrotermal: esta síntesis se basa en la adición de una disolución de las sales metálicas a un pH determinado en un autoclave. Este autoclave se introduce en un horno a elevada temperatura durante un cierto tiempo, produciendo la precipitación del HDL [62].
- Ultrasonidos: este método de síntesis está basado en la aplicación de ultrasonidos a una disolución acuosa de las sales metálicas y los aniones deseados. Los efectos producidos por los ultrasonidos son derivados de la creación, expansión y destrucción de burbujas pequeñas que aparecen cuando un líquido es sometido a ultrasonidos. Este fenómeno es conocido como cavitación [63].
- Microondas: consiste en la aplicación de radiación de microondas durante el proceso de síntesis del HDL, acelerando los pasos de crecimiento y envejecimiento del sólido. La irradiación de microondas da como resultado materiales de elevada cristalinidad y aporta ciertas variaciones en las propiedades físico-químicos del HDL [60].

Los métodos de síntesis empleados en esta tesis doctoral han sido el método de coprecipitación, precipitación homogénea, sol-gel y reconstrucción. Se han usado tratamientos asistidos por microondas y agentes directores de estructura en algunos de estos procesos de síntesis. Por esta razón, a continuación, profundizaremos en estos métodos.

I.6.1 Síntesis por coprecipitación

Como decíamos anteriormente, de todos los métodos de síntesis de hidróxidos dobles laminares, el más comúnmente utilizado es el método de coprecipitación. Frecuentemente es utilizado para la síntesis de HDLs a gran escala. Se utilizan como precursores las disoluciones acuosas de M^{2+} (o mezclas metálicas de M^{2+}) y M^{3+} (o mezclas), que se adicionan a una disolución acuosa que contiene el anión que se quiere incorporar al HDL. Cuando el anión que se quiere incorporar coincide con el anión de las sales metálicas la adición se realiza directamente sobre agua al pH deseado.

Para garantizar la precipitación simultánea de dos o más cationes es necesario trabajar en condiciones de supersaturación. Normalmente, las condiciones de supersaturación se consiguen a través del control del pH en la disolución. Los dos métodos de coprecipitación más utilizados son la precipitación a baja supersaturación y precipitación a alta supersaturación. El primero de ellos ha sido el empleado en esta tesis doctoral, ya que se conduce a materiales de una elevada cristalinidad y relación metálica cercana a la teórica.

En las condiciones comúnmente empleadas en el método de precipitación a baja supersaturación el pH varía entre 7-11, la temperatura entre 50-80 °C y la concentración metálica es baja [7].

Para la síntesis de HDLs de Mg/Al por el método de coprecipitación se realiza una adición lenta de una disolución de las sales metálicas de $Mg(NO_3)_2{\cdot}6H_2O$ y $Al(NO_3)_3{\cdot}9H_2O$ (relación Mg/Al=2) a un reactor con 500 ml de agua bidestilada y desionizada con agitación vigorosa. Los HDLs tienen una elevada afinidad por los aniones carbonato y, por lo tanto, la síntesis se lleva a cabo con una atmósfera de nitrógeno para evitar la absorción del dióxido de carbono atmosférico que generaría iones carbonato in situ.

Para mantener el pH ajustado a 10, se adiciona de manera controlada una disolución acuosa de NaOH 2M [64,65].

Una vez finalizado el proceso de adición de las sales metálicas, el contenido del reactor se mantiene en agitación a una temperatura de 80 °C durante 24 h. Esta etapa de envejecimiento puede ser también realizada mediante un tratamiento asistido por microondas, introduciendo el reactor en un horno microondas. En la figura 7 se muestra el microondas empleado.

Figura 7. Envejecimiento de un HDL asistido por microondas

Transcurrido este tiempo de envejecimiento, el reactor se deja enfriar para ser filtrado y lavado con abundante agua destilada. Finalmente, el sólido obtenido es secado en estufa a 110 °C. La figura 8 muestra de forma esquemática los pasos seguidos en el proceso de síntesis aplicado.

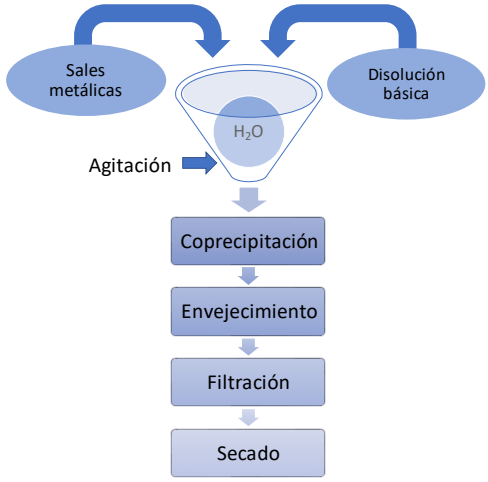

Figura 8. Etapas del procedimiento de síntesis

Los principales factores que deben ser considerados en la síntesis de los HDLs son la naturaleza de los cationes, relación molar, naturaleza de los aniones, pH, temperatura, tipo de envejecimiento y método de coprecipitación (alta o a baja supersaturación). Se ha demostrado que este método de síntesis proporciona al HDL interesantes propiedades, tales como una elevada cristalinidad, tamaños de partícula pequeños, elevada área superficial y diámetro de poro medio-alto [66].

I.6.2 Síntesis por precipitación homogénea

En el método por coprecipitación, la supersaturación del agente precipitante utilizando un medio alcalino fuerte se alcanza rápidamente y se mantiene constante una vez obtenido el pH óptimo. Esto provoca la nucleación continua de los hidróxidos dobles junto al crecimiento de las láminas de forma rápida, resultando una amplia distribución del tamaño de partícula. Al utilizar un retardante como la urea, la etapa de nucleación es independiente del crecimiento y envejecimiento desde el principio [60].

La hidrólisis de la urea permite alcalinizar soluciones de forma lenta y homogénea, lo que facilita el control de las condiciones de precipitación. Este procedimiento es el método de (co)precipitación en fase homogénea más utilizado, permitiendo la obtención de excelentes resultados en la síntesis de hidróxidos, oxohidróxidos, óxidos, hidróxidos mixtos, entre otros.

El método de precipitación homogénea consiste en la disolución de las sales metálicas, en nuestro caso $Mg(NO_3)_2{\cdot}6H_2O$ y $Al(NO_3)_3{\cdot}9H_2O$ en una relación del metal divalente con respecto al metal trivalente de 2 (Mg/Al=2), en el interior de un reactor a una temperatura de 80 °C. A dicha disolución se le añade una cierta cantidad de urea sólida en proporción 10:1 con respecto al metal divalente. A continuación, el reactor es acoplado a un sistema de reflujo o introducido en un reactor de microondas [67,68]. Transcurrido este tiempo, el reactor se deja enfriar y el contenido del mismo se filtra y lava con abundante agua destilada. Finalmente, el sólido obtenido es secado en estufa a 110 °C.

El método de precipitación homogénea asistido por microondas es similar al anterior, con la diferencia de que ahora los reactores son sometidos a una radiación de microondas durante un tiempo determinado y a una temperatura de 80 °C. El control de temperatura se realiza mediante un termopar integrado. El dispositivo experimental se muestra en la figura 9.

Figura 9. Síntesis por el método de precipitación homogénea asistida por microondas

La presencia de urea sólida en el reactor (figura 10), evita el proceso de adición de una disolución alcalina a la disolución metálica, debido a que su descomposición al ir disolviéndose aporta el medio básico.

Entre los 70 y 90 °C, la reacción de descomposición de la urea ocurre en dos etapas:

Formación reversible de cianato de amonio

$$OC(NH_2)_2 \rightleftharpoons OCN^- + NH_4^+$$

Hidrólisis irreversible de los iones cianato

$$OCN^- + 2H_2O + H^+ \rightarrow NH_4^+ + HCO_3^-$$

$$HCO_3^- \rightleftharpoons CO_3^{=} + H^+$$

En condiciones hidrotermales, la cinética de hidrólisis de la urea puede describirse como dos pasos irreversibles sucesivos e independientes del pH [69].

El valor de pH máximo es alcanzado a los pocos segundos de síntesis, como pudo demostrar en sus investigaciones Thomas Brill [70].

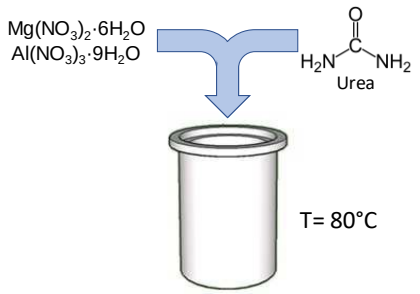

Figura 10. Esquema del reactor de síntesis para el método de la urea

Por todo ello, podemos decir que la síntesis mediante el método de precipitación homogénea con urea es eficiente en la síntesis de HDLs con una elevada cristalinidad [71]. A su vez, la presencia de aniones carbonato en la descomposición de la urea proporciona HDLs con este anión en su región interlaminar.

I.6.4 Síntesis por el método sol-gel

Para llevar a cabo la síntesis de un HDL mediante el método sol-gel se requiere la hidrolisis de sus precursores en una secuencia adecuada. La hidrólisis del precursor se realiza en presencia de ácido, normalmente HCl, permitiendo un control de la velocidad y de la extensión de la reacción.

La síntesis de los HDLs se realiza disolviendo etóxido de magnesio en etanol con una pequeña cantidad de HCl acuoso para obtener un pH de 3 que favorezca la formación de una suspensión coloidal (sol). El sol está formado por pequeñas partículas suspendidas en el disolvente por el movimiento Browniano, donde las interacciones son atribuidas a fuerzas de corto alcance (Van der Waals) y a las cargas superficiales. Esta disolución es sometida a reflujo durante tres horas. A continuación, se añade una disolución con la sal o sales del otro u otros metales que forman el HDL. La disolución resultante es ajustada a pH 10 utilizando amoniaco y calentada a reflujo favoreciendo la formación de un gel. El gel es una red molecular en una fase liquida continua formado por dos fases, donde la fase sólida es una red que atrapa e inmoviliza la fase líquida.

El gel es aislado mediante centrifugación, lavado con agua destilada y secado en estufa a 100 °C. Finalmente, los HDLs obtenidos son intercambiados con carbonato obteniendo una composición aniónica homogénea. El procedimiento de intercambio se llevó a cabo suspendiendo 1 gramo del HDL en una disolución acuosa con 0.345 g de Na_2CO_3. Dicho intercambio fue realizado a 100 °C durante 2 h en agitación vigorosa. Una vez finalizado el proceso de intercambio el HDL se filtró, lavó y secó a una temperatura de 80 °C.

I.6.4 Síntesis por reconstrucción

El método de reconstrucción o rehidratación se basa en la propiedad de "efecto memoria" que poseen los óxidos mixtos procedentes de la calcinación de los HDLs. Estos óxidos mixtos formados se pueden rehidratar en una disolución acuosa con aniones pudiendo recuperar la estructura tipo brucita [72]. El agua se absorbe reconstruyendo las láminas hidroxílicas, incorporándose los nuevos aniones y el agua a la región interlaminar [73].

Actualmente, se están realizando muchas investigaciones empleando el método de reconstrucción [74,75] de HDLs procedentes de óxidos mixtos en la descontaminación de compuestos de aguas conteniendo aniónicos inorgánicos y orgánicos. Algunos ejemplos de esto se presentan en la tabla 2,

***Tabla 2**. Compuestos aniónicos inorgánicos y orgánicos capturados por HDLs mediante el proceso de rehidratación*

Contaminante	Origen	Efectos
Ion arseniato [76] **(AsO_4^{3-})**	Insecticida	Reemplaza el fosfato inorgánico en la glucólisis, como resultado, provoca la perdida de ATP
Ion antimoniato [77] **($Sb(OH)_6^-$)**	Minería e industrial	Metaloide cancerígeno, el cual es fácilmente absorbido por las raíces de las plantas
Ion molibdato [78] **(SbO_4^{2-})**	Metalurgia y minería	Formación de complejos de Mo, los cuales afectan a procesos metabólicos
Ion seleniato [79] **(SeO_3^{2-}; SeO_4^{2-})**	Industrial y suelo	Elevada toxicidad para el ser humano y medio ambiente a elevadas concentraciones
Ion cromato [80] **($Cr_2O_7^{2-}$)**	Industrial	Elevada toxicidad provocando dermatitis cutánea, daño hepático y carcinogenicidad
Ion yoduro [81] **(I^-)**	Residuos radiactivos	Fácil adsorción por el ser humano generando una elevada toxicidad radiactiva

Ion Bromato [82] **(BrO_3^-)**	Purificación del agua	Esta considerado un carcinógeno potencial de difícil eliminación del cuerpo humano
Ion nitrato [83] **(NO_3^-)**	Fertilizantes y abonos	Formación de nitrosaminas cancerígenas, así como problemas de diabetes
Ion Tecnecio [84] **(TcO_4^-)**	Desechos radiactivos	Compuesto de larga vida y muy soluble, el cual no puede ser remedido por los materiales geológicos
Ion Renato [85] **(ReO_4^-)**	Desechos radiactivos	Anión homólogo al ion tecnecio, el cual posee una larga vida y elevada reactividad
Tereftalato (TA) [86]	Fabricación poliéster	Las aguas residuales generadas son ricas en ácido tereftálico, el cual provoca la inhibición de procesos biológicos
Sulfametoxanol [87] **(SMX)**	Industria farmacéutica	Incidencia relativamente alta de resistencia bacteriana a este antibiótico
Dicamba [88]	Pesticidas	Debido a su elevada solubilidad es lixiviado en regiones de cultivo, contaminando las aguas subterráneas
Rojo Congo (CR) [89]	Industria textil	Elevada toxicidad, carcinogenicidad, mutagenicidad y deficiente degradación
Carmín de Índigo [90]	Industria textil	Provoca coloración del agua afectando a sus actividades fotoquímicas
Azul brillante R [91]	Industria textil	Tóxico para muchos microorganismos, causando la destrucción e inhibición de sus capacidades catalíticas

En esta tesis doctoral, nos hemos centrado en el anión cianuro como potencial contaminante del agua. La presencia de aniones cianuro en el agua suele indicar una contaminación de tipo industrial, procedente en la mayoría de los casos de la metalurgia, sobre todo del sector de la joyería, muy abundante en Córdoba y también de instalaciones de tratamiento de materiales metálicos. El cianuro posee una elevada toxicidad por lo que hay que controlar sus vertidos al medio ambiente [92].

En la actualidad, existen diversos métodos para la eliminación del ion cianuro de efluentes industriales. Generalmente se elimina del agua mediante cloración alcalina, pero también se puede eliminar mediante el uso de otros oxidantes químicos [93]. Otras técnicas alternativas son la oxidación fotocatalítica [94], la biorremediación enzimática [95] y la tecnología ómica (cianómica) [96]. En esta tesis doctoral se ha empleado el uso del método de reconstrucción de HDLs de

Mg/Al para la eliminación de aniones cianuro del agua. Este punto se abordará con más detalle en el capítulo III.

I.6.4. Síntesis empelando agentes directores de estructura.

En la actualidad, se están realizando nuevas investigaciones relacionadas con el uso de agentes directores de estructura o "templates" en la síntesis de HLDs. El uso de estos agentes proporciona a los HDLs nuevas propiedades, tales como una estructura mesoporosa jerarquizada y una elevada superficie específica.

El papel que juegan estos "templates" en la síntesis de materiales, afecta principalmente a los procesos de cristalización. Es bien conocido el uso de agentes directores de estructura para la síntesis de materiales tales como M41S [97], PMOs [98], carbón mesoporoso [99], etc, pero en el caso de los HDLs no está aclarado su papel [100]. Por ello, lo hemos abordado en el capítulo V de esta tesis doctoral.

El uso de agentes directores de estructura permite controlar la estructura porosa y el área superficial de los HDLs. Se han realizado diversas investigaciones usando partículas "templates" de poliestireno [101] o micelas de copolímeros de bloque [98] (como el Pluronic F-127 [102] y Pluronic 123 [100]). Dichos "templates" poseen la característica de ser no iónicos. La utilización de compuestos iónicos en la síntesis de HDLs provocaría un efecto competitivo con el precursor en la incorporación en la región interlaminar.

Como ha sido mencionado, en la síntesis del HDL el control del pH es vital, por ello no se puede utilizar cualquier agente director de estructura. Así, nos centraremos en el Pluronic 123 (P123), un tensoactivo no iónico ampliamente utilizado en la formación de compuestos mesoporosos.

La síntesis ha sido realizada utilizando el método de coprecipitación anteriormente explicado, pero añadiendo un 2% en peso de Pluronic-123 al reactor que contiene los 500 ml de agua bidestilada y desionizada.

El P123 es un copolímero simétrico formado por el polietilenglicol (PEO) y el polipropilenglicol (PPO). Su estructura es a base de bloques donde podemos encontrarlo como PEO-PPO-PEO (figura 11).

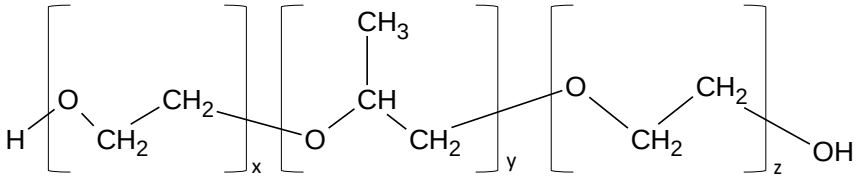

Figura 11. Estructura polimérica del Pluronic 123

I.7. CARACTERIZACIÓN DE HIDRÓXIDOS DOBLES LAMINARES

Las principales técnicas de caracterización utilizadas para la determinación de la composición, propiedades estructurales y texturales, morfológicas y físico-químicas de los hidróxidos dobles laminares se muestran en la tabla 1.

Tabla 1. *Técnicas de caracterización comunes usadas para la determinación estructural de los HDLs*

TÉCNICA DE CARACTERIZACIÓN	OBJETIVO
Acoplamiento de plasma inductivo-espectroscopía de masas	Análisis elemental y relación metálica
Fluorescencia de Rayos X	
Difracción de Rayos X	Caracterización estructural
Espectroscopia Infrarroja y Raman	Caracterización del anión interlaminar y estudio de los grupos hidroxilo de las láminas de tipo brucita
Resonancia Magnética Nuclear	Caracterización del entorno catiónico y aniónico
ATG/ATD	Cuantificación de la cantidad de agua en el sólido, anión interlaminar y cambios de fase
Porosimetría de adsorción-desorción de nitrógeno	Determinación de las propiedades texturales
Microscopía electrónica de barrido	Caracterización morfológica
Microscopía electrónica de transición	
Desorción a temperatura programada	Determinación de las propiedades químico-superficiales

I.7.1 Determinación de la relación metálica.

La determinación de la relación metálica en un HDL se realiza a partir de los datos obtenidos tras la cuantificación de los metales que lo forman. Esta cuantificación se puede realizar empleando diferentes técnicas instrumentales como el acoplamiento de plasma inductivo-espectrometría de masas (ICP-MS), la espectroscopia de fluorescencia de rayos X (XRF) o la espectroscopía de absorción atómica (AAS). En este trabajo hemos empleado tanto la ICP-MS como la XRF. Con

ambas técnicas se obtienen resultados similares y la diferencia fundamental es que con la segunda la muestra puede ser recuperada.

En la ICP-MS es necesario realizar una digestión, normalmente con ácido nítrico, para oxidar los metales presentes en la misma, para posteriormente se ionizados por un plasma de argón acoplado inductivamente para su posterior separación y detección mediante espectrometría de masas.

A diferencia de la anterior, en la XRF utilizamos la muestra sin necesidad de tratamiento previo. La muestra es "bombardeada" con rayos X de alta energía o rayos gamma excitando la muestra, para posteriormente emitir rayos X secundarios característicos del material.

I.7.2 Caracterización Estructural de los HDLs.

La difracción de rayos X (XRD) es la técnica principal en la caracterización estructural de HDLs. Esta técnica no destructiva proporciona información sobre la estructura cristalina del material y permite determinar los parámetros de red.

En la difracción de Rayos X se hace incidir un haz de rayos X sobre una muestra en polvo pulverizada y extendida de forma plana y uniforme sobre un portamuestras. La XRD puede interpretarse mediante un modelo de reflexiones de fotones por los planos cristalográficos del material (figura 12).

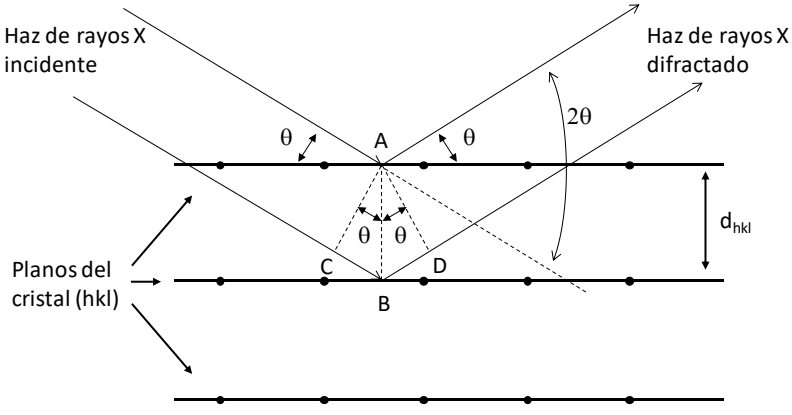

Figura 12. Esquema del proceso de difracción

La condición para que los haces reflejados se encuentren en fase viene dada por la ley de Bragg:

$$n \cdot \lambda = 2 \cdot d \cdot \operatorname{sen} \theta$$

donde λ es la longitud de onda de la radiación incidente, d es el espaciado entre los planos cristalográficos, n un número entero y θ es el ángulo que forma el haz incidente y el plano de reflexión.

La figura 13 muestra un difractograma típico de un hidróxido doble laminar de Mg/Al con anión carbonato en su región interlaminar. Presenta en su perfil líneas estrechas e intensas a valores de 2θ bajos y líneas menos intensas generalmente asimétricas a valores angulares mayores.

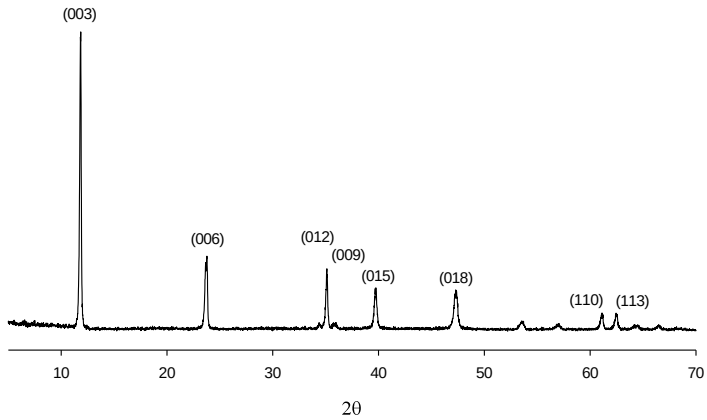

Figura 13. Difractograma de rayos X típico de un HDL de Mg/Al

El análisis por difracción de rayos X permite diferenciar entre reflexiones basales (00l) (bandas intensas y estrechas a bajos valores de d) y reflexiones no basales. Mediante el análisis de un XRD podemos obtener información sobre:

- Las reflexiones basales correspondientes a sucesivos órdenes del espaciado basal c´, que representa la distancia entre dos láminas de un HDL medida desde el centro de una lámina, es decir sería la distancia interlaminar más el grosor de una lámina.

- La reflexión (110) puede emplearse para calcular el parámetro a ($a=2d_{(110)}$). El parámetro a se puede asimilar a la distancia entre dos cationes contiguos en una lámina del HDL.
- El parámetro c ($c=3c'$) dependerá del tipo de anión, valor de x y grado de hidratación y es el triple de la distancia interlaminar.

En el caso de existir más de un anión en la región interlaminar, se apreciarían varias reflexiones basales o un espaciado basal en una fase interestratificada con secuencias alternativas de láminas combinadas [40].

I.7.3. Técnicas espectroscópicas en la caracterización de los HDLs

En la actualidad, para la caracterización de los HDLs se emplean diferentes técnicas espectroscópicas, incluyendo la espectroscopia infrarroja con transformada de Fourier (FT-IR) [7], la espectroscopia Raman [103] y la resonancia magnética nuclear de estado sólido (MAS-NMR) [98].

Las dos primeras se emplean, básicamente, para la determinación del anión interlaminar y el estudio de los grupos hidroxilos de las láminas de tipo brucita y del agua interlaminar. La MAS-NMR tiene aplicaciones más concretas para el estudio del entorno molecular de los diferentes núcleos que conforman el HDL. En este trabajo hemos empleado la espectroscopia infrarroja con transformada de Fourier (FT-IR) y la espectroscopia Raman.

La FT-IR es una técnica basada en la absorción de radiación infrarroja por los enlaces de una molécula, en la que los electrones son excitados hasta niveles vibracionales superiores. Cada tipo de enlace absorbe radiación a una frecuencia distinta, lo que permite determinar los grupos funcionales de la molécula estudiada.

El análisis por FT-IR ha sido usado para la identificación de los aniones interlaminares y los grupos hidroxilos procedentes de la estructura tipo brucita. En los HDLs podemos asignar un conjunto de bandas características. La figura 14 muestra el espectro FT-IR de un HDL con anión nitrato en su región interlaminar. Todos los HDLs presentan una absorción ancha entre 2800-3700 cm^{-1} atribuida a

las vibraciones de tensión de los O-H de los grupos hidroxilos de las láminas tipo brucita y del agua interlaminar. Sobre los 1600 cm^{-1} aparece una banda asignada a la vibración de deformación del agua. En la zona de 1000-1800 cm^{-1} se encuentran las bandas vibracionales de los aniones y finalmente a valores inferiores a los 1000 cm^{-1} aparecen varias bandas relacionadas con las vibraciones catión-oxígeno.

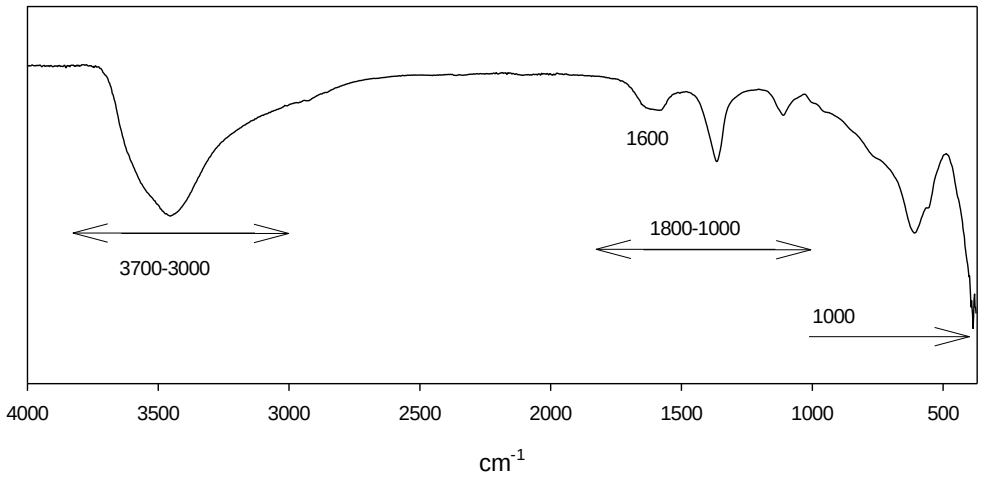

Figura 14. Espectro FT-IR típico de un HDL

La espectroscopia Raman es una técnica basada en los efectos de interacción de la luz con una muestra. El "efecto Raman" se produce cuando un haz de luz láser monocromática incide en una muestra y es dispersada inelásticamente. Esta radiación dispersada ofrece información sobre las vibraciones de los enlaces atómicos en las moléculas de la muestra excitada por la energía de la luz incidente.

La figura 15 muestra el espectro Raman de un HDL con anión nitrato en su región interlaminar. La banda a 557 cm^{-1} se asigna a las vibraciones de red de las láminas octaédricas de tipo brucita, Al-O-Mg, la cual aparece en todos los HDLs de MgAl [103]. Las bandas correspondientes a 1055 y 710 cm^{-1} han sido asignadas a las vibraciones del anión nitrato [104]. Finalmente, se observan unas bandas intensas y anchas alrededor de 3500 cm^{-1}, asignadas a las vibraciones características de los grupos O-H.

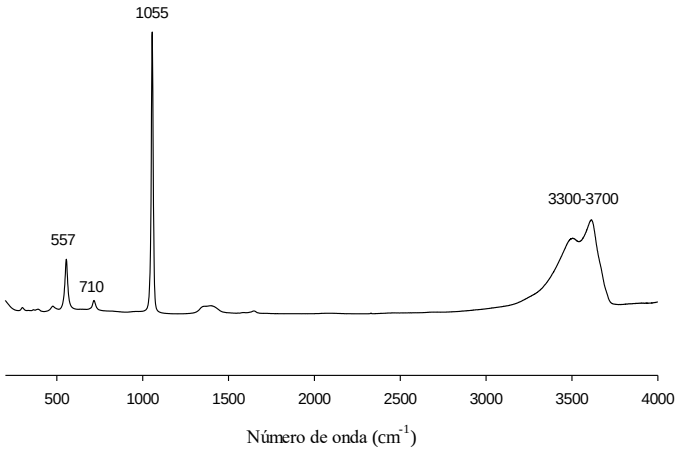

Figura 15. Espectro Raman típico de un HDL de Mg/Al con nitrato

I.7.4 Análisis termogravimétrico / análisis térmico diferencial (ATG/ATD)

El análisis térmico consiste en el estudio de las variaciones provocadas en las propiedades (físicas y/o químicas) de una muestra mientras es sometida a una variación de temperatura controlada. Esta técnica se ha empleado principalmente para determinar la cantidad de agua de cristalización y la cantidad de aniones en los HDLs.

La figura 16 muestra una curva ATG/ATD típica de un HDL de relación Mg/Al=2 con carbonato como anión en la región interlaminar. En la curva ATG/ATD se observan tres etapas comprendidas entre 30-250 °C, 250-500°C y T>500 °C, atribuidas a la pérdida de agua interlaminar, de los grupos hidroxilos estructurales y carbonato interlaminar, respectivamente.

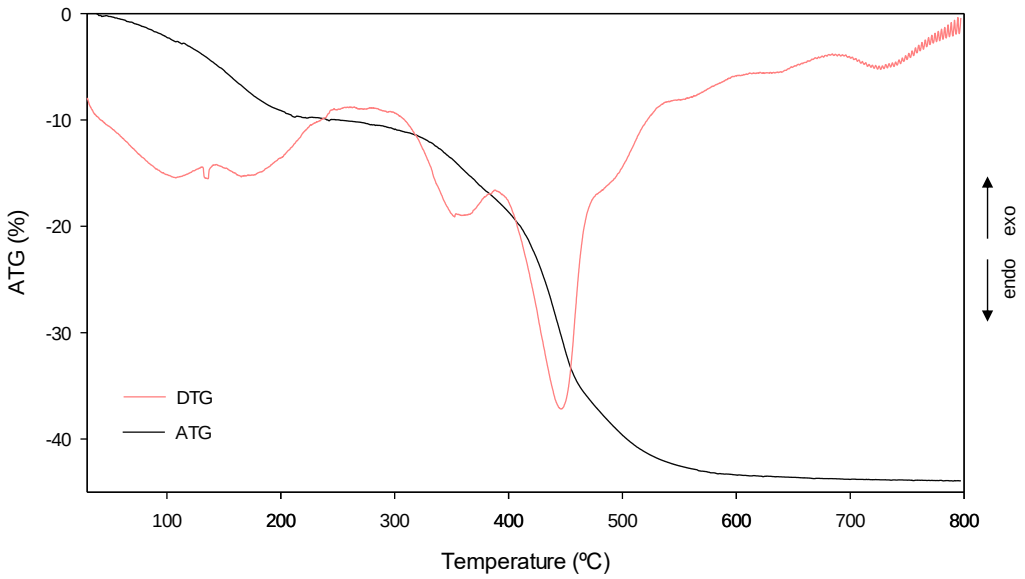

Figura 16. Curvas ATG/ATD para un HDL de Mg/Al con carbonato

En la primera etapa (hasta los 250 °C) se aprecia sobre 100 °C un pequeño hombro correspondientes a la eliminación del agua fisisorbida en el material. La eliminación de las moléculas de agua interlaminar es la responsable de la pérdida de peso producida sobre los 250 °C.

En la segunda etapa, a temperaturas cercanas a los 300 °C, se forma la fase totalmente deshidratada, provocando una disminución del espaciado interlaminar para "reacomodar" al anión carbonato. Para ello se requiere la sustitución de los grupos hidroxilos (originales del HDL) por grupos O^- (de los iones carbonato) en los vértices de algunos octaedros $M(OH)_6$ de las láminas, acortando la distancia entre ellas. Entre los 450 y 500 °C se lleva a cabo la descarbonatación y deshidroxilación de las láminas.

En la tercera etapa, a partir de los 500 °C se produce una pequeña pérdida de peso correspondiente a procesos de deshidroxilación de los óxidos mixtos formados, conduciendo a la formación de fases espinela.

Finalmente, el análisis térmico diferencial (ATD) proporciona información sobre el tipo de transformación provocada durante el tratamiento térmico, ya sea exotérmico o endotérmico [105].

I.7.5 Determinación de las propiedades texturales

La porosimetría de adsorción-desorción de nitrógeno determina la superficie específica (S_{BET}), volumen acumulado de poro (V_p), diámetro de poro (d_p) y la función de tamaño y distribución de poros de un material. La adsorción física es un fenómeno superficial por el que un líquido o un gas (adsorbato, normalmente nitrógeno) se acumula en la superficie de un sólido (adsorbente, en nuestro caso, el HDL). Dependiendo del tipo de adsorción podemos agrupar las isotermas en seis grupos siguiendo la clasificación de la IUPAC [60,106].

El resultado del análisis mediante porosimetría de adsorción-desorción de nitrógeno de un HDL es una isoterma de adsorción-desorción (figura 17), donde se representa la cantidad de gas adsorbido en función de la presión relativa (P/P_0) en el intervalo $0<P/P_0<1$, siendo P, la presión de vapor de equilibrio del adsorbato y P_0, la presión de vapor de adsorbato líquido puro [7].

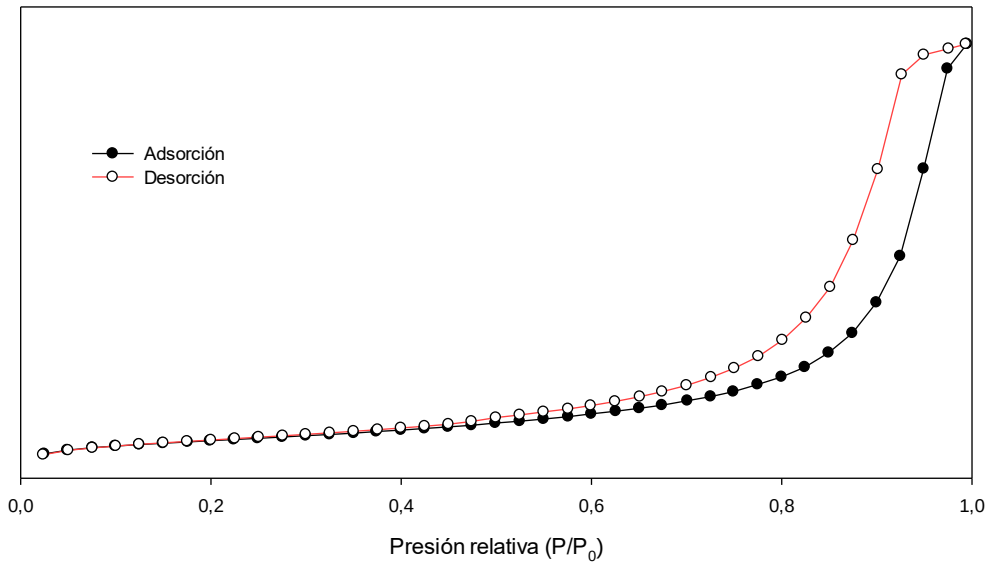

Figura 17. Isoterma de adsorción-desorción de un HDL

I.7.6 Determinación de la morfología.

Existen diversas técnicas de caracterización para determinar la morfología de un HDL. Las técnicas de microscopía electrónica se basan en la interacción de un haz de electrones de alta energía para generar una imagen. Entre las técnicas de microscopía electrónica más utilizadas podemos encontrar la microscopía electrónica de barrido (SEM) y la microscopía electrónica de transmisión (TEM).

Mediante un microscopio electrónico de barrido (SEM) se puede reconocer la superficie de un sólido mediante un rastreo programado con un haz de electrones de alta energía. Esta técnica nos permite observar y estudiar la superficie de sólidos deshidratados y eléctricamente conductores. En muestras poco conductoras es necesario realizar un pretratamiento de las mismas basado en un recubrimiento del material con metales conductores (Au, Pt o C) [64].

La microscopía electrónica de transmisión (TEM) se utiliza ampliamente como técnica de caracterización para obtener información acerca de la microestructura, morfología y distribución de tamaño de las partículas obtenidas. Esta técnica se fundamenta en la formación de una imagen mediante el uso de lentes, utilizando un haz de electrones en lugar de luz como fuente de iluminación. Una vez que el haz atraviesa la muestra, una lente objetivo forma la imagen, que a su vez es amplificada y proyectada por un conjunto de lentes proyectoras [64].

I.7.6. Determinación de las propiedades químico-superficiales.

Los hidróxidos dobles laminares, tras la calcinación, se transforman en óxidos mixtos con propiedades químico-superficiales de gran interés. Estas nuevas propiedades pueden ser medidas mediante quimisorción (etapa esencial en los procesos catalíticos), donde la molécula adsorbida forma un complejo intermedio superficial susceptible de dar una reacción química. Los análisis de quimisorción se aplican para determinar la eficiencia relativa del catalizador en la promoción de una reacción en particular. Permiten estudiar el envenenamiento de catalizadores y controlar la pérdida de la actividad catalítica con el tiempo de uso. Las técnicas de quimisorción a temperatura programada estudian el efecto de la temperatura

sobre la superficie de reacción, basadas en los centros ácidos o básicos propios de los metales que los componen.

Mediante la desorción a temperatura programada de CO_2 (TPD) podemos obtener información sobre la basicidad superficial del material, así como la fortaleza y distribución de los centros básicos. La caracterización de los centros básicos de un oxido mixto procedente de la calcinación de un HDL se lleva a cabo mediante la quimisorción de una mezcla gaseosa de Ar/CO_2 [107].

La figura 18 muestra un perfil TPD de un óxido mixto procedente de la calcinación de un HDL de Mg/Al [108]. Generalmente, el perfil TPD-CO_2 de los óxidos mixtos presenta tres tipos de centros básicos activos: Centros básicos de fortaleza débil (grupos OH- de la superficie), centros básicos de fortaleza media (grupos Mg^{2+}-O^{2-} y Al^{3+}-O^{2-}) y centros básicos de fortaleza fuerte (aniones O^{2-}) [108].

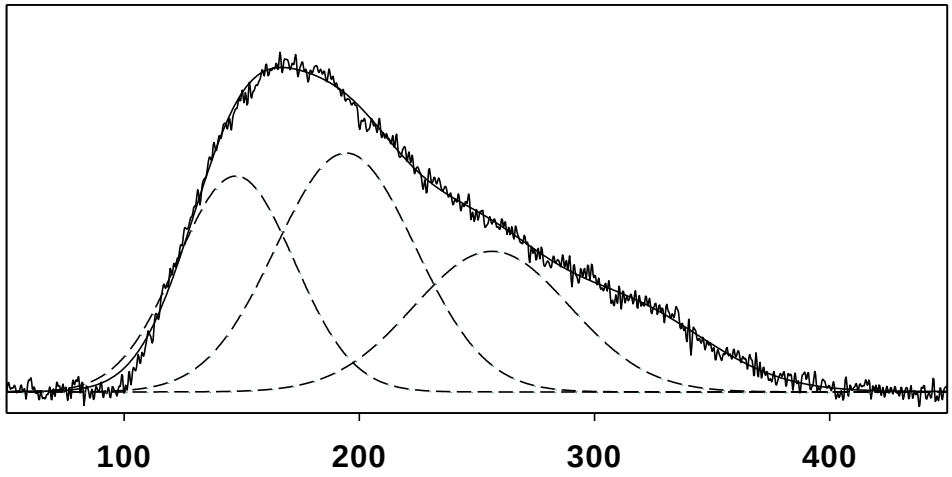

Figura 18. Perfil TPD-CO^2 de un óxido mixto de Mg/Al

I.8. APLICACIONES DE LOS HIDRÓXIDOS DOBLES LAMINARES

Desde los años 70 del siglo pasado, la aplicación a nivel industrial de los hidróxidos dobles laminares ha ido en auge, sobre todo en su empleo como catalizadores para reacciones de hidrogenación [109]. En la actualidad, los HDLs y sus productos de calcinación presentan diversas aplicaciones en distintos ámbitos científicos y/o industriales, tal y como se recoge en la figura 19.

Figura 19. Principales aplicaciones de los HDLs

Una de las ventajas más importantes de los HDLs radica en la modificación de sus propiedades físico-químicas adquiridas al variar su composición y metodología de síntesis. Esto permite obtener materiales que pueden ser utilizados en multitud de aplicaciones.

I.8.1. Adsorbente de sustancias contaminantes

El medio ambiente engloba a todos los seres vivos de nuestro planeta [110]. El efecto que ejerce sobre él la contaminación es debido a la presencia de sustancias o formas de energía no deseables en concentraciones que afecten a la salud y bienestar de las personas, animales y/o plantas.

Los contaminantes pueden tener un origen natural o antropogénico. Este segundo puede originarse en fuentes estacionarias o en fuentes móviles. Los contaminantes emitidos directamente por ambas fuentes de manera continua pueden tener una naturaleza muy amplia, provocando la contaminación del agua, aire y suelo. De esta forma, encontramos contaminantes de naturaleza física, química [111] (inorgánicos y/o orgánicos) y biológicos [110] (nutrientes, fármacos, microorganismos, entre otros).

Si nos centramos en la contaminación hídrica, podemos decir que procede mayoritariamente de instalaciones industriales y de actividades agrarias y/o

ganaderas. El desarrollo industrial genera toneladas de agua residual, haciendo necesario la descontaminación de esta para su posterior incorporación al medio ambiente. Muchos compuestos químicos orgánicos e inorgánicos identificados en aguas residuales industriales son objeto de una regulación referente a su toxicidad o a sus efectos a largo plazo en el medio ambiente [112].

Debido a las propiedades de reconstrucción e intercambio aniónico de los HDLs, se posicionan como potenciales adsorbentes para la eliminación de contaminantes aniónicos inorgánicos y orgánicos del agua [113–115].

Por ello, se han realizado multitud de estudios basados en el uso de HDLs para la adsorción de contaminantes aniónicos del agua, ya que proseen una elevada capacidad de adsorción. Existe una amplia variedad de contaminantes aniónicos estudiados [116] como son los haluros [117], oxoaniones no metálicos [118], aniones oxometalatos [119], complejos aniónicos de metales de transición [120] y otros muchos de naturaleza orgánica. En la tabla 3 se muestran algunos de estos estudios realizados descritos en la literatura.

Tabla 3*. Compuestos aniónicos inorgánicos y orgánicos adsorbidos por HDLs mediante el proceso de intercambio iónico*

Contaminante	Origen	Efectos
Ion Fluoruro [121] **(F^-)**	Industrial	Provoca enfermedades óseas y moteado dental
Ion Cloruro [122] **(Cl^-)**	Vertederos	Corrosión de las tuberías de desagüe, y efectos perjudiciales al cultivo agrícola
Ion Bromuro [123] **(Br^-)**	Áreas costeras	Peligro debido a la transformación del anión bromato (carcinogénico)
Ion perclorato [124] **(ClO_4^-)**	Pirotecnia y herbicida	Afecta a la glándula tiroides en los humanos, provocando la inhibición en la incorporación de yodo
Ion fosfato [113] **(PO_4^{3-})**	Fertilizantes y detergentes	En exceso, provoca la eutrofización de lagos, lagunas, ríos y mares
Ion cromato [125] **(CrO_4^{2-})**	Industrial	Carácter carcinogénico y elevada toxicidad
Ion Vanadato [118] **(VO_4^{3-})**	Industrial	Es acumulado en el aire, provocando bronquitis, neumonías e irritación
Polioxometalato [126] **($[PW_{12}O_{40}]^{3-}$)**	Industrial, epoxidación	El volframio está considerado como altamente tóxico con peligro de explosión e incendio

Complejos metálicos [127] **($[Ru(CN)_4L]^{2-}$)**	Electrocatálisis	Compuesto soluble, altamente tóxico y carcinógeno
Benzoato [128] **($C_6H_5COO^-$)**	Aditivo	En exceso, puede provocar dificultades respiratorias, perdida de consciencia, sangre en orina y heces
Bencenosulfonatos [129]	Uso doméstico	En elevadas concentraciones provoca efectos tóxicos por inhalación o ingestión
Azul de Bromotimol [130]	Industrial	Tinte no degradable, de naturaleza tóxica, mutagénica y carcinogénica
Naranja de metilo [131] **(MO)**	Industrial	Peligrosidad leve, generando irritación en el tracto gastrointestinal por ingestión
Polietileno sulfonado [132] **(PSS)**	Residuos farmacoquímicos	Baja toxicidad, en exceso puede provocar problema respiratorios y necrosis

I.8.2. Soporte de moléculas de interés

Los métodos de intercambio iónico y rehidratación son comúnmente usados para sintetizar nuevos HDLs. Cuando en el espacio interlaminar intercalamos compuestos orgánicos aniónicos, surgen unos nuevos materiales denominados genéricamente organo-HDLs. Algunos de estos organo-HDLs se muestran en la tabla 4.

***Tabla 4**. Nuevos órgano-HDLs y nuevas propiedades adquiridas.*

Nuevo HDL	Anión	Propiedad adquirida
LDH-Cholate [133]	Colato	Proporciona al HDL la capacidad de adsorber contaminantes emergentes del agua
ILs/LHDs [134]	Sales de amonio	Aumento de la capacidad de adsorción de colorantes reactivos
CaAl-Co (II)-His-LDH [135]	Histidina	Los HDL protegen a los aniones intercalados de la degradación fotoquímica y permiten la liberación controlada de los mismos
CaAl-Co (II)-Cys-LDH	Cisteína	
CaAl-Co (II)-Tyr-LDH	Tirosina	
S_x-LDH [136]	Polisulfuro	Los HDLs obtienen la capacidad de poder adsorber cationes de uranio, los cuales son potenciales contaminantes
Gly-LDH [137]	Glicina	Los Gly-LDH poseen una mayor selectividad y capacidad de adsorción de oxoaniones

CA/Mg-Al LDH [138]	Acetato de celulosa	Este nuevo órgano-HDL permite la eliminación de sustancias farmacéuticas de las aguas residuales
MnFe-LDH/PMS [139]	Peroximonosulfato (PMS)	Este HDL permite la activación del PMS para la degradación de contaminantes orgánicos
HT-DDS [140,141]	Dodecilsulfato	Capacidad de adsorción de hidrocarburos aromáticos policíclicos (HAP), retardante de llama
SOS-LDH [142] **SDS-LDH** **SOBS-LDH** **SDBS-LDH**	Octilsulfato Dodecilsulfato 4-octilbencenosulfonato Dodecilbencenosulfonato	Obtención de propiedades superficiales hidrofóbicas, permitiendo la adsorción de compuestos orgánicos no iónicos
SCD-LDH [143]	Ciclodextrina	Proporciona al HDL la capacidad de adsorber compuestos orgánicos no iónicos como derivados del fenol
NA-LDH-OA [144]	Oleato sódico	Conduce a un mayor almacenamiento y rápida difusión de iones por la interlámina, actuando como electrodos supercapacitores positivos
RL-LDH [145]	Bio-surfactante rhamnolipid	Mejora la sacarificación enzimática y la producción de etanol de Artemisia ordosica
Curcumin-LDH [146]	Curcumina	La combinación de la curcumina-HDL con irradiciación LED azul, podría amplificar el efecto citotóxico y proapoptótico de la curcumina
CS-LDH [147]	Quitosán	El quitosán le confiere al HDL una elevada capacidad de remoción y un proceso de adsorción rápida de Pb^{2+} y Cd^{2+} en agua
BC-LDH [148]	Biochar	El biochar confiere al HDL la capacidad de adsorber compuestos tales como fosforo (P) procedente de la producción agrícola

En esta tesis doctoral hemos aprovechado la propiedad de intercambio iónico de los HDLs para obtener nuevos materiales de esta naturaleza conteniendo aniones desoxicolato y colato en su región interlaminar. El mecanismo de intercambio ha sido realizado mediante un tratamiento asistido por microondas, permitiendo disminuir sustancialmente el tiempo necesario para el intercambio de 48h a 1h. A su vez, nuestro grupo de investigación se encuentra realizando diversas

investigaciones basadas en la adsorción de contaminantes emergentes en aguas con estos nuevos órgano-HDLs. La síntesis y caracterización de estos HDLs será detallada de manera exhaustiva en el capítulo IV.

I.8.3. Catalizadores de procesos orgánicos

Los HDLs y sus productos de calcinación se han aplicado en multitud de procesos orgánicos catalizados tanto en química fina como en química industrial [149,150]. En este apartado, únicamente vamos a hacer referencia al uso de sólidos calcinados en procesos de catálisis básica.

Existen multitud de procesos catalíticos de naturaleza básica que pueden ser realizados con óxidos mixtos obtenidos a partir de HDLs. Entre ellos podemos destacar la condensación aldólica [151,152], la condensación de Claisen-Schmidt [153] y la condensación de Knoevenagel [154]; la reducción de Meerwein-Ponndorf-Verley (MPV) [155]; la reacción de Henry [156,157]; isomerizaciones [158,159] y polimerizaciones [160], entre otras.

De todas estas reacciones, nos centraremos en la reacción de reducción de compuestos carbonílicos de Meerwein-Ponndorf-Verley (MPV). Esta reacción está basada en la transferencia de hidrógeno desde un alcohol, preferentemente secundario, hasta un compuesto carbonílico. Este es un método sencillo para la obtención de alcoholes de cualquier naturaleza. En condiciones suaves se obtiene una elevada selectividad en la reducción de los grupos carbonilos. En la figura 20 se muestra el esquema general de la reacción de MPV.

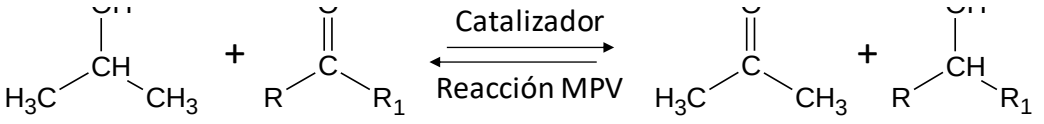

Figura 20. Reacción de Meerwein-Poondorf-Verley

Normalmente, esta reacción suele estar catalizada por un alcóxido metálico, en fase homogénea. En los últimos años, se han realizado múltiples estudios acerca del uso de catalizadores heterogéneos en la reacción de MPV. Entre ellos podemos destacar los óxidos metálicos (MgO, Al_2O_3, TiO_2, ZrO_4) [161–163], fosfatos de

magnesio [164], hidróxidos dobles laminares [165], sólidos mesoporos [166,167] y compuestos zeolíticos [168,169]. Los óxidos mixtos derivados de HDLs también se han empleado como catalizadores de esta reacción.

Concretamente, nuestro grupo de investigación posee una amplia experiencia en el uso de estos sólidos como catalizadores de la reacción de este proceso[170–178]. En el capítulo V de esta tesis doctoral empleamos óxidos mixtos procedentes de la calcinación de HDLs sintetizados por diferentes métodos de síntesis en la reacción de MPV.

Toda esta labor investigadora nos ha llevado a proponer el mecanismo de reacción mostrado en la figura 21, según el cual la transferencia de hidrógeno es producida por un proceso concertado a través de un intermedio cíclico de seis eslabones, formado por el alcohol secundario y el aldehído o cetona diana. Ambos se encuentran adsorbidos sobre un par ácido-base de la superficie del óxido mixto de magnesio y aluminio. La fortaleza del centro ácido-base es crucial para llevar a cabo dicha reacción. El paso determinante de la velocidad se encuentra en la interacción ejercida entre el alcohol con el centro ácido-base provocando su disociación al correspondiente alcóxido.

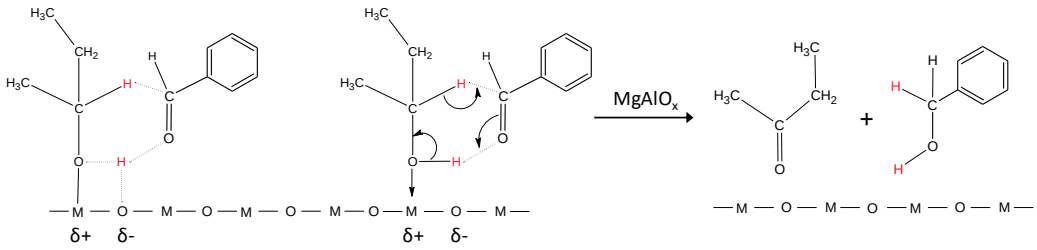

Figura 21. Mecanismo para la reacción de MPV catalizada por óxidos mixtos procedentes de la calcinación de un HDL de Mg/Al

I.8.4. Otras aplicaciones

En las dos últimas décadas, el interés por los hidróxidos dobles laminares ha aumentado sustancialmente. Esto es debido a su fácil síntesis, versatilidad en el alojamiento de iones interlaminares y las múltiples aplicaciones en diferentes ámbitos científicos [179]. Los HDLs han tenido un notable protagonismo en áreas

como ciencias de los materiales [180] e industrial [181], pudiendo actuar como electrodos [182], materiales diseñados por modelado computacional [183], fotocatalizadores [184], emisores de luz [185], sensores biológicos [186], almacenadores de energía [187], catalizadores en la producción de biodiesel [188] y retardantes de llama [189].

El uso de los HDLs en el campo de la medicina y biología ha tenido una importante repercusión en los últimos años. Dichos materiales han sido utilizados como medicamentos antiácidos debido a su inocuidad y su elevado número de grupos hidroxilos a lo largo de su estructura [190]. Actualmente, se están realizando multitud de investigaciones relacionadas con el uso de HDLs en la liberación controlada de fármacos [191], la captación celular y liberacion de genes [192], actividad antimicrobiana [193] o tratamientos contra el cáncer [194].

I.9. BIBLIOGRAFÍA

[1] W. Feitknecht, M. Gerber, Zur Kenntnis der Doppelhydroxyde und basisehen Doppelsalze, Helv. Chim. Acta, 25 (1942) 131–137.

[2] R. Allmann, The crustal structure of pyroaurite, Acta Crystallogr., B24 (1968) 972–977.

[3] L. Ingram, H.F.W. Taylor, The crystal structures of sjögrenite and pyroaurite, Mineral. Mag., 36 (1967) 465–479.

[4] F. Rutley, Mineralogy, Thomas Murby & Company, 1802.

[5] L. Pauling, The principles determining the structure of complex ionic crystals, J. Am. Chem. Soc., 51 (1929) 1010–1026.

[6] C. Klein, C.S. Hurlbut, Manual de mineralogía, Reverté, 1996.

[7] M. Mora, Utilización de soportes de Pd soportado sobre hidrotalcita en la reacción de acoplamiento cruzado de Suzuki, Tesis Doctoral, Universidad de Córdoba, 2008.

[8] M. Gastuche, G. Brown, M. Mortland, Mixed magnesium-aluminiun hydroxides. I. Preparation and characterization of compounds formed in dialysed systems, Clay Miner., 7 (1967) 177–192.

[9] A. Khan, D. O`Hara, Layered double hydroxides: Structure and Bonding, Berlín, 2006.

[10] G. Guadalupe, C. Arizaga, K.G. Satyanarayana, F. Wypych, Layered hydroxide salts : Synthesis , properties and potential applications, Solid State Ionics, 178 (2007) 1143–1162.

[11] A. Aramendıa, V. Borau, M. Marinas, M. Luque, R. Ruiz, F.J. Urbano, Synthesis and characterization of a novel Mg/In hydrotalcite-like compound, Mater. Lett., (2000) 118–121.

[12] G. Carja, R. Nakamura, T. Aida, H. Niiyama, Textural properties of layered double hydroxides : effect of magnesium substitution by copper or iron, Microporous Mesoporous Mater., 47 (2001) 275–284.

[13] Y. Minati, T. Takei, S. Yanagida, N. Kumada, Hybridization of Ni–Cr, Cu–Cr, and Zn–Cr layered double hydroxides with polyoxometalates and their catalytic behavior, J. Ceram. Soc. Japan, 125 (2017) 747–752.

[14] L. Feng, Y. Yuan, B. Dong, Y.X. Zhang, X. Liu, C. Jing, F. Dong, D. Bin Jiang, 2D-2D growth of NiFe LDH nanoflakes on montmorillonite for cationic and anionic dye adsorption performance, J. Colloid Interface Sci., 540 (2019) 398–409.

[15] J.W. Boclair, P.S. Braterman, J. Jiang, S. Lou, F. Yarberry, Layered double hydroxide stability. 2. Formation of Cr(III)-containing layered double hydroxides directly from solution, Chem. Mater., 11 (1999) 303–307.

[16] E. Zhu, X. Hong, Z. Ye, K.S. Hui, K.N. Hui, Influence of various experimental parameters on the capacitive removal of phosphate from aqueous solutions using LDHs/AC composite electrodes, Sep. Purif. Technol., 215 (2019) 454–462.

[17] M.A. Aramendia, Y. Avile, V. Borau, M. Marinas, R. Ruiz, F.J. Urbano, Comparative study of Mg/Al and Mg/Ga layered double hydroxides, Microporous Mesoporous Mater., 29 (1999) 319–328.

[18] M. Yu, H. Li, N. Du, W. Hou, Understanding Li-Al-CO3 layered double hydroxides. (I) Urea-supported hydrothermal synthesis, J. Colloid Interface Sci., 547 (2019) 183–189.

[19] J. Qu, L. Sha, Z. Xu, Z. He, M. Wu, C. Wu, Q. Zhang, Calcium chloride addition to overcome the barriers for synthesizing new Ca-Ti layered double hydroxide by mechanochemistry, Appl. Clay Sci., 173 (2019) 29–34.

[20] Z. Yan, S. Liu, Y. Zhang, T. Wang, S. Luo, W. Chu, F. Jing, The role of Zr in NiZrAl oxides catalyst and the evaluation on steam reforming of glycerol for hydrogen product, Catal. Today, 319 (2019) 229–238.

[21] Z. Gao, F. Liu, L. Wang, F. Luo, Highly efficient transfer hydrodeoxygenation of vanillin over Sn4+-induced highly dispersed Cu-based catalyst, Appl. Surf. Sci., 480 (2019) 548–556.

[22] S. Naseem, B. Gevers, R. Boldt, F.J.W.J. Labuschagné, A. Leuteritz, Comparison of transition metal (Fe, Co, Ni, Cu, and Zn) containing tri-metal layered double hydroxides (LDHs) prepared by urea hydrolysis, RSC Adv., 9 (2019) 3030–3040.

[23] D. Wang, Q. Zhu, Y. Su, J. Li, A. Wang, Z. Xing, Preparation of MgAlFe-LDHs as

a deicer corrosion inhibitor to reduce corrosion of chloride ions in deicing salts, Ecotoxicol. Environ. Saf., 174 (2019) 164–174.

[24] W.Y. Hernández, K. De Vlieger, P. Van Der Voort, A. Verberckmoes, Ni–Cu Hydrotalcite-Derived Mixed Oxides as Highly Selective and Stable Catalysts for the Synthesis of β-Branched Bioalcohols by the Guerbet Reaction, ChemSusChem, 9 (2016) 3196–3205.

[25] W. Hofmeister, H. Von Platen, Crystal chemistry and atomic order in brucite-related double-layer structures, Crystallogr. Rev., 3 (1992) 3–29.

[26] G.W. Brindley, S. Kikkawa, A crystal-chemical study of Mg , Al and Ni , N hydroxy-perchlorates and hydroxy-carbonates, Am. Mineral., 64 (1979) 836–843.

[27] A.I. Khan, D. O`Hara, Intercalation chemistry of layered double hydroxides: recent developments and applications, J. Mater. Chem., (2002) 3191–3198.

[28] R.P. Bontchev, S. Liu, J.L. Krumhansl, J. Voigt, T.M. Nenoff, Synthesis, Characterization, and Ion Exchange Properties of Hydrotalcite $Mg_6Al_2(OH)_{16}(A)_x(A')_{2-x}\cdot 4H_2O$ (A, A' = Cl^- , Br^- , I^- , and NO_3^- , $2 \geq x \geq 0$) Derivatives, Chem. Mater., 15 (2003) 3669–3675.

[29] B. Sadeghalvad, A. Azadmehr, A. Hezarkhani, A new approach to improve sulfate uptake from contaminated aqueous solution : Metal layered double hydroxides functionalized metasomatic rock, Sep. Sci. Technol., 663 (2019) 453–464.

[30] L. Alidokht, S. Oustan, A. Khataee, Removal of chromate from aqueous solution by reduction with nanoscale Fe–Al layered double hydroxide, Res. Chem. Intermed., 44 (2018) 2319–2331.

[31] J. Das, B.S. Patra, N. Baliarsingh, K.M. Parida, Adsorption of phosphate by layered double hydroxides in aqueous solutions, Appl. Clay Sci., 32 (2006) 252–260.

[32] J.W. Boclair, P.S. Braterman, B.D. Brister, Z. Wang, F. Yarberry, Physical and chemical interactions between Mg:Al layered double hydroxide and hexacyanoferrate, J. Solid State Chem., 161 (2001) 249–258.

[33] K. Inomata, M. Ogawa, Preparation and Properties of Mg/Al Layered Double

Hydroxide–Oleate and –Stearate Intercalation Compounds, Bull. Chem. Soc. Jpn., 79 (2006) 336–342.

[34] R. Tanaka, I. Ogino, S.R. Mukai, Synthesis of Mg–Al Mixed Oxides with Markedly High Surface Areas from Layered Double Hydroxides with Organic Sulfonates, ACS Omega, 3 (2018) 16916–16923.

[35] E.E. Gaskell, T. Ha, A.R. Hamilton, Ibuprofen intercalation and release from different layered double hydroxides, Ther. Delivey, 9 (2018) 653–666.

[36] H. Wang, J. Wu, L. Zheng, X. Cheng, H. Wang, J. Wu, L. Zheng, X. Cheng, Preparation and Properties of ZnAl Layered Double Hydroxide/Polycaprolactone Nanocomposites for Use in Drug Delivery Preparation and Properties of ZnAl Layered Double Hydroxide / Polycaprolactone, Polym. Plast. Technol. Eng., 00 (2018) 1–9.

[37] F. Zhu, L. Wang, S. Liao, Y. Zhu, W. Luo, X. Huang, F. Jiao, X. Chen, Applied Clay Science Co-assembly of exfoliated Mg / Al layered double hydroxides nanosheets with sulfobutyl ether- β -cyclodextrin for enantioseparation of racemic propranolol, Appl. Clay Sci., 162 (2018) 138–145.

[38] Z. Yin, K. Dideriksen, M. Abdelmoula, C. Ruby, F.M. Michel, M.J. Bjerrum, H.C.B. Hansen, Structure of single sheet iron oxides produced from surfactant interlayered green rusts, Appl. Clay Sci., 170 (2019) 86–96.

[39] D.R. Martínez, G.G. Carbajal, Hidróxidos dobles laminares: Arcillas sintéticas con aplicaciones en nanotecnología, Av. Quim., 7 (2012) 87–99.

[40] T. Hibino, Anion Selectivity of Layered Double Hydroxides: Effects of Crystallinity and Charge Density, Eur. J. Inorg. Chem., 2018 (2018) 722–730.

[41] S. Miyata, Anion-exchange propierties of hydrotalcite-like compunds, Clays Clay Miner., 31 (1983) 305–311.

[42] H. Wang, X. Liu, Y. Wu, C. Hou, Y. Qiu, K. Guo, Microwave-Assisted Synthesis of Ethylene Glycol-Intercalated NiAl LDHs and Their Application for Intracrystalline Catalytic Esterification with Naphthenic Acids in Crude Oil, Energy Fuels, 31 (2017) 9898–9904.

[43] Y. Kameshima, H. Yoshizaki, A. Nakajima, K. Okada, Preparation of sodium oleate/layered double hydroxide composites with acid-resistant properties,

298 (2006) 624–628.

[44] M. Trikeriotis, D.F. Ghanotakis, Intercalation of hydrophilic and hydrophobic antibiotics in layered double hydroxides, 332 (2007) 176–184.

[45] C. Andronescu, S.A. Garea, E. Vasile, H. Iovu, Synthesis and characterization of polybenzoxazine / layered double hydroxides nanocomposites, Compos. Sci. Technol., 95 (2014) 29–37.

[46] G. Martínez, M. a Gómez, Ciclodextrinas : Complejos De Inclusión Con Polímeros, Rev. Iberoam. Polim., 8 (2007) 300–312.

[47] W. Hu, X. Wu, F. Jiao, W. Yang, Y. Zhou, Preparation and characterization of magnetic Fe3O4@sulfonated β-cyclodextrin intercalated layered double hydroxides for methylene blue removal, Desalin. Water Treat., 57 (2016) 25830–25841.

[48] L. Qiu, W. Chen, B. Qu, Morphology and thermal stabilization mechanism of LLDPE / MMT and LLDPE / LDH nanocomposites, Polymer (Guildf)., 47 (2006) 922–930.

[49] T. Stanimirova, T. Hibino, V. Balek, Thermal behavior of Mg-Al-CO_3 Layered double hydroxide characterized by emanation thermal analysis, J. OfT Hermal Anal. Calorim., 84 (2006) 473–478.

[50] D. Madej, Examination of dehydration and dehydroxylation of synthetic layered (oxy)hydroxides through thermal analysis (TG-DSC-EGA-MS) and a discussion to the second Pauling's rule, Inorganica Chim. Acta, 482 (2018) 402–410.

[51] V. Rives, Comment on " Direct Observation of a Metastable Solid Phase of Mg/Al/CO3-Layered Double Hydroxide by Means of High-Temperature in Situ Powder XRD and DTA/TG," Inorg. Chem., (1999) 406–407.

[52] W. Kagunya, Z. Hassan, W. Jones, Catalytic Properties of Layered Double Hydroxides and Their Calcined Derivatives, Inorg. Chem., 35 (1996) 5970–5974.

[53] K.L. Erickson, T.E. Bostrom, R.L. Frost, A study of structural memory effects in synthetic hydrotalcites using environmental SEM, 59 (2005) 226–229.

[54] D. Li, M. Lu, Y. Cai, Y. Cao, Y. Zhan, L. Jiang, Synthesis of high surface area

MgAl2O4 spinel as catalyst support via layered double hydroxides-containing precursor, Appl. Clay Sci., 132–133 (2016) 243–250.

[55] F. Cavani, F. Trifirò, A. Vaccari, Hydrotalcite-type anionic clays: Preparation, properties and applications., Catal. Today, 11 (1991) 173–301.

[56] U. Costantino, F. Marmottini, M. Nocchetti, R. Vivani, New Synthetic Routes to Hydrotalcite-Like Compounds – Characterisation and Properties of the Obtained Materials, Eur. J. Inorg. Chem., 1998 (1998) 1439–1446.

[57] M. Herrero, Nanomateriales híbridos orgánicos/inorgánicos con hidróxidos dobles laminares., Salamanca, 2008.

[58] K. Chibwe, W. Jones, Intercalation of Organic and Inorganic Anions into Layered Double Hydroxides, J. Chem. Soc. Chem. Commun. Artic., 14 (1989) 926–927.

[59] J. Pérez-Ramirez, G. Mul, F. Kapteijn, J.A. Moulijn, On the stability of the thermally decomposed Co–Al hydrotalcite against retrotopotactic transformation, Mater. Res. Bull., 36 (2001) 1767–1775.

[60] C. Forano, T. Hibino, F. Leroux, Layered double hydroxide, in: Handb. Clay Sci., 2006: pp. 1021–1095.

[61] J. He, M. Wei, B. Li, D. Evans, X. Duan, Preparation of Layered Double Hydroxides, Struct. Bond., 119 (2006) 89–119.

[62] A. Fahami, F.S. Al-hazmi, A.A. Al-ghamdi, W.E. Mahmoud, G.W. Beall, Structural characterization of chlorine intercalated Mg-Al layered double hydroxides : A comparative study between mechanochemistry and hydrothermal methods, J. Alloys Compd., 683 (2016) 100–107.

[63] Q. Chang, L. Zhu, Z. Luo, M. Lei, S. Zhang, H. Tang, Sono-assisted preparation of magnetic magnesium – aluminum layered double hydroxides and their application for removing fluoride, Ultrason. - Sonochemistry, 18 (2011) 553–561.

[64] G. Mendoza Damián, Síntesis y Caracterización de Hidróxidos dobles Laminares (HDL) con adición de cationes M^{4+}, 2017.

[65] S.Y. Lee, K.-W. Jung, J.-W. Choi, Y.J. Lee, In situ synthesis of hierarchical cobalt-aluminum layered double hydroxide on boehmite surface for efficient

removal of arsenate from aqueous solutions: Effects of solution chemistry factors and sorption mechanism, Chem. Eng. J., 368 (2019) 914–923.

[66] E.L. Crepaldi, P.C. Pavan, J.B. Valim, Comparative Study of the Coprecipitation Methods for the Preparation of Layered Double Hydroxides, J. Braz. Chem. Soc., 11 (2000) 64–70.

[67] S.P. Lonkar, J.M. Raquez, P. Dubois, One-Pot Microwave-Assisted Synthesis of Graphene/Layered Double Hydroxide (LDH) Nanohybrids, Nano-Micro Lett., 7 (2015) 332–340.

[68] S. Chilukoti, T. Thangavel, Enhanced adsorption of Congo red on microwave synthesized layered Zn-Al double hydroxides and its adsorption behaviour using mixture of dyes from aqueous solution, Inorg. Chem. Commun., 100 (2019) 107–117.

[69] M. 2003 Jobbágy, Síntesis , caracterización y propiedades de hidróxidos dobles laminares, 2003.

[70] M.L. Kieke, J.W. Schoppelrei, T.B. Brill, Spectroscopy of Hydrothermal Reactions. 1. The CO_2–H_2O System and Kinetics of Urea Decomposition in an FTIR Spectroscopy Flow Reactor Cell Operable to 725 K and 335 bar, J. Phys. Chem., 100 (1996) 7455–7462.

[71] P. Yang, J. Yu, Z. Wang, Q. Liu, T. Wu, Urea method for the synthesis of hydrotalcites, React. Kinet. Catal. Lett., 83 (2004) 275–282.

[72] K. Goh, T. Lim, Z. Dong, Application of layered double hydroxides for removal of oxyanions : A review, Water Res., 42 (2008) 1343–1368.

[73] A. Chatterjee, P. Bharadiya, D. Hansora, Layered double hydroxide based bionanocomposites, Appl. Clay Sci., 177 (2019) 19–36.

[74] W.M.A. El Rouby, S.I. El-Dek, M.E. Goher, S.G. Noaemy, Efficient water decontamination using layered double hydroxide beads nanocomposites, Environ. Sci. Pollut. Res., 70 (2018) 1–19.

[75] G. Mascolo, M.C. Mascolo, On the synthesis of layered double hydroxides (LDHs) by reconstruction method based on the “memory effect,” Microporous Mesoporous Mater., 214 (2015) 246–248.

[76] X. Dai, S. Zhang, G.I.N. Waterhouse, H. Fan, S. Ai, Recyclable polyvinyl alcohol

sponge containing flower-like layered double hydroxide microspheres for efficient removal of As(V) anions and anionic dyes from water, J. Hazard. Mater., 367 (2019) 286–292.

[77] C. Ardau, F. Frau, P. Lattanzi, Antimony Removal from Aqueous Solutions by the Use of Zn-Al Sulphate Layered Double Hydroxide, Water. Air. Soil Pollut., 227 (2016) 344.

[78] C. Ardau, F. Frau, E. Dore, P. Lattanzi, Molybdate sorption by Zn-Al sulphate layered double hydroxides, Appl. Clay Sci., 65–66 (2012) 128–133.

[79] L. Constantino, J. Nunes, A. Maffei, A. Urbano, J.M. Santos, Sorption-desorption of selenite and selenate on Mg-Al layered double hydroxide in competition with nitrate , sulfate and phosphate, Chemosphere, 181 (2017) 627–634.

[80] M.A.H. Hafez, I.M.M. Kenawy, Z.M.E. Abd, R.R. Elmorsi, K.S. Abou-el-sherbini, Removal of Cr (VI) from aqueous media on calcined (Mg-Zn)/(Al-Fe)-(CO3)/Cl layered double hydroxides, Desalin. Water Treat., 148 (2019) 270–284.

[81] C. Li, Y. Wei, X. Wang, X. Yin, Efficient and rapid adsorption of iodide ion from aqueous solution by porous silica spheres loaded with calcined Mg-Al layered double hydroxide, J. Taiwan Inst. Chem. Eng., 85 (2018) 193–200.

[82] Y. Yang, Q. Ding, D. Wen, M. Yang, Y. Wang, N. Liu, X. Zhang, Bromate removal from aqueous solution with novel flower-like Mg-Al-layered double hydroxides, Environ. Sci. Pollut. Res., 25 (2018) 27503–27513.

[83] D. Ivánová, P. Albert, J. Kavuli, Applied Clay Science Nitrate removal from model aqueous solutions and real water by calcined Mg/Al layered double hydroxides, Appl. Clay Sci., 152 (2018) 65–72.

[84] M.J. Kang, K.S. Chun, S.W. Rhee, Y. Do, Comparison of Sorption Behavior of I^- and TcO_4^- on Mg/AI Layered Double Hydroxide, Radiochim. Acta, 85 (1999) 57–63.

[85] K. Tanaka, N. Kozai, T. Ohnuki, B. Grambow, Study on coordination structure of Re adsorbed on Mg–Al layered double hydroxide using X-ray absorption fine structure, J. Porous Mater., 26 (2018) 1–7.

[86] E.L. Crepaldi, J. Tronto, L.P. Cardoso, B. Valim, Sorption of terephthalate anions by calcined and uncalcined hydrotalcite-like compounds, Colloids Surfaces A Physicochem. Eng., 211 (2002) 103–114.

[87] E.H. Mourid, M. Lakraimi, L. Benaziz, E.H. Elkhattabi, A. Legrouri, Wastewater treatment test by removal of the sulfamethoxazole antibiotic by a calcined layered double hydroxide, Appl. Clay Sci., 168 (2019) 87–95.

[88] Y. You, H. Zhao, G.F. Vance, Adsorption of dicamba (3,6-dichloro-2-methoxy benzoic acid) in aqueous solution by calcined-layered double hydroxide, Appl. Clay Sci., 21 (2002) 217–226.

[89] C. Lei, M. Pi, P. Kuang, Y. Guo, F. Zhang, Organic dye removal from aqueous solutions by hierarchical calcined Ni-Fe layered double hydroxide : Isotherm , kinetic and mechanism studies, J. Colloid Interface Sci., 496 (2017) 158–166.

[90] H. Bessaha, M. Bouraada, L. Deménorval, Removal of indigo carmine and green bezanyl-F2B from water using calcined and uncalcined Zn/AlþFe layered double, J. Water Desalin., 7 (2016) 152–161.

[91] M.X. Zhu, Y.P. Li, M. Xie, H.Z. Xin, Sorption of an anionic dye by uncalcined and calcined layered double hydroxides: A case study, J. Hazard. Mater., 120 (2005) 163–171.

[92] M.J. Logsdon, K. Hagelstein, T.I. Mudder, The management of cyanide in gold extraction, Internactional council on metals and the environment, 1999.

[93] L. Seung-Mok, T. Diwakar, Application of ferrate(VI) in the treatment of industrial wastes containing metal-complexed cyanides: A green treatment, J. Environ. Sci., 21 (2009) 1347–1352.

[94] Y. Guo, Y. Wang, S. Zhao, Z. Liu, H. Chang, X. Zhao, Photocatalytic oxidation of free cyanide over graphitic carbon nitride nanosheets under visible light, Chem. Eng. J., 369 (2019) 553–562.

[95] M. Sharma, Y. Akhter, S. Chatterjee, A review on remediation of cyanide containing industrial wastes using biological systems with special reference to enzymatic degradation, World J. Microbiol. Biotechnol., 35 (2019) 1–14.

[96] V.M. Luque-Almagro, C. Moreno-Vivián, M.D. Roldán, Biodegradation of

cyanide wastes from mining and jewellery industries, Curr. Opin. Biotechnol., 38 (2016) 9–13.

[97] H. Ding, Y. Zhang, Z. Xiao, J. Zhang, P. Bai, N. Li, X. Guo, Synthesis of Hierarchically Porous Zeolite Composites with Enhanced Catalytic Activity: Effect of Different Long-Chain Structure Directing Agents, Cryst. Growth Des., 18 (2018) 1730–1737.

[98] M.L. Maria Isabel, Síntesis de materiales híbridos organosilícicos y su aplicación como adsorbentes y catalizadores, 2015.

[99] B. Sakintuna, Y. Yürüm, Templated Porous Carbons : A Review Article, Ind. Eng. Chem. Res., 44 (2005) 2893–2902.

[100] J. Wang, J. Zhou, Z. Li, Y. He, S. Lin, Q. Liu, M. Zhang, Z. Jiang, Mesoporous mixed metal oxides derived from P123-templated Mg-Al layered double hydroxides, J. Solid State Chem., 183 (2010) 2511–2515.

[101] E. Géraud, S. Rafqah, M. Sarakha, C. Forano, V. Prevot, Three Dimensionally Ordered Macroporous Layered Double Hydroxides : Preparation by Templated Impregnation/Coprecipitation and Pattern Stability upon Calcination, Chem. Mater., 20 (2008) 1116–1125.

[102] Y. Oka, Y. Kuroda, T. Matsuno, K. Kamata, H. Wada, A. Shimojima, K. Kuroda, Preparation of Mesoporous Basic Oxides through Assembly of Monodispersed Mg-Al Layered Double Hydroxide Nanoparticles, Chem. - A Eur. J., 23 (2017) 9362–9368.

[103] M. Mora, C. Jiménez-Sanchidrián, J. Rafael Ruiz, Raman spectroscopy study of layered-double hydroxides containing magnesium and trivalent metals, Mater. Lett., 120 (2014) 193–195.

[104] J.T. Kloprogge, D. Wharton, L. Hickey, R.L. Frost, Infrared and Raman study of interlayer anions CO32-, NO3– , SO42– and ClO4 in Mg/Al- hydrotalcite, Am. Mineral., 87 (2002) 623–629.

[105] T.S. Stanimirova, I. Vergilov, G. Kirov, Thermal decomposition products of hydrotalcite-like compounds : low-temperature metaphases, J. Mater. Sci., 4 (1999) 4153–4161.

[106] D. Tichit, S. Ribet, B. Coq, Characterization of Calcined and Reduced Multi-

Component Co-Ni-Mg-Al-Layered Double Hydroxides, Eur. J. Inorg. Chem, 2 (2001) 539–546.

[107] J. Kuljiraseth, A. Wangriya, J.M.C. Malones, W. Klysubun, S. Jitkarnka, Synthesis and characterization of AMO LDH-derived mixed oxides with various Mg/Al ratios as acid–basic catalysts for esterification of benzoic acid with 2-ethylhexanol, Appl. Catal. B Environ., 243 (2019) 415–427.

[108] O.D. Pavel, D. Tichit, I.C. Marcu, Acido-basic and catalytic properties of transition-metal containing Mg-Al hydrotalcites and their corresponding mixed oxides, Appl. Clay Sci., 61 (2012) 52–58.

[109] D.P. Debecker, E.M. Gaigneaux, G. Busca, Exploring, tuning, and exploiting the basicity of hydrotalcites for applications in heterogeneous catalysis, Chem. - A Eur. J., 15 (2009) 3920–3935.

[110] C. Orozco, A. Pérez, M.N. González, J.M. Alfayate, Contaminación Ambiental. Una visión desde la Química, 2005.

[111] X. Liang, Y. Zang, Y. Xu, X. Tan, W. Hou, L. Wang, Y. Sun, Sorption of metal cations on layered double hydroxides, Colloids Surfaces A Physicochem. Eng. Asp., 433 (2013) 122–131.

[112] A. Rodríguez Férnandez-Alba, P. Letón García, R. Rosal García, M. Dorado Valiño, S. Villar Fernández, J.M. Sanz García, Tratamientos Avanzados De Aguas Residuales Industriales, 2006.

[113] B. Bekele, L. Lundehøj, N.D. Jensen, U.G. Nielsen, C. Forano, Sequestration of orthophosphate by $Ca_2Al\text{-}NO_3$ layered double hydroxide – Insight into reactivity and mechanism, Appl. Clay Sci., 176 (2019) 49–57.

[114] L.J. Aguilera, L.A. Palacio, A.C. Faro, Synthesis of NiAl layered double hydroxides intercalated with aliphatic dibasic anions and their exchange with heptamolybdate, Appl. Clay Sci., 176 (2019) 29–37.

[115] K. Abdellaoui, I. Pavlovic, M. Bouhent, A. Benhamou, C. Barriga, A comparative study of the amaranth azo dye adsorption/desorption from aqueous solutions by layered double hydroxides, Appl. Clay Sci., 143 (2017) 142–150.

[116] C. Forano, Environmental remediation involving layered double hydroxides,

in: Clay Surfaces Fundam. Appl., Elsevier Ltd, 2004: pp. 425–458.

[117] M. Szabados, G. Varga, Z. Kónya, Á. Kukovecz, S. Carlson, P. Sipos, I. Pálinkó, Ultrasonically-enhanced preparation, characterization of CaFe-layered double hydroxides with various interlayer halide, azide and oxo anions (CO_3^{2-}, NO_3^-, ClO_4^-), Ultrason. - Sonochemistry, 40 (2018) 853–860.

[118] K.H. Goh, T.T. Lim, A. Banas, Z. Dong, Sorption characteristics and mechanisms of oxyanions and oxyhalides having different molecular properties on Mg/Al layered double hydroxide nanoparticles, J. Hazard. Mater., 179 (2010) 818–827.

[119] M. Xu, B. Bi, B. Xu, Z. Sun, L. Xu, Polyoxometalate-intercalated ZnAlFe-layered double hydroxides for adsorbing removal and photocatalytic degradation of cationic dye, Appl. Clay Sci., 157 (2018) 86–91.

[120] J. Qiu, G. Villemure, Anionic clay modified electrodes: Electron transfer mediated by electroactive nickel, cobalt or manganese sites in layered double hydroxide films, J. Electroanal. Chem., 428 (1997) 165–172.

[121] Y. Yang, X. Du, A. Abudula, Z. Zhang, X. Ma, K. Tang, Highly efficient defluoridation using a porous MWCNT@NiMn-LDH composites based on ion transport of EDL coupled with ligand exchange mechanism, Sep. Purif. Technol., 223 (2019) 154–161.

[122] C. Chung, H. Jung, J. Kwon, B. Jang, J. Kim, Use of calcium aluminum–layered double hydroxide to control chloride ion penetration of cement-based materials, J. Struct. Integr. Maint., 4 (2019) 37–42.

[123] N. Chubar, V. Gerda, D. Banerjee, Influence of 300 ° C thermal conversion of Fe-Ce hydrous oxides prepared by hydrothermal precipitation on the adsorptive performance of five anions : Insights from EXAFS/XANES , XRD and FTIR (companion paper), J. Colloid Interface Sci., 491 (2017) 111–122.

[124] I.R. Colinas, R.C. Silva, S.R.J. Oliver, Reversible, selective trapping of perchlorate from water in record capacity by a cationic metal-organic framework, Environ. Sci. Technol., 50 (2016) 1949–1954.

[125] H. Chao, Y. Wang, H. Nguyen, Removal of hexavalent chromium from groundwater by Mg / Al-layered double hydroxides using characteristics of

in-situ synthesis, Environ. Pollut., 243 (2018) 620–629.

[126] J. Ma, M. Yang, Q. Chen, S. Zhang, H. Cheng, S. Wang, L. Liu, C. Zhang, Z. Tong, Z. Chen, Comparative study of Keggin-type polyoxometalate pillared layered double hydroxides via two synthetic routes: Characterization and catalytic behavior in green epoxidation of cyclohexene, Appl. Clay Sci., 150 (2017) 210–216.

[127] J.X. He, K. Kobayashi, M. Takahashi, G. Villemure, A. Yamagishi, Preparation of hybrid films of an anionic Ru(II) cyanide polypyridyl complex with layered double hydroxides by the Langmuir-Blodgett method and their use as electrode modifiers, Thin Solid Films, 397 (2001) 255–265.

[128] M. Kaseem, Y.G. Ko, Benzoate intercalated Mg-Al-layered double hydroxides (LDHs) as efficient chloride traps for plasma electrolysis coatings, J. Alloys Compd., 787 (2019) 772–778.

[129] T. Kameda, M. Umetsu, T. Yoshioka, Kinetics and equilibrium studies on the removal of aromatic sulfonates from aqueous solution by Mg-Al oxide, New J. Chem., 39 (2015) 4078–4085.

[130] D. Bharali, R.C. Deka, Preferential adsorption of various anionic and cationic dyes from aqueous solution over ternary CuMgAl layered double hydroxide, Colloids Surfaces A Physicochem. Eng. Asp., 525 (2017) 64–76.

[131] Z. Meng, Y. Zhang, Z. Zhang, Q. Zhang, P.K. Chu, S. Komarneni, F. Lv, Anomalous but massive removal of two organic dye pollutants simultaneously, J. Hazard. Mater., 318 (2016) 54–60.

[132] E.M. Moujahid, J. Besse, F. Leroux, L. Mate, B. Pascal, Synthesis and characterization of a polystyrene sulfonate layered double hydroxide nanocomposite . In-situ polymerization vs . polymer incorporation, J. Mater. Chem., 12 (2002) 3324–3330.

[133] J.F. Naime Filho, F. Silvério, M.J. Dos Reis, J.B. Valim, Adsorption of cholate anions on layered double hydroxides: Effects of temperature, ionic strength and pH, J. Mater. Sci., 43 (2008) 6986–6991.

[134] Q. Zhou, F. Chen, W. Wu, R. Bu, W. Li, F. Yang, Reactive orange 5 removal from aqueous solution using hydroxyl ammonium ionic liquids / layered double

hydroxides intercalation composites, Chem. Eng. J., 285 (2016) 198–206.

[135] G. Varga, Z. Konya, A. Kukovecz, P. Sipos, I. Palinko, Co(II)-amino acid e CaAl-layered double hydroxide composites e Construction and characterization, J. Mol. Struct., 1179 (2019) 263–268.

[136] S. Ma, L. Huang, L. Ma, Y. Shim, S.M. Islam, P. Wang, L. Zhao, S. Wang, G. Sun, X. Yang, M.G. Kanatzidis, E ffi cient Uranium Capture by Polysul fi de/Layered Double Hydroxide Composites, J. Am. Chem. Soc., 137 (2015) 3670–3677.

[137] H. Asiabi, Y. Yamini, M. Shamsayei, Highly selective and efficient removal of arsenic (V), chromium (VI) and selenium (VI) oxyanions by layered double hydroxide intercalated with zwitterionic glycine, J. Hazard. Mater., 339 (2017) 239–247.

[138] M.D. Raicopol, C. Andronescu, S.I. Voicu, E. Vasile, Cellulose acetate/layered double hydroxide adsorptive membranes for efficient removal of pharmaceutical environmental contaminants, Carbohydr. Polym., 214 (2019) 204–212.

[139] L. Hou, X. Li, Q. Yang, F. Chen, S. Wang, Y. Ma, Y. Wu, X. Zhu, X. Huang, D. Wang, Science of the Total Environment Heterogeneous activation of peroxymonosulfate using Mn-Fe layered double hydroxide : Performance and mechanism for organic pollutant degradation, Sci. Total Environ., 663 (2019) 453–464.

[140] F. Bruna, R. Celis, M. Real, J. Cornejo, Organo/LDH nanocomposite as an adsorbent of polycyclic aromatic hydrocarbons in water and soil–water systems, J. Hazard. Mater., 225–226 (2012) 74–80.

[141] L. Qiu, Y. Gao, C. Zhang, Q. Yan, D. O`Hare, Q. Wang, Synthesis of highly efficient flame retardant polypropylene nanocomposites with surfactant intercalated layered double hydroxides, Dalt. Trans., 9 (2017) 2965–2975.

[142] Y. You, H. Zhao, G.F. Vance, Surfactant-enhanced adsorption of organic compounds by layered double hydroxides, Colloids Surfaces A Physicochem. Eng., 205 (2002) 161–172.

[143] X. Xue, Q. Gu, G. Pan, J. Liang, G. Huang, G. Sun, X. Yang, Nanocage Structure Derived from Sulfonated β-Cyclodextrin Intercalated Layered Double

Hydroxides and Selective Adsorption for Phenol Compounds, Inorg. Chem., 53 (2014) 1521–1529.

[144] H. Zhang, M. Tahir, X. Yan, X. Liu, X. Su, L. Zhan, Ni-Al layered double hydroxide with regulated interlayer spacing as electrode for aqueous asymmetric supercapacitor, Chem. Eng. J., 368 (2019) 905–913.

[145] Y. Xiang, Y. Xiang, Y. Jiao, L. Wang, Surfactant-modi fi ed magnetic CaFe-layered double hydroxide for improving enzymatic sacchari fi cation and ethanol production of Artemisia ordosica, Renew. Energy, 138 (2019) 465–473.

[146] K. Khorsandi, R. Hosseinzadeh, F. Shahidi, Photodynamic treatment with anionic nanoclays containing curcumin on human triple-negative breast cancer cells : Cellular and biochemical studies, J. Cell. Biothemistry, 120 (2018) 4998–5009.

[147] F. Lyu, H. Yu, T. Hou, L. Yan, X. Zhang, B. Du, Efficient and fast removal of Pb^{2+} and Cd^{2+} from an aqueous solution using a chitosan/Mg-Al-layered double hydroxide nanocomposite, J. Colloid Interface Sci., 539 (2019) 184–193.

[148] F. Yang, S. Zhang, Y. Sun, D.C.W. Tsang, K. Cheng, Y. Sik, Assembling biochar with various layered double hydroxides for enhancement of phosphorus recovery, J. Hazard. Mater., 365 (2019) 665–673.

[149] B.F. Sels, D.E. De Vos, P.A. Jacobs, Hydrotalcite-like anionic clays in catalytic organic reactions, Catal. Rev. Sci. Eng., 43 (2007) 443–488.

[150] F. Li, X. Duan, Applications of Layered Double Hydroxides, Struct. Bond., 119 (2006) 193–223.

[151] W. Bing, L. Zheng, S. He, D. Rao, M. Xu, L. Zheng, B. Wang, Y. Wang, M. Wei, Insights on Active Sites of CaAl-Hydrotalcite as a High-Performance Solid Base Catalyst toward Aldol Condensation, ACS Catal., 8 (2018) 656–664.

[152] O. Kikhtyanin, L. Čapek, L. Smoláková, Z. Tišler, D. Kadlec, M. Lhotka, P. Diblíková, D. Kubička, Influence of Mg-Al Mixed Oxide Compositions on Their Properties and Performance in Aldol Condensation, Ind. Eng. Chem. Res., 56 (2017) 13411–13422.

[153] R. Pourfaraj, S.Y. Kazemi, S.J. Fatemi, P. Biparva, α- and β-CoNi binary

hydroxides nanostructures: Synthesis, characterization, and application as heterogeneous catalysts, J. Solid State Chem., 265 (2018) 248–256.

[154] T. Li, W. Zhang, W. Chen, H. Miras, Y.-F. Song, Layered double hydroxides anchored ionic liquids as amphiphilic heterogeneous catalysts for Knoevenagel condensation reaction, Dalt. Trans., 47 (2018) 3059–3067.

[155] J. Ruiz, C. Jimenez-Sanchidrian, Heterogeneous Catalysis in the Meerwein-Ponndorf-Verley Reduction of Carbonyl Compounds, Curr. Org. Chem., 11 (2007) 1113–1125.

[156] L. Wang, Y. Wang, X. Wang, X. Feng, X. Ye, J. Fu, Small-Sized Mg – Al LDH Nanosheets Supported on Silica Aerogel with Large Pore Channels : Textural Properties and Basic Catalytic Performance after Activation, Nanomaterials, 8 (2018) 113.

[157] M.H. Abdellattif, M. Mokhtar, MgAl-Layered Double Hydroxide Solid Base Catalysts for Henry Reaction: A Green Protocol, Catalysts, 8 (2018) 133.

[158] X. Jin, Y. Koizumi, K. Yamaguchi, K. Nozaki, N. Mizuno, Selective Synthesis of Primary Anilines from Cyclohexanone Oximes by the Concerted Catalysis of a Mg – Al Layered Double Hydroxide Supported Pd Catalyst, J. Am. Chem. Soc., 139 (2017) 13821–13829.

[159] Y. Wang, W. Gao, S. Kazumi, Y. Fang, L. Shi, Y. Yoneyama, G. Yang, N. Tsubaki, Solvent-free anchoring nano-sized zeolite on layered double hydroxide for highly selective transformation of syngas to gasoline-range hydrocarbons, Fuel, 253 (2019) 249–256.

[160] Y. Chen, P. Xu, M. Arai, J. Sun, Cycloaddition of Carbon Dioxide to Epoxides for the Synthesis of Cyclic Carbonates with a Mixed Catalyst of Layered Double Hydroxide and Tetrabutylammonium Bromide at Ambient Temperature, Adv. Synth. Catal., 361 (2019) 335–344.

[161] Z. Young, R. Davis, Hydrogen Transfer Reactions Relevant to Guerbet Coupling of Alcohols over Hydroxyapatite and Magnesium Oxide Catalysts, Catal. Sci. Technol., 8 (2018) 1722–1729.

[162] R. López-Asensio, J.A. Cecilia, C.P. Jiménez-Gómez, C. García-sancho, R. Moreno-Tost, Selective production of furfuryl alcohol from furfural by

catalytic transfer hydrogenation over commercial aluminas, Appl. Catal. A, Gen., 556 (2018) 1–9.

[163] T. Komanoya, K. Nakajima, M. Kitano, M. Hara, Synergistic Catalysis by Lewis Acid and Base Sites on ZrO_2 for Meerwein–Ponndorf–Verley Reduction, J. Phys. Chem., 119 (2015) 26540–26546.

[164] M.A. Aramendía, V. Borau, C. Jimenez, J.M. Marinas, F.J. Romero, The Meerwein – Ponndorf – Verley – Oppenauer reaction between 2-hexanol and cyclohexanone on magnesium phosphates, Catal. Letters, 58 (1999) 53–58.

[165] Z. Xiao, Insight into the Meerwein-Ponndorf-Verley reduction of cinnamaldehyde over MgAl oxides catalysts, Mol. Catal., 436 (2017) 1–9.

[166] B. Zhang, F. Xie, J. Yuan, L. Wang, B. Deng, Meerwein-Ponndorf-Verley reaction of acetophenone over ZrO2 -La2O3/MCM-41: Influence of loading order of ZrO_2 and La_2O_3, Catal. Commun., 92 (2017) 46–50.

[167] R. López-Asensio, C. Jiménez, C. García, R. Moreno-tost, J.A. Cecilia, P. Maireles-torres, Influence of Structure-modifying Agents in the Synthesis of Zr-doped SBA-15 Silica and Their Use as Catalysts in the Furfural Hydrogenation to Obtain High Value-added Products through the Meerwein-Ponndorf-Verley Reduction, Int. J. Mol. Sci., 20 (2019) 828.

[168] N.O. Popovych, P.I. Kyriienko, Y. Millot, L. Valentin, J. Gurgul, R.P. Socha, Ż. Jan, S.O. Soloviev, S. Dzwigaj, Sn-BEA zeolites prepared by two-step postsynthesis method: Physicochemical properties and catalytic activity in processes based on MPV reduction, Microporous Mesoporous Mater., 268 (2018) 178–188.

[169] F. Gonell, M. Boronat, A. Corma, Structure-reactivity relationship in isolated Zr sites present in Zr-zeolite and ZrO_2 for the Meerwein-Ponndorf-Verley reaction, Catal. Sci. Technol., 7 (2017) 2865–2873.

[170] M. Mora, M.I. López, C. Jiménez-Sanchidrián, J.R. Ruiz, Ca/Al Mixed Oxides as Catalysts for the Meerwein–Ponndorf–Verley Reaction, Catal. Letters, 136 (2010) 192–198.

[171] M. a. Aramendía, V. Borau, C. Jiménez, J.M. Marinas, J.R. Ruiz, F.J. Urbano, Meerwein–Ponndorf–Verley reduction of cycloalkanones over magnesium–

aluminium oxide, J. Chem. Soc. Perkin Trans. 2, 2 (2002) 1122–1125.

[172] J.R. Ruiz, C. Jiménez-Sanchidrián, J.M. Hidalgo, Meerwein–Ponndorf–Verley reaction of acetophenones with 2-propanol over MgAl mixed oxide: The substituent effect, Catal. Commun., 8 (2007) 1036–1040.

[173] J.M. Hidalgo, C. Jiménez-Sanchidrián, J.R. Ruiz, Delaminated layered double hydroxides as catalysts for the Meerwein–Ponndorf–Verley reaction, Appl. Catal. A Gen., 470 (2014) 311–317.

[174] C. Jiménez-Sanchidrián, J.M. Hidalgo, J.R. Ruiz, Reduction of heterocyclic carboxaldehydes via Meerwein–Ponndorf–Verley reaction, Appl. Catal. A Gen., 303 (2006) 23–28.

[175] J.R. Ruiz, C. Jiménez-Sanchidrián, J.M. Hidalgo, J.M. Marinas, Reduction of ketones and aldehydes to alcohols with magnesium – aluminium mixed oxide and 2-propanol, J. Mol. Catal. A Chem., 246 (2006) 190–194.

[176] A. Aramendıa, V. Borau, C. Jiménez, J.M. Marinas, J.R. Ruiz, F.J. Urbano, Activity of Basic Catalysts in the Meerwein–Ponndorf–Verley Reaction of Benzaldehyde with Ethanol, J. Colloid Interface Sci., 238 (2001) 385–389.

[177] C. Jiménez-Sanchidrián, J.R. Ruiz, Tin-containing hydrotalcite-like compounds as catalysts for the Meerwein–Ponndorf–Verley reaction, Appl. Catal. A Gen., 469 (2014) 367–372.

[178] M.A. Aramendía, V. Borau, C. Jiménez, J.M. Marinas, J.R. Ruiz, F.J. Urbano, Catalytic hydrogen transfer from 2-propanol to cyclohexanone over basic Mg–Al oxides, Appl. Catal. A Gen., 255 (2003) 301–308.

[179] C. Taviot-guého, V. Prévot, C. Forano, G. Renaudin, C. Mousty, F. Leroux, Tailoring Hybrid Layered Double Hydroxides for the Development of Innovative Applications, Adv. Funct. Mater., 28 (2017) 1703868.

[180] Y. Sun, X. Gao, N. Yang, X. Tantai, X. Xiao, B. Jiang, Morphology-Controlled Synthesis of Three-Dimensional Hierarchical Flowerlike Mg–Al Layered Double Hydroxides with Enhanced Catalytic Activity for Transesterification, Ind. Eng. Chem. Res., 58 (2019) 7937–7947.

[181] S.S. Ravuru, A. Jana, S. De, Synthesis of NiAl-layered double hydroxide with nitrate intercalation: Application in cyanide removal from steel industry

effluent, J. Hazard. Mater., 373 (2019) 791–800.

[182] X. Zhang, J. Xie, X. Yang, J. Lv, B. Dong, B. Guo, Y. Zhou, Nano-hybridization of VS with Ni e Fe layered double hydroxides for efficient oxygen evolution in alkaline media, Appl. Surf. Sci., 484 (2019) 1010–1018.

[183] G. Pérez-Sánchez, T.L.P. Galvão, J. Tedim, J.R.B. Gomes, A molecular dynamics framework to explore the structure and dynamics of layered double hydroxides, Appl. Clay Sci., 163 (2018) 164–177.

[184] Z. Cai, X. Bu, P. Wang, J.C. Ho, J. Yang, X. Wang, Recent Advances on Layered Double Hydroxide Electrocatalysts for Oxygen Evolution Reaction, J. Mater. Chem. A, 7 (2019) 5069–5089.

[185] H. Chen, Y. Wang, J. Lin, M. Shuai, H. Zhu, Transparent red-emitting silicone resin for color conversion and encapsulation of NUV light-emitting diodes, J. Am. Chem. Soc., 102 (2019) 2718–2726.

[186] J. Zhou, M. Min, Y. Liu, J. Tang, W. Tang, Layered assembly of NiMn-layered double hydroxide on graphene oxide for enhanced non-enzymatic sugars and hydrogen peroxide detection, Sensors Actuators B. Chem., 260 (2018) 408–417.

[187] S. Sanati, Z. Rezvani, g-C3N4 nanosheet@CoAl-layered double hydroxide composites for electrochemical energy storage in supercapacitors, Chem. Eng. J., 362 (2019) 743–757.

[188] L.R. Reyna-Villanueva, J. M. Dias, N.A. Medellín-Castillo, R. Ocampo-Pérez, J.M. Martínez-Rosales, T. Peñaflor-Galindo, G. Alvarez Fuentes, Biodiesel production using layered double hidroxides and derived mixed oxides: The role of the synthesis conditions and the catalysts properties on biodiesel conversion, Fuel, 251 (2019) 285–292.

[189] S. Gómez, Improving the fire behavior of flexible polyurethane foams using eco-friendly fillers, 2018.

[190] C. Del Hoyo, Layered double hydroxides and human health: An overview, Appl. Clay Sci., 36 (2007) 103–121.

[191] E.P. Rebitski, G.P. Souza, S.A.A. Santana, S.B.C. Pergher, A.C.S. Alcântara, Bionanocomposites based on cationic and anionic layered clays as

controlled release devices of amoxicillin, Appl. Clay Sci., 173 (2019) 35–45.

[192] P. Yazdani, E. Mansouri, S. Eyvazi, V. Yousefi, M.S. Hejazi, A. Mesbahi, V. Tarhriz, M. Abolghasemi, Layered double hydroxide nanoparticles as an appealing nanoparticle in gene / plasmid and drug delivery system in C2C12 myoblast cells, Artif. Cells, Nanomedicine, Biotechnol., 47 (2019) 436–442.

[193] F. Peng, D. Wang, D. Zhang, H. Cao, X. Liu, The prospect of layered double hydroxide as bone implants : A study of mechanical properties, cytocompatibility and antibacterial activity, Appl. Clay Sci., 165 (2018) 179–187.

[194] E. Komarala, H. Tyagi, S. Thiyagarajan, L. Pradhan, M. Aslam, D. Bahadur, NIR absorbing Au nanoparticle decorated layered double hydroxide nanohybrids for photothermal therapy and fluorescence imaging of cancer cells, J. Mater. Chem. B, 5 (2017) 3852–3861.

CHAPTER II.

RESULTS AND DISCUSSION

(PAPER 1)

CHAPTER II. VIBRATIONAL SPECTROSCOPIC STUDY OF SOL–GEL LAYERED DOUBLE HYDROXIDES CONTAINING DIFFERENT TRI- AND TETRAVALENT CATIONS

CHAPTER II. PAPER 1

VIBRATIONAL SPECTROSCOPIC STUDY OF SOL–GEL LAYERED DOUBLE HYDROXIDES CONTAINING DIFFERENT TRI- AND TETRAVALENT CATIONS

Daniel Cosano, César Jiménez-Sanchidrián , José Rafael Ruiz,*

Departamento de Química Orgánica,Universidad de Córdoba. Campus de Rabanales, Edificio Marie Curie, Carretera Nacional IV-A, km. 396, 14014 Córdoba (SPAIN)

*Corresponding author. E-mail address: qo1ruarj@uco.es, Tfno: 34 957218638; fax: 34 957212066

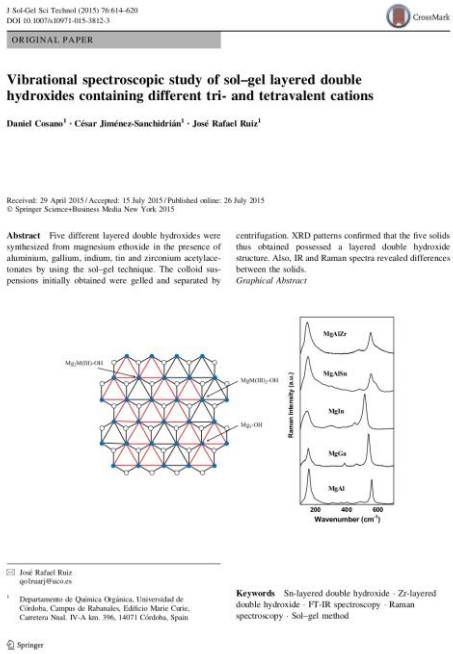

J Sol-Gel Sci Technol (2015) 76:614–620
DOI 10.1007/s10971-015-3812-3

ORIGINAL PAPER

Vibrational spectroscopic study of sol–gel layered double hydroxides containing different tri- and tetravalent cations

Daniel Cosano[1] · César Jiménez-Sanchidrián[1] · José Rafael Ruiz[1]

Received: 29 April 2015 / Accepted: 15 July 2015 / Published online: 26 July 2015

Abstract Five different layered double hydroxides were synthesized from magnesium ethoxide in the presence of aluminium, gallium, indium, tin and zirconium acetylacetonates by using the sol–gel technique. The colloid suspensions initially obtained were gelled and separated by centrifugation. XRD patterns confirmed that the five solids thus obtained possessed a layered double hydroxide structure. Also, IR and Raman spectra revealed differences between the solids.
Graphical Abstract

✉ José Rafael Ruiz
qo1ruarj@uco.es

[1] Departamento de Química Orgánica, Universidad de Córdoba, Campus de Rabanales, Edificio Marie Curie, Carretera Nnal. IV-A km. 396, 14071 Córdoba, Spain

Keywords Sn-layered double hydroxide · Zr-layered double hydroxide · FT-IR spectroscopy · Raman spectroscopy · Sol–gel method

Springer

ABSTRACT

Five different layered double hydroxides were synthesized from magnesium ethoxide in the presence of aluminium, gallium, indium, tin and zirconium acetylacetonates by using the sol–gel technique. The colloid suspensions initially obtained were gelled and separated by centrifugation. XRD diffraction patterns confirmed that the five solids thus obtained possessed a layered double hydroxide structure. Also, IR and Raman spectra revealed differences between the solids.

Keywords: Sn-layered double hydroxide, Zr-layered double hydroxide, FT-IR spectroscopy, Raman spectroscopy, Sol–gel method.

II.1. INTRODUCTION

Natural and synthetic layered double hydroxides (LDHs) have aroused enormous interest in various scientific areas such as catalysis and adsorption research [1–4]. These compounds are mixed metal hydroxides of general formula $[M(\mathrm{II})_{1-x}M(\mathrm{III})_x(\mathrm{OH})_2]^{x+}[A_{x/n}]^{n-}\cdot m\mathrm{H_2O}$, where M(II) and M(III) denote a divalent and a trivalent metal, respectively, and A is an anion. The structure of LDHs is similar to that of brucite, $Mg(OH)_2$, with Mg^{2+} cations occupying the centres of octahedra joined by their edges to form infinitely superimposed layers linked by hydrogen bonds between hydroxyl groups at octahedral vertices [5]. A wide variety of LDHs containing diverse di- and trivalent cations (Mg, Zn, Cr, Al, Fe, Ni, Co) in combination with different anions (CO_3^{2-}, SO_4^{2-}, NO_3^-, PO_4^{3-}, Cl^-, organic anions) have been reported [4]. Most have been obtained by synthesis, especially by using the co-precipitation method. Alternatives such as the sol–gel method [6–8] and homogeneous precipitation by urea hydrolysis [9–11] have also been used to prepare them and to alter some textural chemical or surface property.

A number of authors have used spectroscopic techniques to characterize Mg/Al layered double hydroxides. However, LDHs containing less common metals such as Ga or In have been less widely examined —and even less have those containing Sn or Zn. The most commonly used techniques for characterizing LDHs are Fourier-transform infrared (FT-IR) spectroscopy and solid-state nuclear magnetic resonance (MAS NMR) spectroscopy of nuclei such as ^{1}H, ^{27}Al or ^{71}Ga [12–14]. Recently, Raman spectroscopy was also successfully used to characterize LDHs of variable chemical composition [15–20]. However, none of these techniques has been used to examine LDHs containing tetravalent metals prepared with the sol–gel method. In this work, we prepared Mg/Al, Mg/Ga, Mg/In, Mg/Al/Sn and Mg/Al/Zr LDHs in Mg/M(III) or Mg/[M(III) + M(IV)] ratios of 3 by using the sol–gel method, and characterized them in structural and surface terms by using Raman spectroscopy in addition to XRD spectroscopy and nitrogen porosimetry.

II.2. MATERIALS AND METHODS

Obtaining intercalated compounds with the sol–gel method requires that their metal precursors be hydrolysed in an appropriate sequence. In order to prepare hydrotalcites containing Mg and Al, Ga or In, we dissolved 0.15 mol of magnesium ethoxide in 200 mL of ethanol containing a small amount of 35% aqueous HCl to obtain a final pH of 3. The solution was refluxed under continuous stirring for 3 h and then supplied with 0.05 mol of aluminium, gallium or indium acetylacetonate dissolved in 200 mL of acetone. The Sn and Zr LDHs were synthesized by adding appropriate amounts of tin or zirconium acetylacetonate (0.005 mol) and using a reduced amount of aluminium salt (0.045 mol). The resulting solution was adjusted to pH 10 by adding aqueous ammonia and refluxed until a gel was formed. The gel was isolated by centrifugation, washed with distilled water several times and dried at 100 ºC in a stove. In order to ensure a homogeneous composition, the solids were ion-exchanged to have carbonate as the sole anion in the interlayer spacing. To this end, the two hydrotalcites were suspended in 50 mL of water containing 0.345 g Na_2CO_3/g hydrotalcite at 100 ºC for 2 h, after which the solids were isolated by centrifugation, washed and dried. This treatment was repeated twice on each hydrotalcite. The Mg/Al, Mg/Ga and Mg/In LDHs were designated MgAl, MgGa and MgIn, respectively, and the Mg/Al/Sn and Mg/Al/Zr LDHs MgAlSn and MgAlZr, respectively.

The five LDHs were analysed by X-ray diffraction spectroscopy in order to check whether they possessed a layered structure, and also by Raman and FT-IR spectroscopies.

The metal ratio in each solid was determined by inductively coupled plasma mass spectrometry (ICP-MS) on a Perkin–Elmer ELAN DRC-e spectrometer. Crystallization water was determined by thermogravimetric analysis. X-ray diffraction patterns were obtained on a Siemens D-5000 diffractometer using CuK_α radiation. Patterns were recorded over the 2θ range from 5 to 70º. Fourier transform infrared (FT-IR) spectra were recorded on a Perkin–Elmer Spectrum 100 FTIR spectrophotometer by co-adding 32 scans with a resolution of 4 cm^{-1}. Samples were prepared by mixing appropriate, powdered aliquots of the solids with KBr as reference. The Raman spectra for the solids were acquired with a

Renishaw Raman instrument (InVia Raman Microscope) equipped with a Leica microscope furnished with various lenses, monochromators and filters, in addition to a CCD. Spectra were obtained by excitation with green laser light (532 nm) from 100 to 2000 cm^{-1}. A total of 32 scans per spectrum were performed in order to improve the signal-to-noise ratio. All spectral treatments (baseline correction, smoothing, normalization and deconvolution) were done with the Peakfit v. 4.11 software package.

II.3. RESULTS AND DISCUSSION

Table 1 shows the formulae of the five synthesized layered double hydroxides. As can be seen, the final metal ratios of the solids were quite close to the theoretical value (3:1), which suggests that the cations were completely incorporated into each layered solid phase.

Table 1. Formulae, experimentally determined metal ratios and lattice parameters of the LDHs.

LDH	Formula	$Mg/M(III)_{exp}$	x[a]	*a*[b]	*c*[b]	t[c]
MgAl	$Mg_{0.754}Al_{0.246}(OH)_2(CO_3)_{0.123}\cdot 0.62H_2O$	3.06	0.246	3.081	23.177	191
MgGa	$Mg_{0.757}Ga_{0.243}(OH)_2(CO_3)_{0.121}\cdot 0.52H_2O$	3.00	0.250	3.143	23.097	134
MgIn	$Mg_{0.744}Al_{0.256}(OH)_2(CO_3)_{0.128}\cdot 0.69H_2O$	2.84	0.260	3.186	23.388	99
MgAlSn	$Mg_{0.743}Al_{0.230}Sn_{0.027}(OH)_2(CO_3)_{0.142}\cdot 0.73H_2O$	3.11	0.243	3.111	23.340	141
MgAlZr	$Mg_{0.749}Al_{0.220}Zr_{0.031}(OH)_2(CO_3)_{0.128}\cdot 0.66H_2O$	2.91	0.254	3.109	23.101	149

[a]x = M(III)([Mg(II)+M(III)+M(IV)]; [b]Lattice parameters (A); [c]Crystal size (A).

III.3.1 XRD study.

The XRD patterns for the five samples (figure 1) are consistent with simple crystal phases with *x* values close to 0.25. The XRD patterns are also consistent with the proposed LDH structure, which consists of layered double hydroxides with brucite like-layers of $[Mg_{1-x}[M(III)M(IV)]_x(OH)_2]^{x+}(CO_3)_{x/2}^{2-}\cdot mH_2O$ composition. From the previous results it follows that the structure of synthesized solids is consistent with that of an LDH; thus, it contains positively charged brucite-like $[Mg_6M(III)_2(OH)_{16}]^{2+}$ layers, with carbonate ions and loosely bound water molecules occupying the interlayer region [21]. The XRD patterns allowed basal (*00l*) reflections —strong peaks at low 2θ values— and non-basal reflections to be

distinguished, thereby facilitating their discrimination from those due to impurities. Basal reflections corresponded to successive orders in the *c* basal space. The weak reflection at ca. 2θ = 60° was indexed as (*110*). This reflection is independent of the particular layer stacking pattern and can thus be used to calculate parameter *a* in the equation $a = 2 \cdot d_{(110)}$ [22], where *a* is the mean cation–cation distance in the brucite-like layer, and *c* is related to the distance between brucite-like layers and obtained from the equation $c = ½ [d_{(003)} + 2 \cdot d_{(006)}]$. As can be seen, *a* increased from Al to In. This suggests that both Ga and In were effectively incorporated into the LDH lattice; in fact, an increase in ionic radius in the trivalent ion should result in an increased distance between cations (the ionic radius for Al^{3+}, Ga^{3+} and In^{3+} is 0.51, 0.62 and 0.83A, respectively). On the other hand, *c* exhibited no clear-cut trend; in any case, it varied little among the LDHs, which is logical since replacing a cation with another of the same charge should have no significant effect on this parameter. The XRD patterns also revealed that the height or width of all peaks decreased with increasing ionic radius of the isovalent ion, which is consistent with previous findings [23,24]. Table 1 also shows the crystallite sizes for the *(003)* and *(006)* diffractions in the LDHs as determined from the Debye–Scherrer equation [25] as a measure of crystallinity along the direction of the *c*-axis. As can be seen, crystallinity decreased with increasing ionic radius of the trivalent cation in the LDHs. Identical conclusions can be drawn for the LDHs containing tetravalent ions (Sn^{4+} or Zr^{4+}). As can be seen, *a* increased and crystallite size decreased; the changes, however, were not so marked as in the LDHs containing Ga^{3+} or In^{3+} because the amount of tetravalent ion incorporated into the LDH structure was not too large.

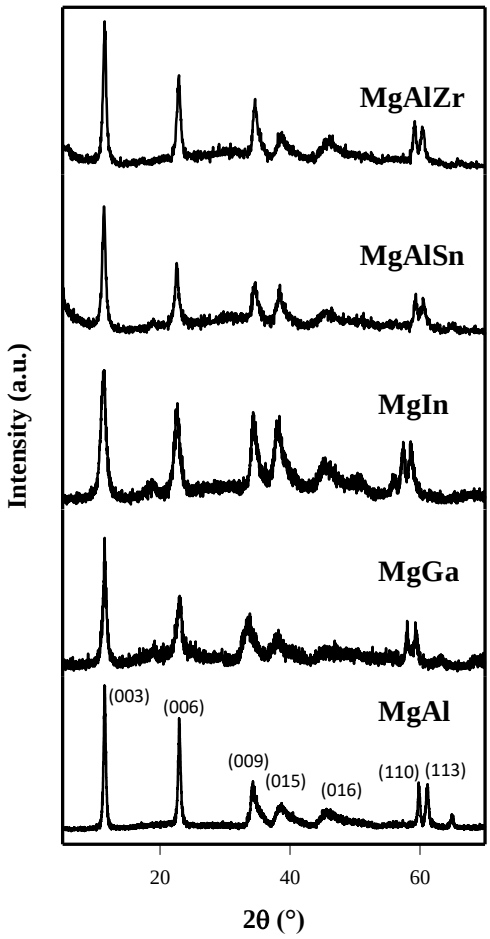

Figure 1. X-ray diffraction patterns for the LDHs.

III.3.2. Spectroscopic study

The amount of charge present in the brucite-like layer of LDHs is dictated by the trivalent—or tetravalent— cation replacing Mg^{2+}. As a result, the cation concentration should be correlated with the number of interlayer ions. Also, all hydroxyl groups in octahedral layers should coordinate to three metal sites. In Mg and Al LDHs, all hydroxyl groups are coordinated to three metal sites; therefore, four different local environments that can be designated Mg_3OH, Mg_2AlOH, $MgAl_2OH$ and Al_3OH are possible. By using ^1H MAS NMR, Sideris *et al*. [26] previously found Mg/Al LDHs with metal ratios higher than 2 to exhibit an orderly distribution of cations in their brucite-like layers; therefore, no contact between

Al^{3+} ions exists or these structural units are present in very low proportions. As a result, Mg^{2+} and Al^{3+} cations adopt a beehive-like structure as shown in Fig. 2 and only two different environments are possible, namely: Mg_2AlOH and Mg_3OH. A similar distribution can be expected from Ga^{3+} and In^{3+}. Also, exchanging a small amount of Al^{3+} with a tetravalent cation should have little effect on the octahedral units.

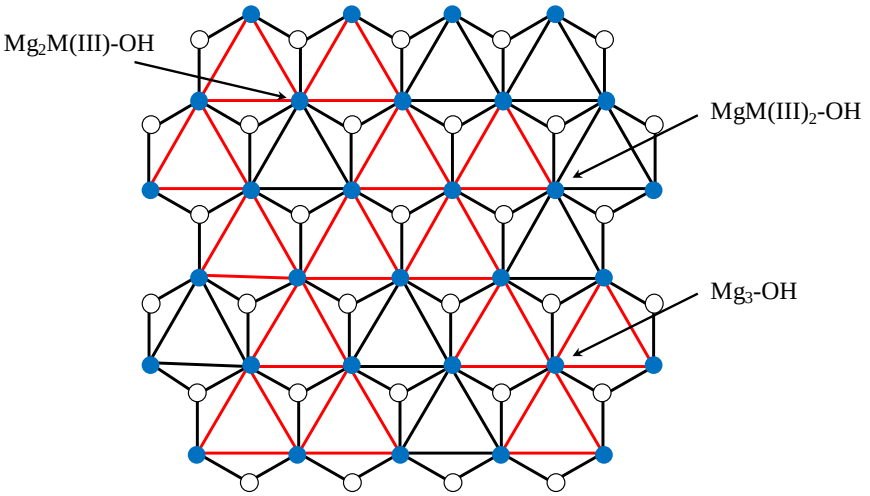

Figure 2. Schematic representation of brucite-like layers with possible distribution of M(III) octahedra (black) and Mg(II) octahedral (red).

In order to identify these structures, we characterized the solids by vibrational spectroscopy. The region where stretching bands for O–H bonds appear in the Raman or IR spectrum range from about 2800 cm^{-1} to 3800 cm^{-1}. The spectrum for an LDH in this region should contain the signals for O–H stretching vibrations in water molecules in the interlayer region and those for O–H groups in brucite-like structural units. However, water is a very poor Raman scatterer, so this technique is of little use with metal-bonded O–H groups in hydrotalcites. This led us to use FT-IR spectroscopy to examine O–H stretching vibrations and Raman spectroscopy for other bonds (viz., stretching vibrations of C–O bonds in carbonate ions, 1000–1100 cm^{-1}, and *M*–O bonds, 100-700 cm^{-1}).

III.3.2.1 Region 2800-3800 cm-1 (FT-IR spectroscopy)

Figure 3 shows the normalized, deconvoluted spectra for the five LDHs over the O–H bond stretching region. All spectra included a strong band at ca. 3450 cm–1 that was assigned to stretching vibrations in Mg-bonded OH groups (Mg-OH) [27,28] in addition to another three. That at the smallest wavenumber (2950–3050 cm^{-1}) can be assigned to stretching vibrations of OH groups in interlayer water molecules bonded to carbonate ions [29]. A third band was observed at ca. 3200 cm^{-1} that was assigned to stretching vibrations of hydroxyl groups in water molecules [30]. Also, a fourth band appeared at ca. 3600 cm^{-1} that can be assigned to stretching vibrations in O–H groups bonded to the trivalent metal. Finally, a fifth, very weak band was observed above 3700 cm^{-1} that was assigned to stretching vibrations in Sn–OH or Zr–OH bonds. These assignations were based on the assumption that an increase in cation charge would shift the bands to greater wavenumbers.

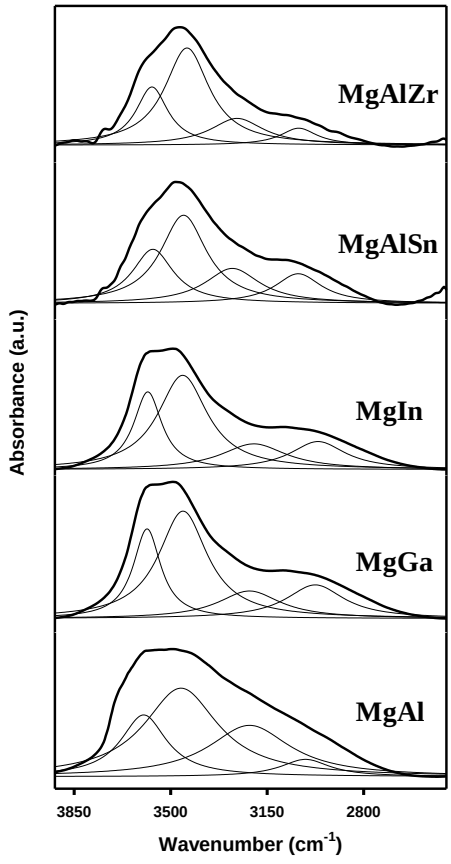

Figure 3. FT-IR spectra in the 2500-3900 region for the LDHs.

Table 2 lists the exact wavenumbers of the bands for each LDH and the corresponding percent areas. As can be seen, the proportions of the stretching bands for Mg–OH, M(III)–OH and M(IV)–OH were similar, which is consistent with the structural formulae of the LDHs —where the amount of magnesium was also similar. In addition, these results seemingly confirm the previous comment regarding the results of Sideris et al. [26] that most of the structural environments were of the Mg_3OH or Mg_2AlOH type. Accordingly, the spectra should exhibit two bands for stretching vibrations in O–H bonds as was in indeed the case. The FT-IR spectra for the LDHs with tetravalent metals exhibited a third vibrational mode corresponding to an Mg_2SnOH or Mg_2ZrOH environment.

LDH	**3900-2500 cm^{-1}**	
	Center (cm^{-1})	**Area (%)**
MgAl	3597	18.3
	3462	27.6
	3213	32.5
	3011	21.6
MgGa	3583	17.3
	3456	26.0
	3198	33.0
	2990	23.7
MgIn	3582	19.5
	3436	26.8
	3220	28.7
	3025	25.0
MgAlSn	3722	6.0
	3584	20.5
	3459	22.0
	3246	28.3
	3037	23.2
MgAlZr	3742	7.6
	3578	18.2
	3452	22.3
	3250	28.1
	3035	23.8

III.3.2.2. Region 1000-1100 cm^{-1} (Raman spectroscopy)

As can be seen in Fig. 4, all solids exhibited a strong signal in this zone. The band was assigned to stretching vibrations of carbonate ion in the interlayer region [16,17]. There is general agreement that the symmetry of carbonate ion depends on how perturbed by neighbouring species it is. Thus, in the absence of perturbations, carbonate ion adopts D_{3h} symmetry. A comprehensive analysis of group theory for carbonate ion reveals that its C–O bonds possess four normal vibration modes designated ν_1 (symmetric stretching, A_1'), ν_2 (out-of-plane bending, A_2''), ν_3 (in-plane bending, E′) and ν_4 (asymmetric stretching, E′). Modes ν_1, ν_3 y ν_4 are Raman-active in perturbed carbonate ions, but only mode ν_1 is in unperturbed ions. Because carbonate ions in the interlayer region of LDHs can be altered by water molecules in that region and hydroxyl groups in brucite-like octahedral layers, they can be assumed to be unperturbed and hence to possess a single active Raman vibration mode (ν_1) and to exhibit a single Raman signal. In fact, as can be seen from Fig. 4, the Raman spectra for the LDHs exhibited a strong band in the zone 1000–1100 cm^{-1}, which is that where ν_1 typically appears. However, the wavenumber for all LDHs (ca. 1060 cm^{-1}) was smaller than that for free carbonate ion, which is also the case with magnesite ($MgCO_3$, 1094 cm^{-1}) and calcite ($CaCO_3$, 1088 cm^{-1}) [31,32]. The decreased wavenumber can be ascribed to the above-described interactions of carbonate ions in the interlayer region of LDHs.

However, as can be seen from Fig. 4, the strong signal at ca. 1060 cm^{-1} can be deconvoluted into several smaller bands suggesting the presence of various types of carbonate ions in the interlayer regions (viz., carbonate ions subject to various types of interactions). Since, as noted earlier, the trivalent metal lies in a single environment, carbonate ion also has a single environment to interact with the metal. Also, because the trivalent ion (Al^{3+}, Ga^{3+} or In^{3+}) is the more abundant, the band at 1060 cm^{-1} can be assigned to carbonate ions bonded to it. The other, much weaker bands fell above and below the wavenumber of the main band and were assigned to “free” carbonate ions (i.e. ions bonded to neither the brucite-like layer nor interlayer water [33]); also, the band at the higher wavenumber was assigned to carbonate ions strongly hydrogen-bonded to water molecules. It should

be noted that the main band was slightly shifted to lower wavenumbers with increase in cation size. Finally, inserting a tetravalent cation had little effect on the shift and only caused a slight decrease in wavenumber.

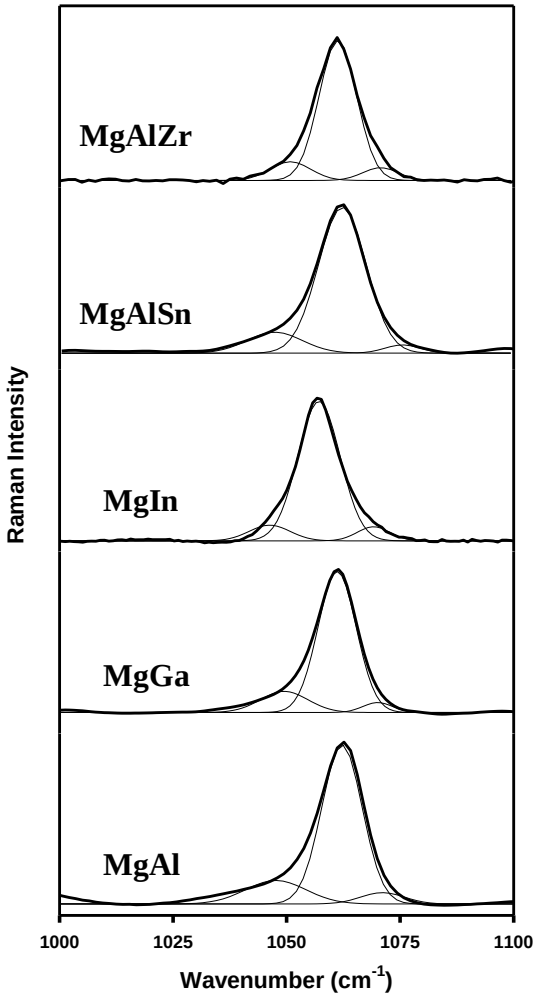

Figure 4. Raman spectra for LDHs in 1000-1100 cm^{-1} region.

III.3.2.3. Region 1000-1100 cm^{-1} (Raman spectroscopy)

This zone contained the stretching vibration bands for *M*–O bonds. Figure 5 shows the Raman spectra for the LDHs in this zone. As can be seen, the most salient bands appeared at ca. 150, 470 and 560 cm^{-1}. The latter two were unequivocally assigned to symmetric stretching vibrations in Al–OH bonds (modes A_{1g} and E_g, respectively [34]). As with the stretching vibration band for C–O bonds, the

wavenumber decreased markedly with increasing size of the cation (from 559 cm^{-1} in solid MgAl to 538 cm^{-1} in MgGa and 514 cm^{-1} in the indium-containing LDH). Therefore, this signal can be used to unambiguously distinguish LDHs containing different trivalent metals. Inserting a tetravalent metal into an Mg/Al LDH shifts the stretching vibration band for Al–OH bonds by 6–8 cm^{-1}; however, the most salient result is that it distorts the band —a sign of the presence of a tetravalent cation. The cation also affected the band at ca. 470 cm^{-1}; however, the effect was much less marked and hence more difficult to observe. Finally, the band at ca. 140–160 cm^{-1} cannot be unambiguously assigned but the shift it undergoes from Al^{3+} to In^{3+} suggests that it is due to Mg–O–*M*(III) bonds —some authors, however, have assigned it to deformation vibrations in O–*M*–O bonds [35].

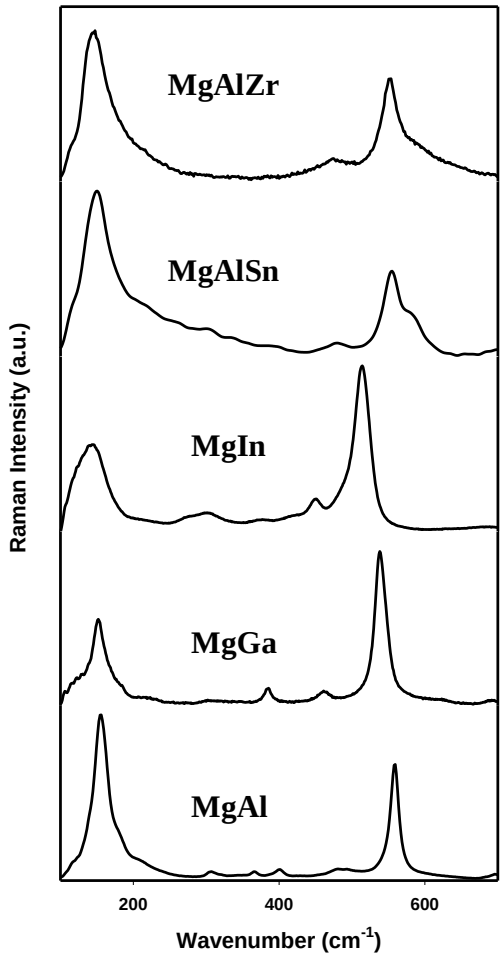

Figure 5. Raman spectra for LDHs in 100-700 cm^{-1} region.

II.4. CONCLUSIONS

Five magnesium LDHs containing various trivalent metals (aluminium, gallium and indium) and tetravalent metals (tin and zirconium) in a metal ratio of 3 [(Mg/*M*(III) + *M*(IV)] were prepared by using the sol–gel method. XRD patterns revealed that the five solids possess a layered double hydroxide structure and a metal ratio very close to the theoretical value. The environment of hydroxyl groups was studied in detail by using IR spectroscopy, and the interlayer anion and metal–oxygen bonds were examined by Raman spectroscopy. The IR zone from 2800 to 3900 cm^{-1} was quite similar for the five solids and seemingly confirms the presence of Mg_3OH and Mg_2Al-OH environments in the LDHs since only two stretching vibration modes for metal-bonded OH groups were observed. Also, the presence of a trivalent cation other than aluminium or the insertion of a small amount of a tetravalent ion in the LDH crystal network had little effect on the FT-IR spectra for the solids in this zone. Raman spectra were recorded in two different zones. One spanned the wavenumber range 1000–1100 cm^{-1} and contained the signal for stretching vibrations in carbonate, its position changing with the size of the trivalent cation —inserting a tetravalent cation had no effect on it, however. The other zone, 135–700 cm^{-1}, was that exhibiting the greatest differences between LDHs [especially in the signal for the stretching vibration of *M*(III)–OH bonds, which can be used to unequivocally distinguish between LDHs].

ACKNOWLEDGEMENTS

The authors wish to acknowledge funding of this work by Spain's Ministerio de Educación, Cultura y Deporte (Project MAT-2013-44463-R), Junta de Andalucía and FEDER Funds.

REFERENCES

[1] M. J. Logsdon, K. Hagelstein, T. I. Mudder, The management of cyanide in gold extraction. International Council on Metals and the Environments, 1999.

[2] A. Smith, T. I. Mudder, The environmental geochemistry of cyanide. Rev. Econ. Geol. V. 6, G. S. Plumlee, M. J. Logsdon (Eds.), 1993.

[3] M. Islam, R. Patel, Nitrate sorption by thermally activated Mg/Al chloride hydrotalcite-like compound, J. Hazard. Mater. 169 (2009) 524-531.

[4] M. Islam, R. Patel, Synthesis and physicochemical characterization of Zn/Al chloride layered double hydroxide and evaluation of its nitrate removal efficiency, Desalination 256 (2010) 120-128.

[5] J. Du, D. A. Sabatini, E. C. Butler, Synthesis, characterization, and evaluation of simple aluminum-based adsorbents for fluoride removal from drinking water, Chemosphere 101 (2014) 21-27.

[6] R. Chitrakar, S. Tezuka, A. Sonoda, K. Sakane, K. Ooi, T. Hirotsu, Adsorption of phosphate from seawater on calcined MgMn-layered double hydroxides, J. Coll. Interf. Sci. 290 (2005) 45-51.

[7] M. Zhang, B. Gao, Y. Yao, M. Inyang, Phosphate removal ability of biochar/MgAl-LDH ultra-fine composites prepared by liquid-phase deposition, Chemosphere 92 (2013) 1042-1407.

[8] M. J. Kang, S. W. Rhee, H. Moon, V. Neck, Th. Fanghänel, Sorption of MO_4^- (M = Tc, Re) on Mg/Al layered double hydroxide by anion exchange, Radiochim. Acta 75 (1996) 169-173.

[9] M. J. Kang, K. S. Chun, S. W. Rhee, Y. Do, Comparison of sorption behavior of I^- and TcO_4^- on Mg/Al layered double hydroxide, Radiochim. Acta 85 (1999) 57-63.

[10] K. Nejati, S. Davary, M. Saati. Study of 2,4-dichlorophenoxyacetic acid (2,4-D) removal by Cu-Fe-layered double hydroxide from aqueous solution, Appl. Surf. Sci. 280 (2013) 67-73.

[11] N. Sadik, E. Sabbar, M. Mountadar, M. Lakraimi, Elimination of the pesticide 2,4-D by synthesized anion clays starting from marine water, J. Mater. Environ. Sci. 3 (2012) 379-390.

[12] S. J. Santosa, E. K. Kunarti, Karmanto, Synthesis and utilization of Mg/Al hydrotalcite for removing disolved humic acid, Appl. Surf. Sci. 254 (2008) 7612-7617.

[13] Q. Zhao, S. Tian, L. Yan, Q. Zhang, P. Ning, Novel HCN sorbents based on layered double hydroxides: Sorption mechanism and performance, J. Hazard. Mater. 285 (2015) 250-258.

[14] R. R. Dash, C. Balomajumder, A. Kumar, Remolval of cyanide from water and wastewater using granular activated carbon, Chem. Eng. J. 146 (2009) 408-413.

[15] F. Cavani, F. Trifiro, A. Vaccari, Hydrotalcite-type anionic clays: Preparation, properties and applications, Catal. Today 11 (1991) 173-301.

[16] D. P. Debecker, E. M. Gaigneaux, G. Busca, Exploring, tuning, and exploiting the basicity of hydrotalcites for applications in heterogeneous catalysis, Chem. Eur. J. 15 (2009) 3920-3935.

[17] D. Tichit, M. N. Bennani, F. Figueras, J. R. Ruiz, Decomposition processes and characterization of the surface basicity of Cl^- and CO_3^{2-} hydrotalcites, Langmuir 14 (1998) 2086-2091.

[18] M. Mora, M. I. López, C. Jiménez-Sanchidrián, J. R. Ruiz, Near- and mid-infrared spectroscopy of layered double hydroxides containing various di- and tri-valent metals, J. Porous Mater. 20 (2013) 351-357.

[19] W. T. Reichle, S. Y. Kang, D. S. Everhardt, The nature of the thermal decomposition of a catalytically active anionic clay mineral, J. Catal. 101 (1986) 352-359.

[20] V. A. Drits, T. N. Sokolova, G. V. Sokolova, V. I. Chercashin, New members of the hydrotalcite-manasseite group, Clays Clay Miner. 35 (1987) 401-417.

[21] S. Velu, D. P. Sabde, N. Shah, S. Sivasanker, New Hydrotalcite-like Anionic Clays Containing Zr4+ in the Layers: Synthesis and Physicochemical Properties. Chem. Mater. 10 (1998) 3451-3458.

[22] M. A. Aramendia, V. Borau, J. M. Luque, J. M. Marinas, J. R. Ruiz, F. J. Urbano, Catalytic hydrogen transfer from 2-propanol to cyclohexanone over basic Mg-Al oxides, Appl. Catal. A: General 255 (2003) 301-308.

[23] M. A. Aramendia, Y. Avilés, J. A. Benitez, V. Borau, J. M. Marinas, J. R. Ruiz, F. J. Urbano, Comparative study of Mg/Al and Mg/Ga layered double hydroxides, Microp. Mesop. Mater. 29 (1999) 319-328.

[24] M. A. Aramendia, Y. Avilés, V. Borau, J. M. Luque, J. M., Marinas, J. R. Ruiz, F. J. Urbano, Thermal decomposition of Mg/Al and Mg/Ga layered-double hydroxides: A spectroscopic study. J. Mater. Chem. 9 (1999) 1603-1607.

[25] F. Millange, R. I. Walton, D. O´Hare, D., Time-resolved in situ X-ray diffraction study of the liquid-phase reconstructitm of Mg-Al-carboaate hydrotalcite-like compounds, J. Mater. Chem. 10 (2000) 1713-1720.

[26] E. C. Kruissink, L. L. van Reijen, J. R. H. Ross, Coprecipitated nickel-alumina catalysts for methanation at high temperature. Part 1. - Chemical composition and structure of the precipitates, J. Chem. Soc., Faraday Trans. I 77 (1981) 649-663.

[27] N. Das, R. Das, R., Insertion of chromium (III) ascorbate complex into layered double hydroxide through reduction of intercalated chromate by ascorbic acid, Appl. Clay Sci. 42 (2008) 90-94.

CHAPTER III.

RESULTS AND DISCUSSION

(PAPER 2)

CAPITULO III. PAPER 2

USE OF RAMAN SPECTROSCOPY TO ASSESS THE EFFICIENCY OF MgAl MIXED OXIDES IN REMOVING CYANIDE FROM AQUEOUS SOLUTIONS

Daniel Cosano, Carlos Esquinas, César Jiménez-Sanchidrián and José Rafael Ruiz,*

Departamento de Química Orgánica,Universidad de Córdoba. Campus de Rabanales, Edificio Marie Curie, Carretera Nacional IV-A, km. 396, 14014 Córdoba (SPAIN)

*Corresponding author. E-mail address: qo1ruarj@uco.es, Tfno: 34 957218638; fax: 34 957212066

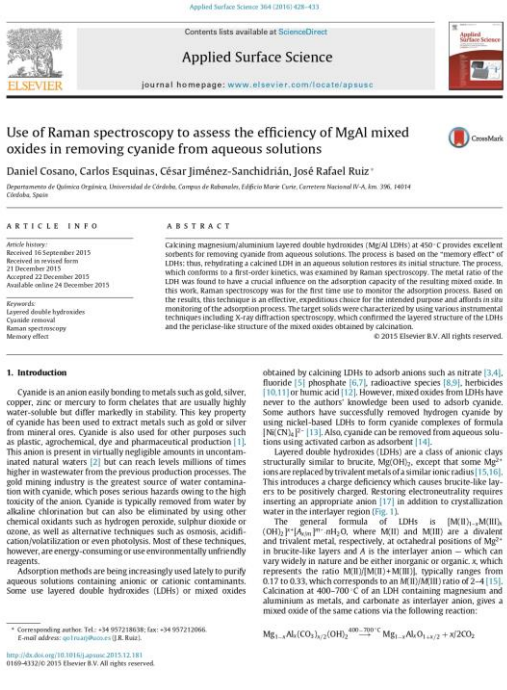

Applied Surface Science 364 (2016) 628–633

Contents lists available at ScienceDirect

Applied Surface Science

journal homepage: www.elsevier.com/locate/apsusc

Use of Raman spectroscopy to assess the efficiency of MgAl mixed oxides in removing cyanide from aqueous solutions

Daniel Cosano, Carlos Esquinas, César Jiménez-Sanchidrián, José Rafael Ruiz *

Departamento de Química Orgánica, Universidad de Córdoba, Campus de Rabanales, Edificio Marie Curie, Carretera Nacional IV-A, km. 396, 14014 Córdoba, Spain

ARTICLE INFO

Article history:
Received 16 September 2015
Received in revised form
21 December 2015
Accepted 22 December 2015
Available online 24 December 2015

Keywords:
Layered double hydroxides
Cyanide removal
Raman spectroscopy
Memory effect

ABSTRACT

Calcining magnesium/aluminium layered double hydroxides (MgAl LDHs) at 450 °C provides excellent sorbents for removing cyanide from aqueous solutions. The process is based on the "memory effect" of LDHs: thus, rehydrating a calcined LDH in an aqueous solution restores its initial structure. The process, which conforms to a first-order kinetics, was examined by Raman spectroscopy. The metal ratio of the LDH was found to have a crucial influence on the adsorption capacity of the resulting mixed oxide. In this work, Raman spectroscopy was for the first time use to monitor the adsorption process. Based on the results, this technique is an effective, expeditious choice for the intended purpose and affords *in situ* monitoring of the adsorption process. The target solids were characterized by using various instrumental techniques including X-ray diffraction spectroscopy, which confirmed the layered structure of the LDHs and the periclase-like structure of the mixed oxides obtained by calcination.

1. Introduction

Cyanide is an anion easily bonding to metals such as gold, silver, copper, zinc or mercury to form chelates that are usually highly water-soluble but differ markedly in stability. This key property of cyanide has been used to extract metals such as gold or silver from mineral ores. Cyanide is also used for other purposes such as plastic, agrochemical, dye and pharmaceutical production [1]. This anion is present in virtually negligible amounts in uncontaminated natural waters [2] but can reach levels millions of times higher in wastewater from the previous production processes. The gold mining industry is the greatest source of water contamination with cyanide, which poses serious hazards owing to the high toxicity of the anion. Cyanide is typically removed from water by alkaline chlorination but can also be eliminated by using other chemical oxidants such as hydrogen peroxide, sulphur dioxide or ozone, as well as alternative techniques such as osmosis, acidification/volatilization or even photolysis. Most of these techniques, however, are energy-consuming or use environmentally unfriendly reagents.

Adsorption methods are being increasingly used lately to purify aqueous solutions containing anionic or cationic contaminants. Some use layered double hydroxides (LDHs) or mixed oxides obtained by calcining LDHs to adsorb anions such as nitrate [3,4], fluoride [5] phosphate [6,7], radioactive species [8,9], herbicides [10,11] or humic acid [12]. However, mixed oxides from LDHs have never to the authors' knowledge been used to adsorb cyanide. Some authors have successfully removed hydrogen cyanide by using nickel-based LDHs to form cyanide complexes of formula $[Ni(CN)_4]^{2-}$ [13]. Also, cyanide can be removed from aqueous solutions using activated carbon as adsorbent [14].

Layered double hydroxides (LDHs) are a class of anionic clays structurally similar to brucite, $Mg(OH)_2$, except that some Mg^{2+} ions are replaced by trivalent metals of a similar ionic radius[15,16]. This introduces a charge deficiency which causes brucite-like layers to be positively charged. Restoring electroneutrality requires inserting an appropriate anion [17] in addition to crystallization water in the interlayer region (Fig. 1).

The general formula of LDHs is $[M(II)_{1-x}M(III)_x(OH)_2]^{x+}[A_{x/n}]^{n-}\cdot mH_2O$, where M(II) and M(III) are a divalent and trivalent metal, respectively, at octahedral positions of Mg^{2+} in brucite-like layers and *A* is the interlayer anion – which can vary widely in nature and be either inorganic or organic. x, which represents the ratio M(II)/[M(II)+M(III)], typically ranges from 0.17 to 0.33, which corresponds to an M(II)/M(III) ratio of 2–4 [15]. Calcination at 400–700 °C of an LDH containing magnesium and aluminium as metals, and carbonate as interlayer anion, gives a mixed oxide of the same cations via the following reaction:

$$Mg_{1-x}Al_x(CO_3)_{x/2}(OH)_2 \xrightarrow{400-700\,^{\circ}C} Mg_{1-x}Al_xO_{1+x/2} + x/2CO_2$$

* Corresponding author. Tel.: +34 957218638; fax: +34 957212066.
E-mail address: qo1ruarj@uco.es (J.R. Ruiz).

http://dx.doi.org/10.1016/j.apsusc.2015.12.181
0169-4332/

ABSTRACT

Calcining magnesium/aluminium layered double hydroxides (Mg/Al LDHs) at 450 ºC provides excellent sorbents for removing cyanide from aqueous solutions. The process is based on the "memory effect" of LDHs; thus, rehydrating a calcined LDH in an aqueous solution restores its initial structure. The process, which conforms to a first-order kinetics, was examined by Raman spectroscopy. The metal ratio of the LDH was found to have a crucial influence on the adsorption capacity of the resulting mixed oxide. In this work, Raman spectroscopy was for the first time use to monitor the adsorption process. Based on the results, this technique is an effective, expeditious choice for the intended purpose and affords in situ monitoring of the adsorption process. The target solids were characterized by using various instrumental techniques including X-ray diffraction spectroscopy, which confirmed the layered structure of the LDHs and the periclase-like structure of the mixed oxides obtained by calcination.

Keywords: Layered double hydroxides, cyanide removal, Raman spectroscopy, memory effect.

III.1. INTRODUCTION

Cyanide is an anion easily bonding to metals such as gold, silver, copper, zinc or mercury to form chelates that are usually highly water-soluble but differ markedly in stability. This key property of cyanide has been used to extract metals such as gold or silver from mineral ores. Cyanide is also used for other purposes such as plastic, agrochemical, dye and pharmaceutical production [1]. This anion is present in virtually negligible amounts in uncontaminated natural waters [2] but can reach levels millions of times higher in wastewater from the previous production processes. The gold mining industry is the greatest source of water contamination with cyanide, which poses serious hazards owing to the high toxicity of the anion. Cyanide is typically removed from water by alkaline chlorination but can also be eliminated by using other chemical oxidants such as hydrogen peroxide, sulphur dioxide or ozone, as well as alternative techniques such as osmosis, acidification/volatilization or even photolysis. Most of these techniques, however, are energy-consuming or use environmentally unfriendly reagents.

Adsorption methods are being increasingly used lately to purify aqueous solutions containing anionic or cationic contaminants. Some use layered double hydroxides (LDHs) or mixed oxides obtained by calcining LDHs to adsorb anions such as nitrate [3,4], fluoride [5] phosphate [6,7], radioactive species [8,9], herbicides [10,11] or humic acid [12]. However, mixed oxides from LDHs have never to the authors 'knowledge been used to adsorb cyanide. Some authors have successfully removed hydrogen cyanide by using nickel-based LDHs to form cyanide complexes of formula $[Ni(CN)_4]^{2-}$ [13]. Also, cyanide can be removed from aqueous solutions using activated carbon as adsorbent [14].

Layered double hydroxides (LDHs) are a class of anionic clays structurally similar to brucite, $Mg(OH)_2$, except that some Mg^{2+} ions are replaced by trivalent metals of a similar ionic radius [15,16]. This introduces a charge deficiency which causes brucite-like layers to be positively charged. Restoring electroneutrality requires inserting an appropriate anion [17] in addition to crystallization water in the interlayer region (figure 1).

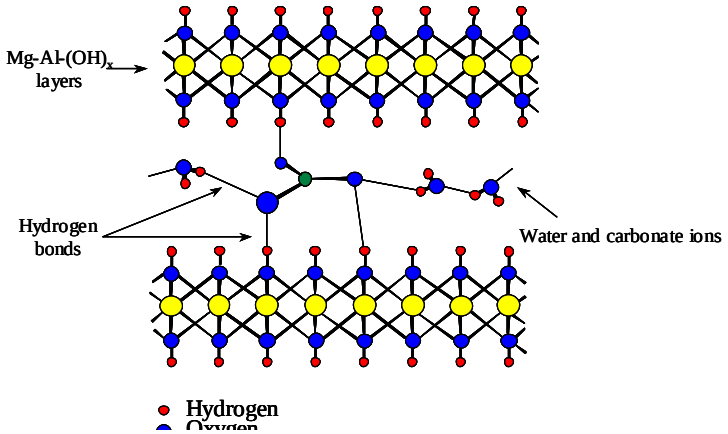

Figure 1. Structure of layered double hydroxide containing Mg(II), Al(III) and carbonate as interlayer anion.

The general formula of LDHs is $[M(\mathrm{II})_{1-x}M(\mathrm{III})_x(\mathrm{OH})_2]^{x+}[A_{x/m}]^{m-}\cdot n\mathrm{H_2O}$, where M(II) and M(III) are a divalent and trivalent metal, respectively, at octahedral positions of Mg^{2+} in brucite-like layers and A is the interlayer anion —which can vary widely in nature and be either inorganic or organic. x, which represents the ratio $M(\mathrm{II})/[M(\mathrm{II}) + M(\mathrm{III})]$, typically ranges from 0.17 to 0.33, which corresponds to an $M(\mathrm{II})/M(\mathrm{III})$ ratio of 2–4 [15]. Calcination at 400–700 ºC of an LDH containing magnesium and aluminium as metals, and carbonate as interlayer anion, gives a mixed oxide of the same cations via the following reaction:

$$Mg_{1-x}Al_x(CO_3)_{x/2}(OH)_2 \xrightarrow{400-700\,^{\circ}C} Mg_{1-x}Al_xO_{1+x/2} + x/2\ CO_2$$

Rehydrating the resulting oxide restores the original LDH structure (Cavani et al., 1991) except that the interlayer anion is now that present in the rehydrating aqueous solution:

$$Mg_{1-x}Al_xO_{1+x/2} + x/n\ A^{n-} + (1 + x/2)H_2O \longrightarrow Mg_{1-x}Al_xA_{\frac{x}{n}}(OH)_2 + xOH^-$$

The reaction occurs at variable temperatures and can even be effected by water vapour, which introduces hydroxyl groups in the interlayer region [17]. In any case, the rehydration process involves the release of OH^- ions and the combination of the mixed oxide with A^{n-} ions in solution. This property, known as the “memory effect”,

was used in this work to develop a method for removing cyanide ions from aqueous solutions by using a magnesium–aluminium mixed oxide.

As noted earlier, LDHs and their calcination products have been widely used to remove anionic contaminants from various types of aqueous matrices on the grounds of their high adsorption capacity. In this work, we used a calcined Mg/Al LDH to remove cyanide from aqueous solutions. One other novelty of our proposal is the use of Raman spectroscopy, a highly sensitive technique subject to no interferences, to monitor the course of cyanide adsorption by the mixed oxide in real time.

III.2. EXPERIMENTAL

II.2.1 Preparation of the materials

The LDHs used was prepared by using a coprecipitation method described elsewhere [18]. In a typical synthetic run, a solution containing 0.3 mol of $Mg(NO_3)_2{\cdot}6H_2O$ and 0.15 mol of $Al(NO_3)_3{\cdot}9H_2O$ in 250 mL of de-ionized water was used (Mg/Al = 2). The solution was slowly dropped over 500 mL of an Na_2CO_3 solution at pH 10 at 60 °C under vigorous stirring, the pH was kept constant by adding appropriate volumes of 1 M NaOH during precipitation. The suspension thus obtained was kept at 80 °C for 24 h, after which the solid was filtered and washed with 2 L of de-ionized water. The layered double hydroxide thus prepared was ion-exchanged with carbonate to remove nitrate ions intercalated between layers. The procedure involved suspending the solid in a solution containing 0.345 g of Na_2CO_3 in 50 mL of bidistilled, de-ionized water per gram of hydrotalcite at 100 °C for 2 h. Then, the solid was filtered off *in vacuo* and washed with 200 mL of bidistilled, de-ionized water. The new LDH thus obtained was subjected to further ion-exchange under the same conditions, and named MgAl-2. This solid was calcined at 450 °C in the air for 8 h, using a temperature gradient of 1 °C/min and named MgAl-2-450. A similar procedure was used to prepare two other LDHs in theoretical metal ratios of 3 and 4 that were named MgAl-3 and MgAl-4, respectively, and calcined at 450 ºC to obtain the solids MgAl-3-450 and MgAl-4-450, respectively.

III.2.2 Characterization of the materials

The Mg/Al ratio of each solid was determined by inductively coupled plasma mass spectrometry (ICP-MS) on an ELAN DRC-E Perkin Elmer ICP-MS instrument operated under standard conditions. X-ray diffraction (XRD) analysis was performed on a Siemens D-5000 diffractometer using CuK$_{\alpha}$ radiation over the range 5–80º. Raman spectra for the solids were acquired with a Renishaw Raman instrument (InVia Raman Microscope) equipped with a Leica microscope furnished with various lenses, monochromators and filters in addition to a CCD. Spectra were obtained by excitation with green laser light (532 nm) from 150 to 1500 cm^{-1}. A total of 32 scans per spectrum were done in order to improve the signal-to-noise ratio. Thermogravimetric analyses were performed on a Setaram Setsys 12 instrument by heating in an argon atmosphere from 25 to 800°C at 10°C/min.

III.2.3 Adsoprtion experiments

Adsorption tests were performed by placing in a flask a 0.25 L volume of a solution containing a 9 mg/L concentration of potassium cyanide (Aldrich ref. 31252) in decarbonated, de-ionized water at the pH resulting from dissolution at room temperature (22 ºC). The solution was then supplied with 0.16 mg of mixed oxide (MgAl-*x*-450) and fitted with a refluxing condenser for vigorous agitation of the flask contents for a present time. Samples of the solution were withdrawn at regular intervals to quantify the amount of adsorbed cyanide by Raman spectroscopy. Following centrifugation at 5000 rpm for 8 min to remove suspended solid, Raman spectra were recorded under the same conditions as those for the LDH and its calcination product, albeit over the wavenumber range 2040–2100 cm^{-1}.

The kinetics of adsorption was studied by using a volume of 0.25 L of the previous solution at 22 ºC under the above-described conditions. The amount of cyanide ion adsorbed by the calcined LDHs was calculated from the following equation:

$$q_t = \frac{[CN^-]_o - [CN^-]_t}{m} \cdot V$$

where q_t is the sorption capacity of the calcined LDH at time t, in mg CN^-/g_{ads}, V is the solution volume (L), $[CN^-]_0$ and $[CN^-]_t$ (mg/L) are the cyanide concentrations at time zero and t, respectively, and m is the amount of calcined LDH (g_{ads}) used as sorbent.

Adsorption tests under different conditions were used to identify the most suitable LDH for the intended purpose, which was then used to establish a kinetic model at different temperatures.

III.3. RESULTS AND DISCUSSION

III.3.1 Characterization of materials.

Table 1 shows the metal ratio x = Al/(Mg + Al) for each LDH and its calcination product, as well as the formula of each solid. The amount of water present in each LDH was determined from thermogravimetric data as described below. The theoretical values were consistent with experimental data, which suggests that the cations were thoroughly incorporated into the solid phase.

Table 1. Theoretical and experimental values of x, and of the lattice parameters, for the LDHs and their calcination products.

SOLID	X_{THER}	X_{EXP}	A (A)	C (A)	FORMULA
MGAL-2	0.33	0.37	3.046	22.860	$Mg_{0.631}Al_{0.369}(OH)_2(CO_3)_{0.185}\cdot 0.65H_2O$
MGAL-3	0.25	0.29	3.052	22.878	$Mg_{0.710}Al_{0.290}(OH)_2(CO_3)_{0.145}\cdot 0.61H_2O$
MGAL-4	0.20	0.22	3.068	23.421	$Mg_{0.779}Al_{0.221}(OH)_2(CO_3)_{0.110}\cdot 0.60H_2O$
MGAL-2-450	0.33	0.37	4.159	-	$Mg_{0.671}Al_{0.369}O_{1.185}$
MGAL-3-450	0.25	0.29	4.175	-	$Mg_{0.710}Al_{0.290}O_{1.145}$
MGAL-4-450	0.20	0.22	4.189	-	$Mg_{0.779}Al_{0.221}O_{1.110}$

Figure 2 shows the X-day diffraction patterns for the three Mg/Al solids. All exhibited the typical signals for hydrotalcite [19], namely: symmetric, strong, narrow peaks for the (003), (006), (110) and (113) planes, and broader, less symmetric peaks for the (009), (015) and (018) planes, all of which are typical of clay minerals with a layered structure. Table 1 shows the

experimental lattice parameters *a* and *c* as determined from the XRD patterns. As can be seen, *a* increased with decreasing metal ratio, *x*, which is consistent with the increasing distance between cations in brucite-like layers as the proportion of trivalent cation —aluminium here— is increased [20]. Parameter *c* also increased with decrease in *x*, but its dependence on the metal ratio has not been unambiguously established [20].

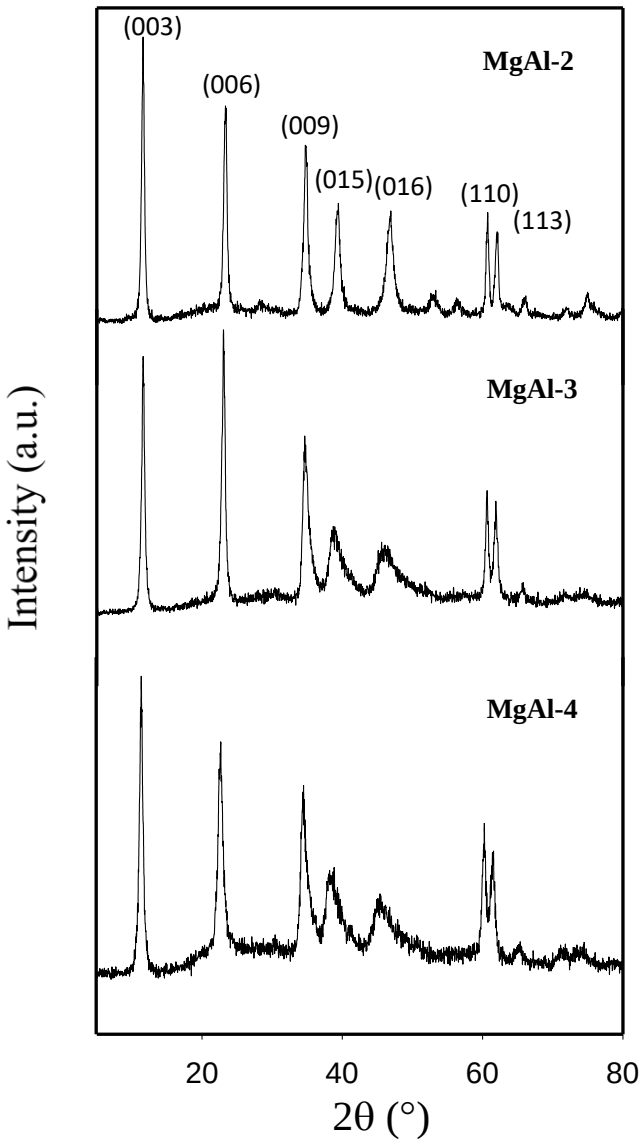

Figure 2. XRD patterns for the as prepared LDHs.

The thermal decomposition of LDHs containing Mg and Al alone above 450 ºC seemingly gives completely crystalline phases of a periclase-like Mg/Al mixed oxide with a lattice parameter *a* that is smaller than that of pure periclase (MgO) by the likely effect of a small amount of Al^{3+} ions being dissolved in the MgO lattice to form solid solutions [15,21,22]. In this work, *a* was calculated from the XRD patterns for the (200) and (220) planes, using the following equation: $a = d_x (h^2 + k^2 + l^2)^{1/2}$. The average *a* values from the XRD patterns for the solids calcined at 450 ºC (Fig. 3) are shown in Table 1. As can be seen, all were smaller than that for pure MgO, which is 4.211 [23].

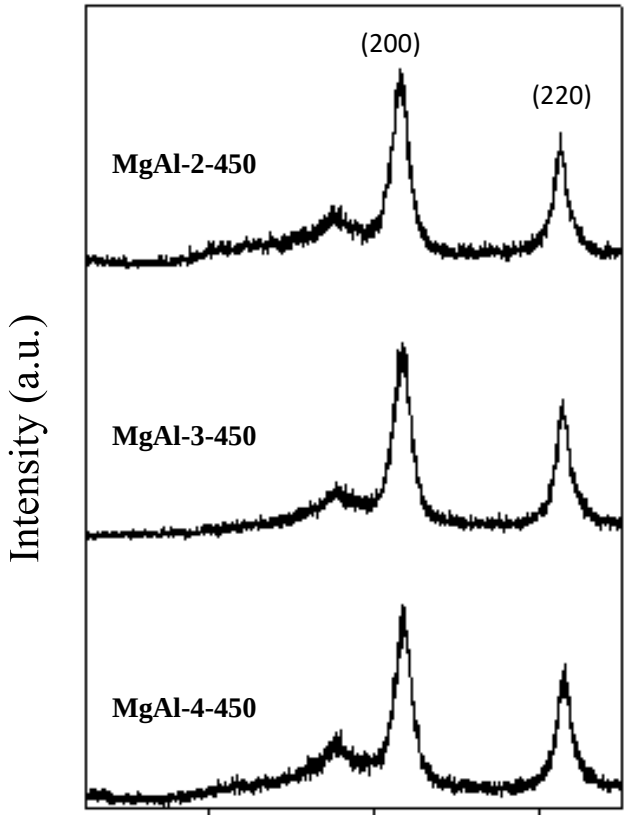

Figure 3. XRD patterns for the calcined LDHs.

Figure 4 shows the thermogravimetric curves for the three LDHs. The decomposition profiles were similar to those previously reported for these materials [24,25]; also, the total weight loss invariably exceeded 40%. The solids exhibited three distinct weight loss regions. One spanned the temperature range 25–220 ºC and exhibited an endothermic peak at ca. 200 ºC that can be assigned to the release of water from interparticle pores [26]. Another region exhibited an endothermic peak at ca. 400 ºC due to the release of carbonate ions from the interlayer region and hydroxyl ions from brucite-like layers [26]. The third region cannot be unequivocally assigned but was seemingly due to sustained release of water probably resulting from dehydroxylation of the mixed oxides formed ($MgAlO_x$) above 450 ºC.

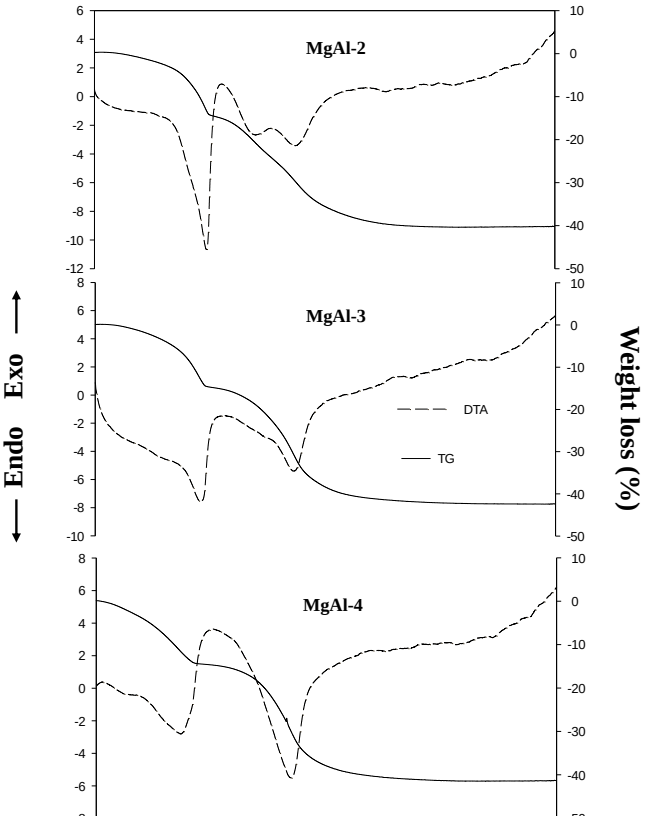

Figure 4. TG and DTA curves for the as prepared LDHs

III.3.2. Adsorption experiments

The Mg/Al ratio in the mixed oxides obtained by calcining the layered double hydroxides was the first variable to be examined with a view to identifying the best performer in removing (adsorbing) cyanide. Figure 5 shows the variation of the proportion of cyanide adsorbed by the MgAl-*x*-450 solids as a function of time.

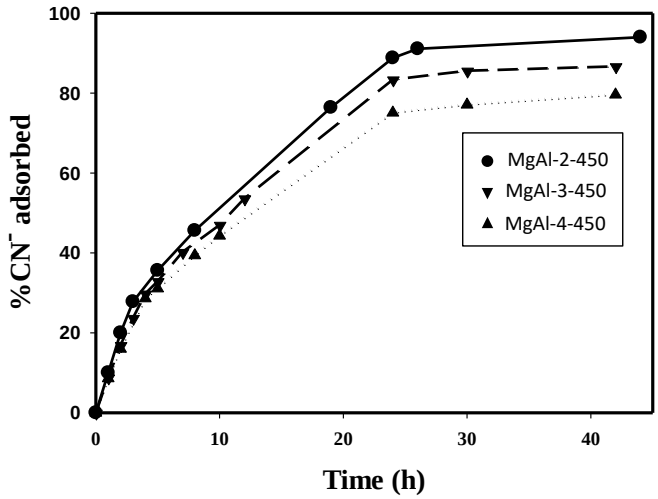

Figure 5. Influence of time on cyanide adsorption by the calcined LDHs.

As can be seen, the amount of cyanide adsorbed changed little —and similarly— at an early stage. However, as time elapsed and the cyanide concentration in solution decreased, the adsorption capacity of the solids increased with decreasing Mg/Al ratio. Also, only MgAl-2-450 succeeded in reducing the cyanide concentration below the legally established maximum level (1 ppm) within 24 h. This result can be ascribed to the increased amount of Al present in MgAl-2-450 since the metal was ultimately responsible for cyanide adsorption by effect of its positive charge being partly offset by the negative charge of cyanide ion. As noted under Experimental, the time course of the process was monitored via the Raman signal for stretching vibrations in C≡N bonds at 2080 cm^{-1}. This was the only signal observed in this spectral region, which afforded direct, uninterfered integration — and hence quantitation— of cyanide. By way of example, Fig. 6 shows the profile for solid MgAl-2-450.

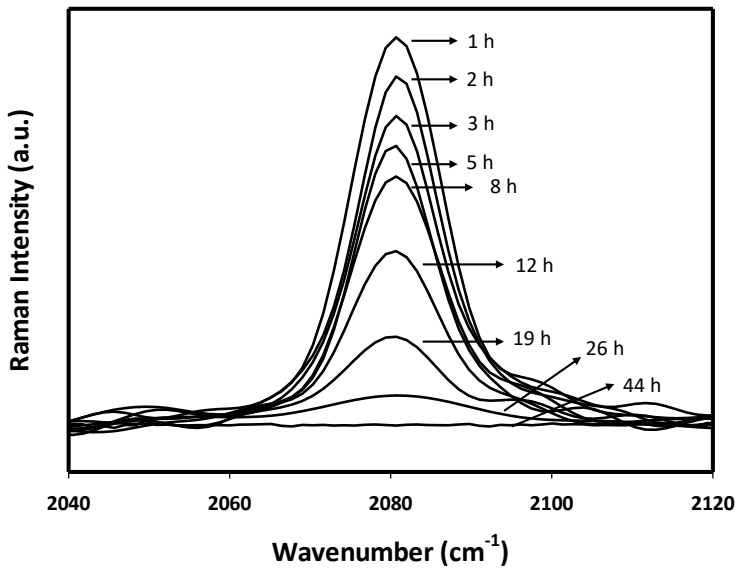

Figura 6. Time course of the signal for stretching vibrations in C≡N bonds during the adsorption of cyanide ion. *T* = 22 ºC. Initial cyanide concentration = 9 mg/L. Amount of solid = 0.16 g (MgAl-2-450).

A kinetic study of the adsorption process followed. As noted earlier, the adsorption curves of Fig. 5 suggest that cyanide ion was rapidly adsorbed early in the process —until about 24 h, when equilibrium was reached an the equilibrium concentration, q_e, determined. Recent adsorption experiments with anions such as nitrate [3,4] and similar solids, revealed that the kinetics of the process conformed to a first-order Lagergren model based on which adsorption in solid/liquid systems is governed by the following equation:

$$\ln (q_e - q_t) = \ln q_e - k_{ads} \cdot t$$

where q_e and q_t are the amounts of cyanide adsorbed at equilibrium and time t, respectively, both in mg CN^-/g_{ads}, and k_{ads} is the rate constant for the process. Linearity in a plot of ln ($q_e - q_t$) against time confirms the validity of the Lagergren model. Table 2 shows the kinetic results and correlation coefficients (R^2) for the three mixed oxides.

Once the solid with an Mg/Al ratio of 2 (viz., MgAl-2-450) was found to be that with the highest cyanide adsorption capacity, the influence of temperature on its

performance was assessed. There is evidence that temperature has a strong effect on the ability of calcined LDHs to adsorb anions [4,27]. We examined cyanide adsorption by solid MgAl-2-450 at 22, 50, 70 and 90 °C. As can be seen from Fig. 7, the adsorption capacity of the solid increased with increasing temperature. Usually, physisorption processes are exothermic; therefore, the adsorption capacity of the solid should have decreased with increasing temperature. This suggests that the adsorption of cyanide on a calcined LDH involves some endothermic chemical reaction.

The energy of activation for the adsorption process was calculated by using Arrhenius' law in logarithmic form:

$$\ln k_{ads} = \ln A - (E_a/RT)$$

Plotting the adsorption rate in the form of k_{ads} against the reciprocal temperature gave a straight line with an acceptable correlation coefficient (R^2 = 0.949). The slope of the curve, $-(E_a/R)$, provided the energy of activation and the intercept, $\ln A$, the Arrhenius constant.

The energy of activation for diffusion-controlled adsorption processes is lower than 20 kJ/mol (Ho et al., 2000). The calculated E_a value for the adsorption of cyanide on a calcined LDH was 159 kJ/mol. Therefore, the adsorption process must be governed by a reaction of cyanide with the mixed oxide rather than by diffusion.

III.4. CONCLUSIONS

Raman spectroscopy is an effective, accurate, expeditious technique for monitoring and quantifying the adsorption of cyanide ion on a mixed oxide obtained by calcining a layered double hydroxide (LDH). Cyanide is adsorbed by a rehydration process based on a "memory effect" that restores the initial structure of the LDH. The absorption rate was found to decrease with increase in metal (Mg/Al) ratio of the LDH used as precursor for the mixed oxide, and to peak for the oxide with Mg/Al = 2. The kinetics of the process conformed to a first-order Lagergren model. The fact that the cyanide adsorption rate increased with increasing temperature suggests that the process is endothermic. Based on the energy of activation for the process, the adsorption of cyanide is governed by its reaction with the mixed oxide rather than by diffusion. Calcination of the LDH after adsorption of cyanide restores the original mixed oxide, which can thus be reused as a cyanide sorbent.

ACKNOWLEDGMENTS

The authors gratefully acknowledge funding by Spain's Ministerio de Educación y Ciencia (Project MAT-2013-44463-R), Feder Funds and to the Consejería de Innovación, Ciencia y Empresa de la Junta de Andalucía. The staff of the Central Service for Research Support (SCAI) at the University of Córdoba is also acknowledged for its technical support in ICP-MS measurements.

REFERENCES

[1] M. J. Logsdon, K. Hagelstein, T. I. Mudder, The management of cyanide in gold extraction. International Council on Metals and the Environments, 1999.

[2] A. Smith, T. I. Mudder, The environmental geochemistry of cyanide. Rev. Econ. Geol. V. 6, G. S. Plumlee, M. J. Logsdon (Eds.), 1993.

[3] M. Islam, R. Patel, Nitrate sorption by thermally activated Mg/Al chloride hydrotalcite-like compound, J. Hazard. Mater. 169 (2009) 524-531.

[4] M. Islam, R. Patel, Synthesis and physicochemical characterization of Zn/Al chloride layered double hydroxide and evaluation of its nitrate removal efficiency, Desalination 256 (2010) 120-128.

[5] J. Du, D. A. Sabatini, E. C. Butler, Synthesis, characterization, and evaluation of simple aluminum-based adsorbents for fluoride removal from drinking water, Chemosphere 101 (2014) 21-27.

[6] R. Chitrakar, S. Tezuka, A. Sonoda, K. Sakane, K. Ooi, T. Hirotsu, Adsorption of phosphate from seawater on calcined MgMn-layered double hydroxides, J. Coll. Interf. Sci. 290 (2005) 45-51.

[7] M. Zhang, B. Gao, Y. Yao, M. Inyang, Phosphate removal ability of biochar/MgAl-LDH ultra-fine composites prepared by liquid-phase deposition, Chemosphere 92 (2013) 1042-1407.

[8] M. J. Kang, S. W. Rhee, H. Moon, V. Neck, Th. Fanghänel, Sorption of MO_4^- (M = Tc, Re) on Mg/Al layered double hydroxide by anion exchange, Radiochim. Acta 75 (1996) 169-173.

[9] M. J. Kang, K. S. Chun, S. W. Rhee, Y. Do, Comparison of sorption behavior of I^- and TcO_4^- on Mg/Al layered double hydroxide, Radiochim. Acta 85 (1999) 57-63.

[10] K. Nejati, S. Davary, M. Saati. Study of 2,4-dichlorophenoxyacetic acid (2,4-D) removal by Cu-Fe-layered double hydroxide from aqueous solution, Appl. Surf. Sci. 280 (2013) 67-73.

[11] N. Sadik, E. Sabbar, M. Mountadar, M. Lakraimi, Elimination of the pesticide 2,4-D by synthesized anion clays starting from marine water, J. Mater. Environ. Sci. 3 (2012) 379-390.

[12] S. J. Santosa, E. K. Kunarti, Karmanto, Synthesis and utilization of Mg/Al hydrotalcite for removing disolved humic acid, Appl. Surf. Sci. 254 (2008) 7612-7617.

[13] Q. Zhao, S. Tian, L. Yan, Q. Zhang, P. Ning, Novel HCN sorbents based on layered double hydroxides: Sorption mechanism and performance, J. Hazard. Mater. 285 (2015) 250-258.

[14] R. R. Dash, C. Balomajumder, A. Kumar, Remolval of cyanide from water and wastewater using granular activated carbon, Chem. Eng. J. 146 (2009) 408-413.

[15] F. Cavani, F. Trifiro, A. Vaccari, Hydrotalcite-type anionic clays: Preparation, properties and applications, Catal. Today 11 (1991) 173-301.

[16] D. P. Debecker, E. M. Gaigneaux, G. Busca, Exploring, tuning, and exploiting the basicity of hydrotalcites for applications in heterogeneous catalysis, Chem. Eur. J. 15 (2009) 3920-3935.

[17] D. Tichit, M. N. Bennani, F. Figueras, J. R. Ruiz, Decomposition processes and characterization of the surface basicity of Cl^- and CO_3^{2-} hydrotalcites, Langmuir 14 (1998) 2086-2091.

[18] M. Mora, M. I. López, C. Jiménez-Sanchidrián, J. R. Ruiz, Near- and mid-infrared spectroscopy of layered double hydroxides containing various di- and tri-valent metals, J. Porous Mater. 20 (2013) 351-357.

[19] W. T. Reichle, S. Y. Kang, D. S. Everhardt, The nature of the thermal decomposition of a catalytically active anionic clay mineral, J. Catal. 101 (1986) 352-359.

[20] V. A. Drits, T. N. Sokolova, G. V. Sokolova, V. I. Chercashin, New members of the hydrotalcite-manasseite group, Clays Clay Miner. 35 (1987) 401-417.

[21] S. Velu, D. P. Sabde, N. Shah, S. Sivasanker, New Hydrotalcite-like Anionic Clays Containing Zr4+ in the Layers: Synthesis and Physicochemical Properties. Chem. Mater. 10 (1998) 3451-3458.

[22] M. A. Aramendia, V. Borau, J. M. Luque, J. M. Marinas, J. R. Ruiz, F. J. Urbano, Catalytic hydrogen transfer from 2-propanol to cyclohexanone over basic Mg-Al oxides, Appl. Catal. A: General 255 (2003) 301-308.

[23] M. A. Aramendia, Y. Avilés, J. A. Benitez, V. Borau, J. M. Marinas, J. R. Ruiz, F. J. Urbano, Comparative study of Mg/Al and Mg/Ga layered double hydroxides, Microp. Mesop. Mater. 29 (1999) 319-328.

[24] M. A. Aramendia, Y. Avilés, V. Borau, J. M. Luque, J. M., Marinas, J. R. Ruiz, F. J. Urbano, Thermal decomposition of Mg/Al and Mg/Ga layered-double hydroxides: A spectroscopic study. J. Mater. Chem. 9 (1999) 1603-1607.

[25] F. Millange, R. I. Walton, D. O´Hare, D., Time-resolved in situ X-ray diffraction study of the liquid-phase reconstructitm of Mg-Al-carboaate hydrotalcite-like compounds, J. Mater. Chem. 10 (2000) 1713-1720.

[26] E. C. Kruissink, L. L. van Reijen, J. R. H. Ross, Coprecipitated nickel-alumina catalysts for methanation at high temperature. Part 1. - Chemical composition and structure of the precipitates, J. Chem. Soc., Faraday Trans. I 77 (1981) 649-663.

[27] N. Das, R. Das, R., Insertion of chromium (III) ascorbate complex into layered double hydroxide through reduction of intercalated chromate by ascorbic acid, Appl. Clay Sci. 42 (2008) 90-94.

CHAPTER IV.

RESULTS AND DISCUSSION

(PAPER 3)

CAPITULO IV. PAPER 3

MICROWAVE-ASSISTED SYNTHESIS OF HYBRID ORGANO-LAYERED DOUBLE HYDROXIDES CONTAINING CHOLATE AND DEOXYCHOLATE

Daniel Cosano, Dolores Esquivel, Francisco J. Romero, César Jiménez-Sanchidrián , José Rafael Ruiz*

Departamento de Química Orgánica, Universidad de Córdoba. Campus de Rabanales, Edificio Marie Curie, Carretera Nacional IV-A, km. 396, 14014 Córdoba (SPAIN)

*Corresponding author. E-mail address: qo1ruarj@uco.es, Tfno: 34 957218638; fax: 34 957212066

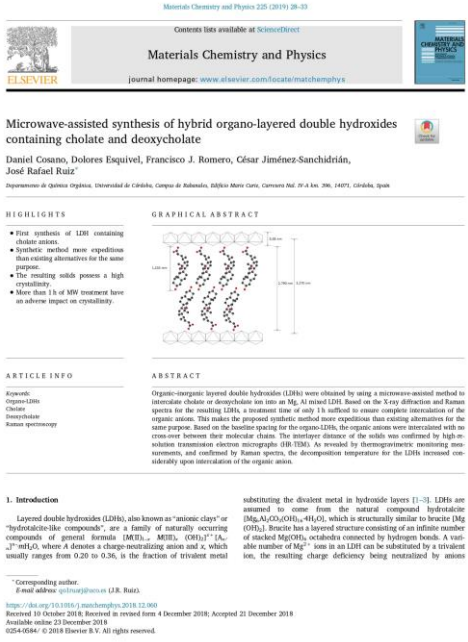

Materials Chemistry and Physics 225 (2019) 28–33

Contents lists available at ScienceDirect

Materials Chemistry and Physics

journal homepage: www.elsevier.com/locate/matchemphys

Microwave-assisted synthesis of hybrid organo-layered double hydroxides containing cholate and deoxycholate

Daniel Cosano, Dolores Esquivel, Francisco J. Romero, César Jiménez-Sanchidrián, José Rafael Ruiz*

Departamento de Química Orgánica, Universidad de Córdoba, Campus de Rabanales, Edificio Marie Curie, Carretera Nal. IV-A km. 396, 14071, Córdoba, Spain

HIGHLIGHTS

- First synthesis of LDH containing cholate anions.
- Synthetic method more expeditious than existing alternatives for the same purpose.
- The resulting solids possess a high crystallinity.
- More than 1 h of MW treatment have an adverse impact on crystallinity.

GRAPHICAL ABSTRACT

ARTICLE INFO

Keywords:
Organo-LDHs
Cholate
Deoxycholate
Raman spectroscopy

ABSTRACT

Organic–inorganic layered double hydroxides (LDHs) were obtained by using a microwave-assisted method to intercalate cholate or deoxycholate ion into an Mg_2Al mixed LDH. Based on the X-ray diffraction and Raman spectra for the resulting LDHs, a treatment time of only 1 h sufficed to ensure complete intercalation of the organic anions. This makes the proposed synthetic method more expeditious than existing alternatives for the same purpose. Based on the baseline spacing for the organo-LDHs, the organic anions were intercalated with no cross-over between their molecular chains. The interlayer distance of the solids was confirmed by high-resolution transmission electron micrographs (HR-TEM). As revealed by thermogravimetric monitoring measurements, and confirmed by Raman spectra, the decomposition temperature for the LDHs increased considerably upon intercalation of the organic anion.

1. Introduction

Layered double hydroxides (LDHs), also known as "anionic clays" or "hydrotalcite-like compounds", are a family of naturally occurring compounds of general formula $[M(II)_{1-x}\ M(III)_x\ (OH)_2]^{x+}\ [A_{x/n}]^{n-}\cdot mH_2O$, where *A* denotes a charge-neutralizing anion and *x*, which usually ranges from 0.20 to 0.36, is the fraction of trivalent metal substituting the divalent metal in hydroxide layers [1–3]. LDHs are assumed to come from the natural compound hydrotalcite ($Mg_6Al_2CO_3(OH)_{16}\cdot 4H_2O$), which is structurally similar to brucite [$Mg(OH)_2$]. Brucite has a layered structure consisting of an infinite number of stacked $Mg(OH)_6$ octahedra connected by hydrogen bonds. A variable number of Mg^{2+} ions in an LDH can be substituted by a trivalent ion, the resulting charge deficiency being neutralized by anions

* Corresponding author.
E-mail address: qo1ruarj@uco.es (J.R. Ruiz).

https://doi.org/10.1016/j.matchemphys.2018.12.060
Received 10 October 2018; Received in revised form 4 December 2018; Accepted 21 December 2018
Available online 23 December 2018
0254-0584/

ABSTRACT

Organic–inorganic layered double hydroxides (LDHs) were obtained by using a microwave-assisted method to intercalate cholate or deoxycholate ion into an Mg,Al mixed LDH. Based on the X-ray diffraction and Raman spectra for the resulting LDHs, a treatment time of only 1 h sufficed to ensure complete intercalation of the organic anions. This makes the proposed synthetic method more expeditious than existing alternatives for the same purpose. Based on the baseline spacing for the organo-LDHs, the organic anions were intercalated with no cross-over between their molecular chains. The interlayer distance of the solids was confirmed by high-resolution transmission electron micrographs (HR-TEM). As revealed by thermogravimetric monitoring measurements, and confirmed by Raman spectra, the decomposition temperature for the LDHs increased considerably upon intercalation of the organic anion.

Keywords: Organo-LDHs, cholate, deoxycholate, Raman spectroscopy.

IV.1. INTRODUCTION

Layered double hydroxides (LDHs), also known as "anionic clays" or "hydrotalcite-like compounds", are a family of naturally occurring compounds of general formula $[M(II)_{1-x}\,M(III)_x(OH)_2]^{x+}[A_{x/n}]^{n-}\cdot mH_2O$, where A denotes a charge-neutralizing anion and x, which usually ranges from 0.20 to 0.36, is the fraction of trivalent metal substituting the divalent metal in hydroxide layers [1–3]. LDHs are assumed to come from the natural compound hydrotalcite $[Mg_6Al_2CO_3(OH)_{16}\cdot 4H_2O]$, which is structurally similar to brucite $[Mg(OH)_2]$. Brucite has a layered structure consisting of an infinite number of stacked $Mg(OH)_6$ octahedra connected by hydrogen bonds. A variable number of Mg^{2+} ions in an LDH can be substituted by a trivalent ion, the resulting charge deficiency being neutralized by anions occupying the space between layers together with water molecules. However, Mg^{2+} can also be substituted by another divalent ion, which has led to the wide variety of LDHs known. The only condition to be fulfilled by the divalent or trivalent metal is having an ionic radius similar to that of magnesium [2]. The three-dimensional structure of the LDH is preserved thanks to electrostatic interactions between the trivalent cation and interlayer anions [2].

The nature of the anion can be very varied, including organic anions [4]. The intercalation of an organic anion into an LDH produces a hybrid (organic–inorganic) solid with a unique microstructure governed by interactions between the anion and inorganic layers in the solid. These hybrid solids can be obtained by direct LDH synthesis, which involves coprecipitation from solutions of a divalent and a trivalent metal in the presence of the organic anion to be intercalated [5,6]. Alternatively, hybrid LDHs can be obtained by anion-exchange [7] or by reconstructing mixed oxides prepared by calcining a precursor LDH. Hybrid LDHs have interesting uses by virtue of their being hydrophobic and hence especially suitable for adsorbing organic compounds [8–10] or metals [11,12] of a high environmental significance. Also, they have proved useful as polymeric additives, magnetic materials, catalysts and catalyst precursors [13].

Most organo-LDHs are obtained by coprecipitation, which provides aggregates consisting of nanocrystals containing hundreds or thousands of layers [14]. In recent years, however, increasing effort has been aimed at producing LDHs of small, uniform particle size in addition to a high specific surface area. One of the most effective methods for this purpose is microwave-assisted treatment [15–20]. Although the earliest organo-LDH thus prepared was reported over twenty years ago [21], relatively few have been produced ever since [22–27].

The aim of this work was to synthesize cholate/Mg,Al and deoxycholate/Mg,Al layered double hydroxides by microwave-assisted ion-exchange from an LDH containing nitrate as interlayer anion. The starting LDH was used as host and the anion (cholate or deoxycholate) as guest. To our knowledge, very few deoxycholate-containing LDHs have to date been reported [28–30]; also, none was obtained by using a similar method. Moreover, no cholate-containing seems to have been reported; rather, the anion has been used as a drug sorbent and the cholate–sorbent couple subsequently intercalated into an LDH [31–33].

IV.2. MATERIALS AND METHODS

IV.2.1. Materials

Sodium cholate hydrate (CH) and sodium deoxycholate (DCH), whose structures are shown in Figure 1, were Sigma–Aldrich ref. 27029 and D6750, respectively. The metal salts [$Mg(NO_3)_2{\cdot}6H_2O$, ref. 141402; $Al(NO_3)_3{\cdot}9H_2O$, ref. 131099] and sodium hydroxide (NaOH, ref. 141687) were supplied by Panreac.

IV.2.2. Synthesis of the nitrate-containing LDH

The nitrate-containing LDH was obtained by coprecipitation in a previous work [34], using two solutions containing 0.25 mol of $MgNO_3{\cdot}6H_2O$ and 0.1 mol of $AlNO_3{\cdot}9H_2O$, respectively, in 200 ml of deionized water [Mg/Al = 2.5]. The mixture was slowly dropped over 500 ml of a solution of NaOH at pH 10 at 60 ºC under vigorous stirring, the pH being kept constant by adding appropriate volumes of 1 M NaOH during precipitation. The suspension thus obtained was kept at 80 ºC for 24 h, after which the solid was filtered and washed with 2 l of deionized water. The solid finally obtained was named LDH-NO_3.

IV.2.3. Synthesis of organo-LDH

The cholate- and deoxycholate-containing LDHs were prepared by microwave-assisted ion-exchange. For this purpose, appropriate amounts of sodium cholate or sodium deoxycholate and LDH-NO_3 were added to 20 ml of de-ionized water. The suspension of LDH in cholate o deoxycholate was placed in a 100 ml Teflon autoclave that was heated in a Flexiwave MA186-001 microwave oven from Milestone S.r.l. operating at 300 W and 90 ºC for 1, 2 or 3 h. This was followed by decantation and washing with de-ionized water. The resulting intercalated solids were named LDH-CH-X (cholate) or LDH-DCH-X (deoxycholate), where X is the treatment time in hours (1, 2 or 3).

IV.2.4. Characterization of LDH

All LDHs were analysed by X-ray diffraction in order to check whether they possessed an LDH structure, and also by Raman spectroscopy. Also, they were assessed for thermal degradation by thermogravimetry and Raman spectroscopy. The Mg/Al ratio in the LDHs was determined by inductively coupled plasma mass spectrometry (ICP-MS) on an ELAN DRC-E Perkin Elmer ICP-MS instrument operating under standard conditions. X-ray diffraction patterns over the 2θ range from 1 to 70º were obtained on a Siemens D-5000 diffractometer using CuK_α radiation. Raman spectra for the solids were acquired with a Renishaw Raman instrument (InVia Raman Microscope) equipped with a Leica microscope furnished with various lenses (5×, 20×, 50× and 100×), monochromators and filters, as well as a CCD. Spectra were obtained by excitation with red laser light (750 nm, 2500–4000 cm^{-1}) and green laser light (532 nm, 100–2000 cm^{-1}). These two lasers provided spectra of increased quality in all windows examined. A total of 32 scans per spectrum were obtained in order to ensure a high signal-to-noise ratio. All spectral treatments (baseline correction, smoothing, normalization and deconvolution) were done with the software package Peakfit v. 4.11. Raman spectra were acquired at increasing temperatures by using a Linkan thermal camera. To this end, a small amount of sample was placed in a glass disc that was fitted to the camera's silver plate. Spectra were thus acquired at 30 ºC intervals,

using a 5× lens and a total of 3 scans per sample. The thermogravimetric analysis was performed by using an amount of sample of 15–20 mg and a 10 ºC/min gradient on a Cahn 2000 thermobalance.

IV.3. RESULTS AND DISCUSSION

IV.3.1. Metal ratio

All LDHs were subjected to elemental analysis. The Mg/Al ratio in LDH-NO_3, which was similar to that for the starting solution (2.43), was slightly lowered upon exchange of nitrate ion by cholate (2.41) or deoxycholate (2.41).

IV.3.2. X-ray diffraction patterns

Figure 2 shows the XRD patterns for the interlayer region of the nitrate- cholate- and deoxycholate-containing LDHs (LDH-NO_3, LDH-CH-X and LDH-DCH-X, respectively). As can be seen from Figure 2a, the pattern for the nitrate-containing solid (LDH-NO_3) was typical of an LDH, with sharp, symmetric, strong lines at low 2θ values, and weaker, less symmetric lines at high 2□ values, and its diffraction pattern has already been commented in a previous work [34]. The XRD spectra allowed us to distinguish baseline reflections (00l), which were sharp, strong lines at low 2θ values, and non-baseline reflections. The baseline reflections corresponded to successive orders of the baseline spacing c' (viz., the distance between two brucite-like layers in the LDH as measured from the centre of the layer or, in other words, the combination of the distance between layers and the layer thickness). The weak reflection above 60º was indexed as (110). Because this reflection is independent of the type of stacking, it can be used to calculate parameter a [$a = 2 \cdot d_{(110)}$]. This parameter can be taken to represent the distance between two neighbouring cations in a brucite-like layer. The calculated values of a are shown in Table 1 together with those of the lattice parameter c, which was obtained from $c = (3/2) \cdot [d_{(003)} + 2 \cdot d_{(006)}]$. Obviously, c depends on the particular intercalated anion and its orientation, and also on the strength of electrostatic interactions between anions and brucite-like layers. The a and c values for the nitrate-containing LDH were similar to those for solids with similar metal ratios and nitrate anion in their interlayer region [2, 35].

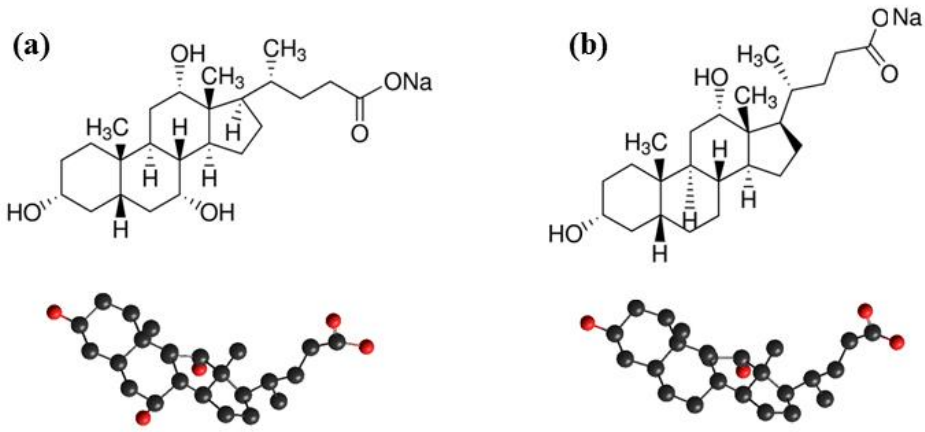

Figure 1. Sodium salt structures and more stable conformations for cholate (a) and deoxycholate (b).

Figures 2b and 2c show the XRD patterns for the organo-LDHs. Clearly, the baseline reflections for these LDHs occurred at lower 2θ values than in LDH-NO_3. Thus, the (003), (006) and (009) reflections appeared at 3.246, 1.645 and 1.201 nm, respectively, in LDH-CH-1, and at 3.186, 1.677 and 1.125 nm, respectively, in LDH-DCH-1. These values are slightly lower, but still similar, to those for deoxycholate-containing LDHs obtained with other synthetic methods [28,30]. Also, as expected for LDHs with a large baseline spacing, the (110) and (113) reflections for the organo-LDHs were overlapped and hence indistinguishable. Based on the (003) and (006) baseline reflections, the crystallinity of these solids decreased with increasing treatment time.

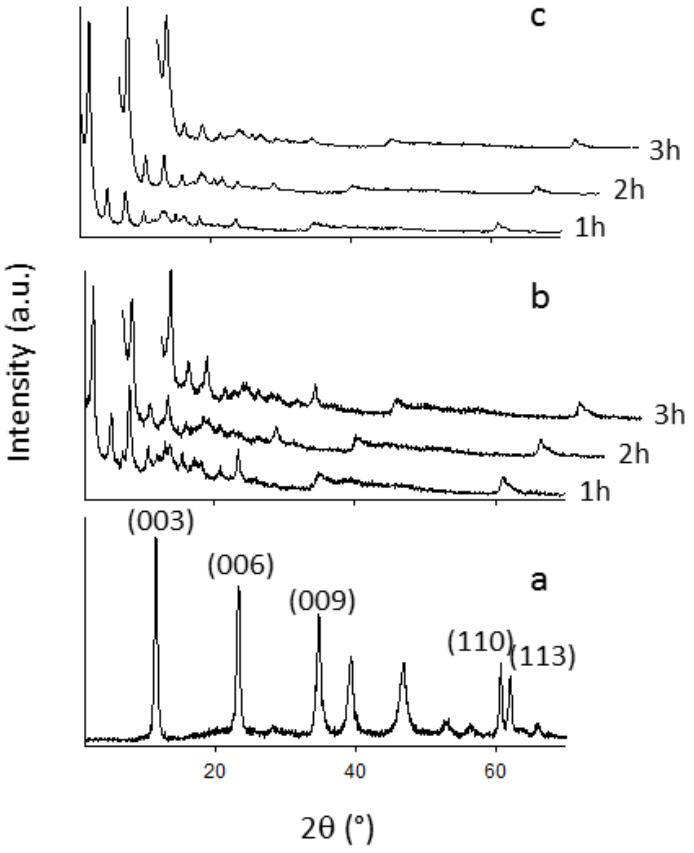

Figure 2. XRD diffraction patterns for: (a) LDH-NO_3; (b) LDH-CH-X y (c) LDH-DCH-X.

As noted earlier, the baseline spacing of LDH-DCH-1 was 3.268 nm, which is similar to but not identical with previously reported values for this organo-LDH [28,30], probably because the deoxycholate molecule adopted a different arrangement in the interlayer region. Quantum mechanical computations with the software Hyperchem Professional 8.0 revealed that the length of a deoxycholate molecule is 1.434 nm. Since the width of a brucite-like layer is 0.48 nm, the baseline spacing for LDH-DCH-1 is consistent with the absence of cross-over in deoxycholate chains (see Fig. 3) The *c* values for the cholate-intercalated LDH suggest that cholate molecules in the interlayer region arranged themselves similarly to deoxycholate molecules.

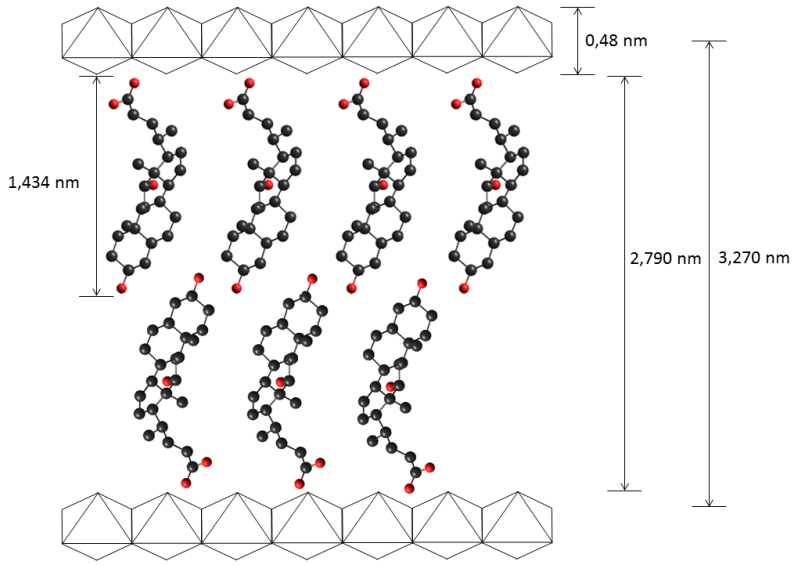

Figure 3. Proposed packaging for deoxycholate chains in the interlaminar region of LDH.

Table 1 shows the lattice parameters for each LDH. As noted earlier, with organic anions these parameters are closely related to the orientation of hydrocarbon chains in the interlayer region as well as with electrostatic interactions between the polar portion of the hydrocarbon part and the brucite-like layers in the LDH —which in turn is dependent on the crystallinity of the solid. Parameter *c* decreased with increasing length of the microwave treatment in both LDH-CD and LDH-DCH, probably as a result of the loss of water from the interlayer region [30]. In fact, the thermogravimetric curves revealed that the amount of interlayer water decreased with time (Table 1). Finally, parameter *a* was very similar for all organo-LDHs as a result of the Mg/Al ratio remaining virtually unchanged during the microwave treatment.

Table 1. Lattice parameters determined for the LDHs.

LDH	*c* (nm)[a]	*a* (nm)[b]
NO_3	2.627	**0,304**
CH-1	9.804	**0.304**
CH-2	9.754	**0.305**
CH-3	9.578	**0.303**
DCH-1	9.810	**0.305**
DCH-2	9.797	**0.305**
DCH-3	9.578	**0.307**

[a]Lattice parameter *c*; [b]Lattice parameter *a*

IV.3.3. Raman spectroscopy

Raman spectroscopy is highly suitable for characterizing the interlayer anion in an LDH [36, 37] and the nature of hydroxyl groups in the solid [37, 38]. In this work, we used it both to check that the anion was successfully intercalated —which was previously confirmed by the XRD patterns— and to ensure that nitrate ion was completely removed from the interlayer region. Figure 4 shows the Raman spectra for all solids. Only those obtained by microwave-assisted heating for 1 h are discussed here as they were the most crystalline. As can be seen from the figure, the spectrum for the nitrate-containing LDH differed markedly from those for the organo-LDHs. In fact, the former only exhibited a strong band at 1056 cm^{-1} for nitrate ion, whereas the latter exhibited a number of bands including those for stretching vibrations of C–H bonds in CH, CH_2 and CH_3 groups in the cholate or deoxycholate molecule, which appeared in the region from 2800 to 3000 cm^{-1}.

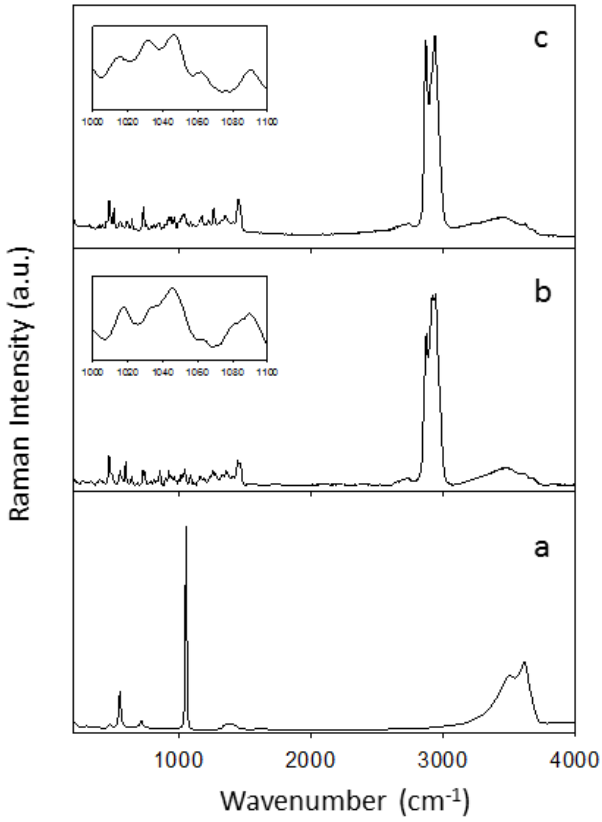

Figure 4. Raman spectra for LDHs: (a) LDH-NO_3; (b) LDH-CH-1; and (c) LDH-DCH-1.

The Raman bands for O–H stretching vibrations typically occur at wavenumbers from 2800 to 3700 cm^{-1}. In an LDH, this zone usually exhibits the bands for O–H bond stretching in interlayer water molecules and brucite-like structural units. However, water is a very poor scatterer, so Raman spectroscopy is poorly suitable for this purpose despite its proven suitability for metal-bound OH groups in brucite-like units [37, 38]. Figure 5 shows the Raman bands for the LDHs in the region 2500–3800 cm^{-1}. The bands for the nitrate-containing LDH (Figure 5a) were exclusively due to hydroxyl groups in LDH layers and in interlayer water; the bands fell at 3612 cm^{-1} and 3508 cm^{-1}, and were assigned to stretching vibrations of OH groups in brucite-like layers of Mg_3OH and Mg_2OH structural units, respectively. The latter band was deconvoluted into three components including the parent band and two others at 3326 and 3115 cm^{-1} (results not shown). Similarly to IR bands for LDHs [5], the Raman band at 3115 cm^{-1} can be assigned to O–H bond stretching of hydroxyl groups hydrogen-bonded to interlayer nitrate ions. In carbonate-containing LDHs, this band has been assigned to stretching vibrations of hydroxyl groups in water molecules acting as acceptors or donors of hydrogen bonds between M_3OH and carbonate ions [39]. The band at 3326 cm^{-1} can be assigned to OH groups of water molecules in the interlayer region.

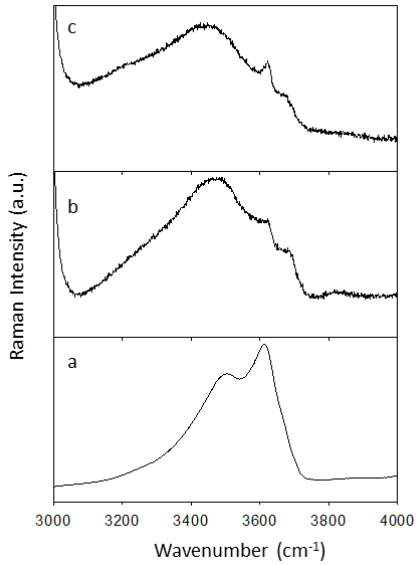

Figure 5. Raman spectra (2500-3800 cm^{-1} region) for LDHs: (a) LDH-NO_3; (b) LDH-CH-1; and (c) LDH-DCH-1.

As can be seen from Figures 5b and 5c, the bands in the 2800–3700 cm^{-1} region for the organo-LDHs were weaker but still allowed the previous types of hydroxyl groups to be identified. Also, the organo-LDHs exhibited an additional band at 3670 cm^{-1} that was assigned to stretching vibrations of hydroxyl groups in cholate or deoxycholate molecules.

In addition to the above-described bands, the spectrum for LDH-NO_3 included a sharp, strong band at 1056 cm^{-1} due to stretching of N–O bonds in interlayer nitrate and two other, weaker bands the most salient of which were those at 550 and 717 cm^{-1}. The former band and another, weaker one at 470 cm^{-1} can be unequivocally assigned to symmetric stretching of Al–OH bonds (specifically, to A_{1g} and E_g vibrations, respectively [40]). The band at 717 cm^{-1} is due to Mg–O bond stretching [41]. These bands were barely distinguishable in the Raman spectra for the organo-LDHS owing to the presence of a large number of cholate and deoxycholate bands in this region. On the other hand, the band at 1056 cm^{-1} was absent from the spectra for the two organo-LDHs (see insets in Figure 4), which confirms that nitrate ion was completely replaced with the organic anions and hence that the microwave treatment was applied under optimum conditions.

IV.3.4. Thermogravimetric analysis and Raman thermal monitoring

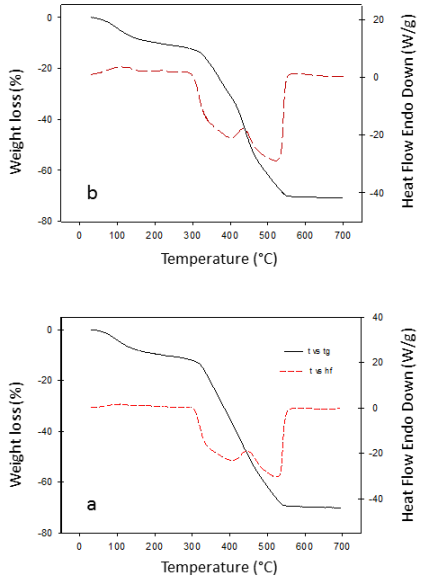

Figure 6. TGA and DTA of (a) LDH-CH-1 and (b) LDH-DCH-1.

As can be seen in Figure 6, the TG–DSG curves for LDH-CH-1 and LDH-DCH-1 were similar. Their weight losses occurred in three distinct stages. The first (25–295 ºC), involved the desorption of physisorbed water and water in the interlayer region. The second (295–550 ºC) caused the decomposition of LDH into a mixed oxide $MgAlO_x$ and the destruction of all organic matter, so it was the stage leading to the greatest weight loss. The last stage (above 550 ºC) was the conversion of the previous oxide into a spinel ($MgAl_2O_4$) [42] with a minimal weight loss. A comparison of these TG–DSC results with those for sodium cholate and deoxycholate (not shown) revealed that both ions decomposed at a higher temperature when intercalated into the LDHs, which was possibly a consequence of interactions between the organic anions and brucite-like layers in the LDH and was confirmed by monitoring the decomposition of the LDHs at a variable temperature under the Raman microscope. Tests were conducted over the typical range for C–H vibrations in cholate and deoxycholate (2700–3100 cm^{-1}). As can be seen from Figure 7, band intensity in this region remained constant up to 290 ºC, above which the LDH structure collapsed through removal of the organic anion and the resulting formation of an Mg/Al mixed oxide.

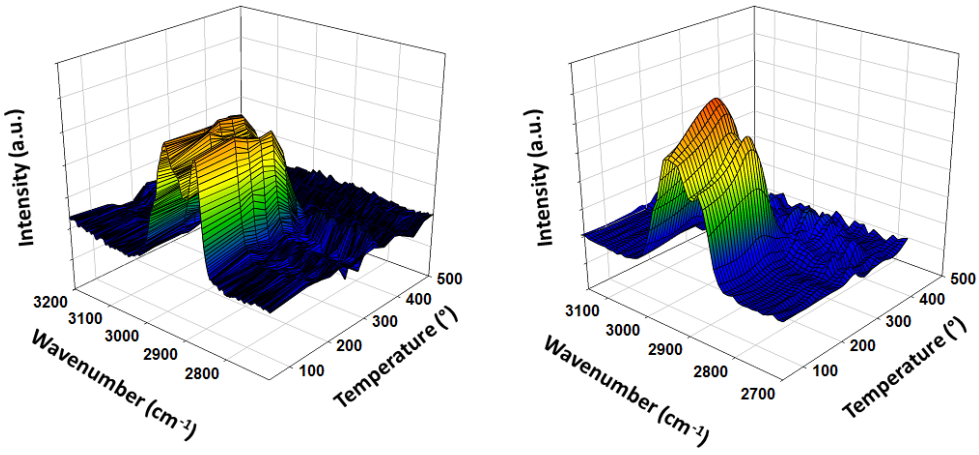

Figure 7. Raman thermal monitoring for organo-LDHs (a) LDH-DCH-1; (b) LDH-DC-1.

IV.3.4. Transmission electronic microscopy

As can be seen in Figure 8, the micrographs for both organo-LDHs showed aggregates of unevenly shaped platelet-like particles. The high-resolution images

revealed that these solids possessed a layered structure with a baseline spacing of ca. 32 nm, which is consistent with the XRD results.

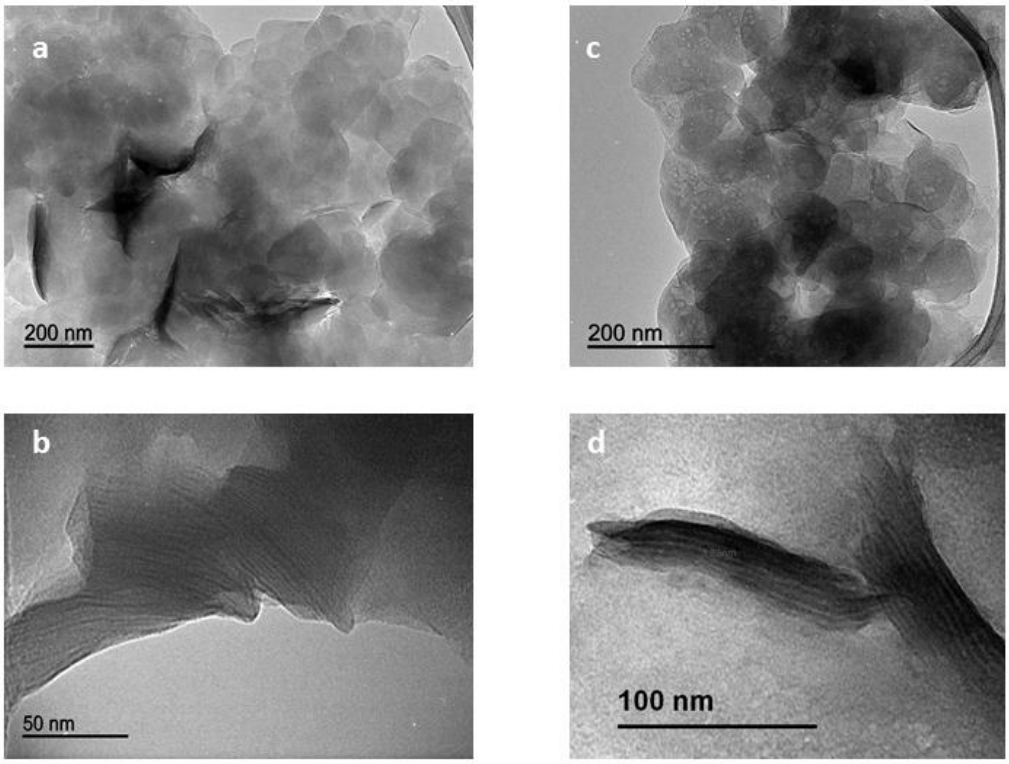

Figure 8. Transmission electron micrographs of (a) LDH-CH-1; (b) LDH-DCH-1 and HR-TEM images for (c) LDH-CH-1 and (d) LDH-DCH-1.

IV.4. CONCLUSIONS

Microwave-assisted anion-exchange provides substantial time savings in synthesizing organo-LDHs. Also, the resulting solids possess a high crystallinity by effect of the starting inorganic anion being completely substituted by the organic anions. More than 1 h of microwave treatment was found to have an adverse impact on crystallinity, however. A cholate-containing LDH was for the first time prepared here whose properties were similar to those of the deoxycholate-containing solid. In both, the interlayer distance as determined by XRD spectroscopy and confirmed by HR-TEM measurements was almost twice the length of a cholate or deoxycholate chain; there was thus no cross-over of organic chains in the LDHs. Finally, Raman spectroscopy was also for the first time used to monitor the thermal decomposition of the organo-LDHs through the stretching vibrations of C–H bonds in cholate and deoxycholate. This allowed the temperature at which the LDHs collapsed by decomposition into an Mg/Al mixed oxide to be precisely established. As shown by the results, intercalating an organic anion into an inorganic LDH considerably raises its decomposition temperature.

ACKNOWLEDGEMENTS

The authors wish to acknowledge funding of this work by Spain's Ministry of Science and Education (Project MAT2013-44463-R), Ramon Areces Foundation, Junta de Andalucía and FEDER Funds.

REFERENCES

[1] S. Miyata. The synthesis of hydrotalcite-like compounds and their structures and physicochemical properties. The systems Mg^{2+}-Al^{3+}-NO_3^-, Mg^{2+}-Al^{3+}-Cl^-, Mg^{2+}-Al^{3+}-ClO_4^-, Ni^{2+}-Al^{3+}-Cl^- and Zn^{2+}-Al^{3+}-Cl^-. Clays Clay Miner. 23 (1975) 369-375.

[2] F. Cavani, F. Trifiro, A. Vaccari. Hydrotalcite-type anionic clays: Preparation, properties and applications. Catal. Today 11 (1991) 173-301.

[3] D. G. Evans, R. C. T. Slade. Structural aspects of layered double hydroxides. Struct. Bond. 119 (2006) 1-87.

[4] P. Nalawade, B. Aware, V. J. Kadam, R. S. Hirlekar. Layered double hydroxides: A review. J. Sci. Ind. Res. 64 (2009) 267-272.

[5] M. Mora, M. I. López, C. Jiménez-Sanchidrián, J. R. Ruiz. Study of organo-hybrid layered double hydroxides by medium and near infrared spectroscopy. Spectrochim. Acta A 78 (2011) 989-995.

[6] V. Rives, M. del Arco, C. Martín. Intercalation of drugs in layered double hydroxides and their controlled release. A review. Appl. Clay Sci. 88-89 (2014) 239-269.

[7] S. Xu, J. Yu, Y. Sun, S. Wu. Synthesis and characterization of organic intercalated layered double hydroxides and their application in bitumen modification. Mater. Chem. Phys. 152 (2015) 54-61.

[8] X. Ruan, S. Huang, H. Chen, G. Qian. Sorption of aqueous organic contaminants onto dodecylsulfate intercalated magnesium ion layered double hydroxides. Appl. Clay Sci. 72 (2013) 96-103.

[9] T. Kameda, M. Saito, Y. Umetsu. Preparation of a composite material for the uptake of bisphenol A from aqueous solutions, the dodecylsulfate ion-intercalated MgAl layer-structured double hydroxide particles. J. Alloys Comp. 402 (2005) 46-52.

[10] X. Guo, O. Yin, H. Yang. Superb adsorption of organic dyes from aqueous solution on hierarchically porous composites constructed by ZnAl-LDH/$Al(OH)_3$ nanosheets. Microp. Mesop. Mater. 259 (2018) 123-133

[11] T. Kameda, T. Shinmyou, T. Yoshioka. Uptake of Nd^{3+} and Sr^{2+} by Li-Al layered double hydroxides intercalated with ethylenediaminetetraacetate. Mater. Chem. Phys. 177 (2016) 8-11.

[12] H. Chen, G. Qian, X. Ruan, R. L. Frost. Removal process of nickel (II) by using dodecylsulfate intercalated calcium aluminum layered double hydroxide. Appl. Clay Sci. 132-133 (2016) 419-424.

[13] M. Berber, I. H. Hofez. Recent advances in layered double hydroxide-based composites: Synthesis, properties and potential applications. Nova Science Publishers, Inc. 2015, 1-227.

[14] Z. P. Xu, G. S. Stevenson, C.-Q. Lu, G. Q. Lu, P. F. Barlett, P. P. Gray. Stable suspension of layered double hydroxide nanoparticles in aqueous solution. J. Am. Chem. Soc. 128 (2006) 36-37.

[15] L. Wang, B. Li, C. Chen, L. Jia. Structural characterization and related properties of the stearate anions intercalated Ni–Al hydrotalcite-like compound prepared by the microwave crystallization. J. Alloys Comp. 508 (2010) 426-432.

[16] D. Tichit, A. Rolland, F. Prinetto, G. Fetter, M. J. Martinez-Ortiz, M. A. Valenzuela, P. Bosch. Comparison of the structural and acid-base properties of Ga- and Al-containing layered double hydroxide obtained by microwave irradiation and conventional aging by synthesis gels. J. Mater. Chem. 12 (2002) 3832-3838.

[17] M. J. Climent, A. Corma, S. Iborra, K. Epping, A. Velty. Increasing the basicity and catalytic activity of hydrotalcites by different synthesis procedures. J. Catal. 725 (2004) 316-326.

[18] P. Benito, F. M. Labajos, J. Rocha, V. Rives. Influence of microwave radiation on the textural properties of layered double hydroxides. Microp. Mesop. Mater. 94 (2006) 148-158.

[19] P. Benito, I. Guinea, F. M. Labajos, J. Rocha, V. Rives. Microwave hydrothermally aged Zn,Al hydrotalcite-like compounds; Influence of the compostion and irradiation conditions. Microp. Mesop. Mater. 110 (2008) 292-302.

[20] X. Xu, D. Li, J. Sing, Y. Lin, Z. Lv, M. Wei, X. Duan. Synthesis of Mg,Al-carbonate layered double hydroxide by an atomic economic reaction. Particuology 8 (2010) 198-201.

[21] S. Komarneni, Q. H. Li, R. Roy. Microwave-hydrothermal porcessing of layered anion exchangers. J. Mater. Res. 11 (1996) 1866-1869.

[22] M. Z. B. Hussein, Z. Zaimal, A. H. Yahaya, H. W. V. Foo. Microwave-assited aging of organic-inorganic hybrid nanocomposite of -naphthalenacetate in the lamella of Zn-Al-layered double hydroxide. J. Mater. Synth. Proc. 10 (2002) 89-95.

[23] M. Herrero, F. M. Labajos, V. Rives. Size control and optimization of intercalated layered double hydroxides. Appl. Clay Sci. 42 (2009) 510-518.

[24] P. Benito, F. M. Labajos, L. Mafra, J. Rocha, V. Rives. Carboxylate-intercalated layered double hydroxides aged under microwave-hydrothermal treatment. J. Solid State Chem. 182 (2009) 18-26.

[25] P. Benito, M. Herrero, F. M. Labajos, V. Rives. Effect of post-synthesis microwave-hydrothermal treatment on the properties of layered double hydroxides and related materials. Appl. Clay Sci. 48 (2010) 218-227.

[26] R. Rosa, C. Leonelli, C. Villa, G. Priarone. Microwave-assited reaction method for the intercalation of carboxylic acid anions into layered double hydroxides. J. Microw. Power Electrom. Ener. 47 (2013) 12-23.

[27] X. Qiu, K. Sasaki, T. Hirajima, K. Ideta, J. Miyawaki. One-step synthesis of layered double hydroxides intercalated gluconate for removal of borate. Sep. Pur. Technol. 123 (2014) 114-123.

[28] M. Ogawa, S. Asai. Hydrothermal synthesis of layered double hydroxides-deoxycholate intercalation compounds. Chem. Mater. 12 (2000) 3253-3255.

[29] T. Wongkerd, A. Luengnaruemitchai, S. Jitkarnka. Phase change of catalysts derived from a LDH-deoxycholate intercalated compound and its impacts on NO reduction from stationary source emissions. Appl. Catal. B: Environm. 78 (2008) 101-111.

[30] X. Wu, S. Wang, N. Du, R. Zhang, W. Hou. Facile synthesis of deoxycholate intercalated layered double hydroxide nanohybrids via a coassembly process. J. Solid State Chem. 203 (2013) 181-186.

[31] K. M. Tyner, S. R. Wchiffman, E. P. Giannelis. Nanohybrids as delivery vehicles for camptothecin. J. Control. Release 95 (2004) 501-514.

[32] M. Trikeriotis, D. F. Ghanotakis. Intercalation of hydrophilic and hydrophobic antibiotics in layered double hydroxides. Int. J. Pharm. 332 (2007) 176-184.

[33] X. Wu, H. Li, S. Song, R. Zhang, W. Hou. Facile synthesis of camptothecin intercalated layered double hydroxide nanohybrids via a coassembly route. Int. J. Pharm. 454 (2013) 453-461.

[34] C. Jiménez-Sanchidrián, J. M. Hidalgo, R. Llamas, J. R. Ruiz. Baeyer-Villiger oxidation of cyclohexanone with hydrogen peroxide/benzonitrile over hydrotalcites as catalysts. Appl. Catal. A 312 (2006) 86-94.

[35] J. C. Villegas, O. H. Giraldo, K. Laubernds, S. L. Suib. New layered double yydroxides containing intercalated manganese oxide species: synthesis and characterization. Inorg. Chem. 42 (2003) 5621-5631.

[36] D. Cosano, C. Esquinas, C. Jiménez-Sanchidrián, J. R. Ruiz. Use of Raman spectroscopy to assess the efficiency of MgAl mixed oxides in removing cyanide from aqueous solutions. Appl. Surf. Sci. 364 (2016) 428-433.

[37] M. Mora, C. Jiménez-Sanchidrián, J. R. Ruiz. Raman spectroscopy study of layered-double hydroxides containing magnesium and trivalent metals. Mat. Lett. 120 (2104) 193-195.

[38] D. Cosano, C Jiménez-Sanchidrián, J. R. Ruiz. Vibrational spectroscopic study of sol–gel layered double hydroxides containing different tri- and tetravalent cations. J. Sol-Gel Sci. Technol. 76 (2015) 614-620.

[39] R. L. Frost, S. J. Palmer, L. M. Grand. Raman spectroscopy of gallium-based hydrotalcites of formula $Mg_6Ga_2(CO_3)(OH)_{16}{\cdot}4H_2O$. J. Raman. Sepctrosc. 41 (2009) 791-796.

[40] J. Perez-Ramirez, G. Mul, J. A. Moulijin. In situ Fourier transform infrared and laser Raman spectroscopic study of the thermal decomposition of Co–Al and Ni–Al hydrotalcites. Vib. Spectrosc. 27 (2001) 75-80.

[41] J. T. Kloprogge, L. Hickey, R. L. Frost. Synthesis and spectroscopic characterization of deuterated hydrotalcite. J. Mater. Sci. Lett. 21 (2002) 603-605.

[42] M. Aramendía, Y. Avilés, J. A. Benítez, V. Borau, C. Jiménez, J. M. Marinas, J R. Ruiz, F. J. Urbano. Comparative study of Mg/Al and Mg/Ga layered double hydroxides. Microp. Mesop. Mater. 29 (1999) 319–328.

CHAPTER V.

RESULTS AND DISCUSSION

(PAPER 4)

CAPITULO V. PAPER 4

MICROWAVE-ASSISTED SYNTHESIS OF BASIC MIXED OXIDES FROM HYDROTALCITES

Daniel Cosano, Jesús Hidalgo Carrillo, Dolores Esquivel, Francisco J. Romero, César Jiménez-Sanchidrián , José Rafael Ruiz*

Departamento de Química Orgánica, Instituto Universitario de Investigación en Química Fina y Nanoquímica IUIQFN, Facultad de Ciencias, Universidad de Córdoba, Campus de Rabanales, Edificio Marie Curie, E-14071 Córdoba, Spain)

*Corresponding author. E-mail address: qo1ruarj@uco.es, Tfno: 34 957218638; fax: 34 957212066

ABSTRACT

Three hydrotalcites were prepared by using three different microwave irradiation methods, namely: coprecipitation in the absence and presence of Pluronic P123 as template, and homogeneous precipitation in the presence of urea. Calcination at 450 ºC of the three hydrotalcites gave $MgAlO_x$ mixed oxides. The textural and surface chemical properties of which were found to depend on the particular synthetic method used. The mixed oxide obtained from the hydrotalcite prepared by homogeneous coprecipitation was that exhibiting the highest specific surface area and basicity, in addition to an also high microporosity. The three mixed oxides were used as catalysts in the Meerwein–Ponndorf–Verley reaction of benzaldehyde with 2-butanol, where their activity was directly proportional to their population of basic surface sites.

Keywords: Hydrotalcite, mixed oxide, Meerweein-Ponndorf-Verley, catalytic hydrogenation.

V.1. INTRODUCTION

Hydrotalcites (HTs), also called layered double hydroxides (LDHs) or anionic clays, are a major family of materials structurally similar to brucite [$Mg(OH)_2$]. In hydrotalcites, a trivalent metal replaces a variable number of magnesium atoms, thereby causing brucite-like hydroxyl layers to acquire positive charge. Such excess charge is offset by anions present together with water molecules in the interlayer region. In addition to a trivalent metal, the magnesium ions can also be replaced by divalent metals, so the general formula of a hydrotalcite is $[M(II)_{(1-x)}M(III)_x]^{x+}[A_{n/x}]^{n-}\cdot mH_2O$, M(II) and M(III) being a divalent and a trivalent metal, respectively; A the interlayer anion; m the number of molecules of interlayer water; and x the $M(III)/[M(II)+M(III)]$ ratio, which usually ranges from 0.20 to 0.33. Unlike cationic clays, hydrotalcites are scarcely abundant in nature; however, they can be easily obtained with various laboratory methods the most widespread of which is coprecipitation at a constant pH [1,2]. The resulting HT is aged by strong stirring at 60–80 ºC in order to make it more crystalline. The HT can also be aged hydrothermally, but efficiently raising its crystallinity takes much longer —a few days in some cases [3,4]. Microwave irradiation, which makes the process much faster than the conventional hydrothermal treatment, has been increasingly used in recent years to obtain HTs of increased crystallinity and better textural properties [5–10]. Also, microwave irradiation is compatible with homogeneous coprecipitation with urea and conventional precipitation in the presence of a surfactant. In any case, the resulting hydrotalcite is usually calcined. Calcining an Mg/Al hydrotalcite at 450–500 ºC gives an $MgAlO_x$ mixed oxide with interesting surface basic properties. The typical hydrotalcite calcination conditions provide little room for particle size and pore architecture control; thus, it is rather difficult to directly obtain mixed oxides with a highly ordered structure, and a uniform pore shape and size distribution. Template-based methods, which have proved highly effective for synthesizing orderly structures, might also be useful for HTs as suggested by the few existing reports on this topic [11–13].

The Meerwein–Ponndorf–Verley (MPV) reaction is a hydride transfer process that can be mediated by a heterogeneous basic catalyst [14]. Thus, a hydride ion is

transferred from an alcohol to a carbonyl compound to form a new carbonyl compound and another alcohol. This process affords the production of alcohols under very mild conditions and is highly selective towards the reduction of C=O bonds in carbonyl groups preferentially over other double bonds, which are left intact [15,16]. Traditionally, the MPV reaction was catalysed by homogeneous catalysts [15,16]. Over the past two decades, however, a variety of acid and basic heterogeneous catalysts have proved effective in the process and provided conversion and selectivity results even better than those of homogeneous catalysts in some cases [14,17]. Also, heterogeneous catalysts have the typical advantages of heterogeneous catalysts including easy recovery or recycling.

Especially prominent among heterogeneous basic catalysts for the MPV reaction are mixed oxides obtained by calcining hydrotalcites [18–20], a process with which our research groups is highly acquainted [21–27].

The primary aim of this work is to prepare hydrotalcites by using various microwave-assisted synthetic methods for their subsequent calcination to obtain mixed oxides with different textural and surface chemical properties. The resulting oxides will be used as catalysts in the MPV reaction of benzaldehyde with 2-butanol. The synthesis methods used to obtain the hydrotalcites will be homogenous coprecipitation, coprecipitation and a less usual method using Pluronic P123 as template. All three methods used under microwave irradiation.

V.2. EXPERIMENTAL

V.2.1. synthesis of hydrotalcites and catalysts

As stated above, hydrotalcites were prepared by coprecipitation, coprecipitation in the presence of a template (Pluronic P123) and homogeneous coprecipitation. The three methods involved aging by microwave irradiation, which reduced the preparation time from 24 h or more to barely 1 h. The resulting hydrotalcites contained magnesium and aluminium in a 2:1 ratio (x = 0.33).

One hydrotalcite was obtained by using the widespread coprecipitation method, which was previously used by our group to prepare various hydrotalcites [21,22]. The solid obtained was named HT-C. This method was also used in combination

with Pluronic P123, which was added in a 2% proportion to 250 mL of water to obtain a second hydrotalcite labelled HT-P123. Finally, homogeneous coprecipitation in the presence of urea was used to obtain a third hydrotalcite. The process involved adding solid urea to a solution containing 0.1 mol of $Mg(NO_3)_2 \cdot 6H_2O$ and 0.05 mol of $Al(NO_3)_3 \cdot 9H_2O$, and heating at 80 ºC in a Flexiwave MA186-001 microwave oven from Milestore S.r.l. operating at 300 w for 1 h, the resulting solid (HT-U) being filtered off and washed with 2 L of de-ionized water.

All three hydrotalcites were calcined in the air at 450 ºC for 8 h to obtain the mixed oxides to be subsequently used as catalysts. The oxides were given the same names as the originating hydrotalcites and the suffix 450 (see table 1).

V.2.2. Characterization of the hydrotalcites and the catalysts.

The characterization of the hydrotalcites has been carried out using different instrumental techniques. The metal ratio has been determined using X-ray fluorescence (XRF). The textural properties of the solids were established from nitrogen adsorption–desorption isotherms at liquid nitrogen temperature, which were recorded on a Micromeritics ASAP-2010 instrument. Samples were outgassed in vacuo at 100 ºC for 12 h prior to use. Hydrotalcites and mixed oxides obtained from them were checked for crystallinity by X-ray diffraction (XRD) analysis. Diffractograms were recorded on a Siemens D-5000 diffractometer using CuK_α radiation over the range 5–70º. The Raman spectra have been acquired in a Renishaw Raman spectrometer (InVia Raman Microscope). This instrument is equipped with a Leica microscope furnished with monochromators, filters and various lenses, and a charge coupled device detector. A green laser light (532 nm) was used to obtain the spectra from 200 to 4000 cm^{-1}. To improve the signal-to-noise ratio, a total of 64 scans per spectrum were performed. Thermal programmed desorption of carbon dioxide was used to determine the chemical surface properties (basicity) of the mixed oxides (Micromeritics Autochem II instrument with a thermal conductivity detector). Samples of calcined hydrotalcites (100 mg) were cleaned in an air stream (20 mL/min Ar, heating at 450 °C at a rate of 10 °C/min for 1 h and then cooled down to 40 °C). Then, solids were saturated with

carbon dioxide (5% CO_2/Ar flow at 20 mL/min for 1 h), physisorbed CO_2 removed with Ar flow (20 mL/min for 0.5 h) and TPD monitored from 50 to 450 °C (5 °C/min), the final temperature being held for 1 h.

V.2.3. Meerwein-Ponndorf-Verley reaction

The Meerwein-Ponndorf-Verley reactions were conducted at 100 ºC in a two-mouthed flask containing 3 mmol of benzaldehyde, 60 mmol of 2-butanol (i.e. the donor–acceptor ratio was 20) and 500 mg of freshly calcined mixed oxide. A reflux condenser was fitted to one of the mouths of the flask. The other mouth of the flask was used to take samples at regular intervals of time. The mixture of reactants and catalyst was stirred throughout the process. CG-MS was used for the identification of the reaction products (Varian 3900 instrument).

V.3. RESULTS AND DISCUSSION

V.3.1. Characterization of hydrotalcites and catalysts.

V.3.1.1. X-ray difraction

Figure 1 shows the XRD patterns for the hydrotalcites, which are typical for this type of compounds and similar to those previously reported by other authors [2] and our own group [21,22]. X-ray diffraction patterns allow one to discriminate between baseline (00*l*) and other reflections. Baseline reflections correspond to successive orders of the baseline spacing (c', which is the distance between two brucite-like layers in a hydrotalcite). Above 60° appears a weak reflection indexed as (110). This reflection can be used to calculate parameter a from the equation $a = 2 \cdot d_{(110)}$. a is equivalent to the distance between two neighbouring cations (Mg-Mg or Mg-Al) in a hydrotalcite layer. Table 1 shows the estimated values of a and those for the lattice parameter c ($c = 3/2 \cdot [d_{(003)} + 2d_{(006)}]$), which is three times c'. Obviously, the nature of the intercalated anion, as well as its orientation and its charge, have a definite influence on the value of this parameter.

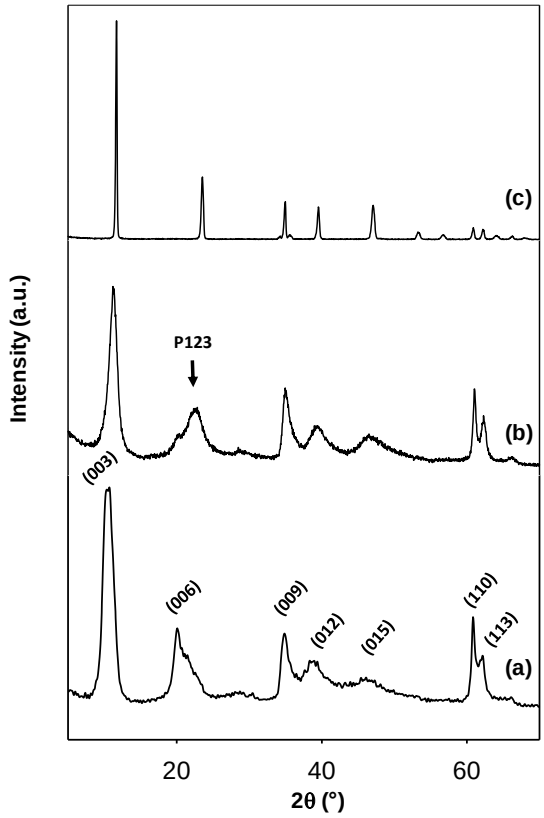

Figure 1. XRD patterns of (a) HT-C; (b) HT-P-123; and (c) HT-U.

As can be seen from figure 1, the solid obtained by homogeneous coprecipitation, HT-U, was the most crystalline. This result is consistent with those of other authors and ourselves [28–30]. The coprecipitation synthetic method and that using Pluronic P123 led to an increased width of the (003) reflection relative to coprecipitation with urea. The increase was a result of the decreased particle size of the hydrotalcites. Also, parameter *c* was smaller for solid HT-U than for those obtained by coprecipitation in the presence or absence of a surfactant (see table 1). The difference, which was quite substantial, suggests that the hydrotalcites might contain a different interlayer anion. In fact, c' values above 8.5 are typical or nitrate-containing hydrotalcites [31,32] and this was the case with HT-C and HT-P123; by contrast, the c' value for HT-U was only 7.553, which suggests that its interlayer anion was carbonate rather than nitrate [2]. The differences in parameter *a* among solids were very small and more strongly related to the actual metal ratio than to

the synthesis method used. In any case, the c' and a values found were consistent with reported values for solids with similar metal ratios containing nitrate or carbonate ions in their interlayer region. Also, solid HT-P123 exhibited a broad band at *ca*. 23º that was assigned to residual surfactant present in the HT.

Table 1. Nomenclature used to designate the hydrotalcites and their calcination products, metal ratio and lattice parameters.

Sample	Synthetic method	Mg/Al ratio[a]	Lattice parameters	
			c (Å)	a (Å)
HT-C	Coprecipitation + MW	2.0	26.303	3.048
HT-P123	Coprecipitation+ P123+ MW	1.9	26.187	3.041
HT-U	Homogeneous coprecipitation + MW	2.0	22.659	3.038
HT-C-450	HT-C calcined at 450 ºC	2.0	-	-
HT-P123-450	HT-P123 calcined at 450 ºC	1.9	-	-
HT-U-450	HT-U calcined at 450 ºC	2.0	-	-

[a]Determined by XRF.

The mixed oxides to be used as catalysts were obtained by calcining the previous three hydrotalcites at 450 ºC. As can be seen from figure 2, their diffraction patterns were very similar and included three bands consistent with the (111), (200) and (220) reflections for periclase MgO. Calcination induced major structural changes. Thus, as previously found by ^{27}Al-MAS NMR [33] spectroscopy, it caused Al^{3+} to switch from octahedral coordination in the hydrotalcites to tetrahedral coordination in the oxides. In this way, Al^{3+} ions entered the crystal network in periclase MgO by replacing Mg^{2+} isomorphically, thereby leading to a periclase-like mixed oxide of general formula $MgAlO_x$. Interestingly, calcining solid HT-P123 removed all residual surfactant through a complex decomposition process [34].

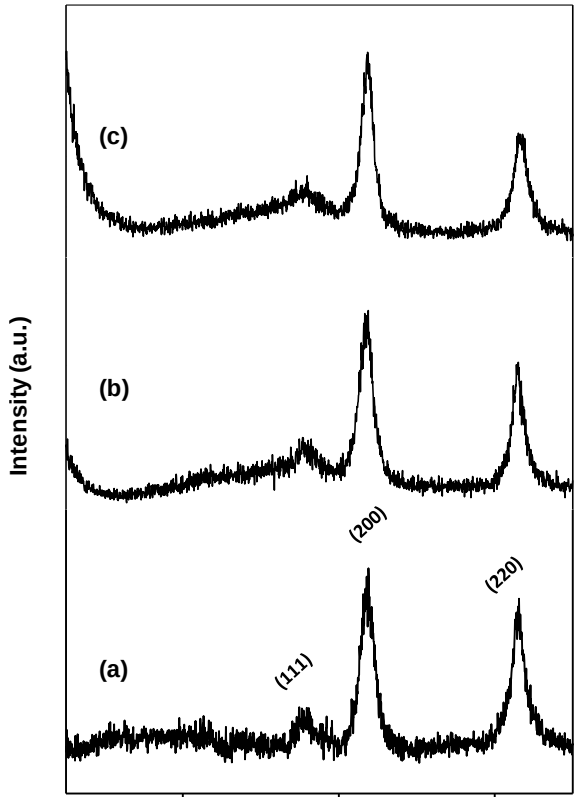

Figure 2. XRD patterns of (a) HT-C-450; (b) HT-P123-450; and (c) HT-U-450.

V.3.1.2. Raman spectroscopy

Like infrared spectroscopy, Raman spectroscopy can be used to identify interlayer anions in hydrotalcites. Our group has successfully used it to characterize hydrotalcites containing cyanide ion [35] and also to examine hydroxyl structural units in a hydrotalcite [36,37]. In this work, we used Raman spectroscopy to identify the anion present in the interlayer region of the hydrotalcites in order to confirm the inferences from the XRD data. Figure 3 shows the Raman spectra for the three hydrotalcites. As can be seen, all exhibited a broad band in the region 3000–3800 cm^{-1} with two

clearly visible peaks at *ca*. 3615 y 3500 cm^{-1} in HT-C and HT-P123. These bands can be assigned to various stretching vibrations of hydroxyl groups in brucite-like layers. As shown in previous work, hydroxyl groups in HTs are coordinated to three metal sites; as a result, there are four potentially different local environments (e.g., Mg_3OH, Mg_2AlOH, $MgAl_2OH$ and Al_3OH for an Mg/Al HT). The band at *ca*. 1055 cm^{-1} in HT-C and HT-P123 can be assigned to N–O bond stretching of interlayer nitrate groups in the HTs. The band appeared at 1061 cm^{-1}, which is typical of C–O bond stretching of carbonate ion [37], in HT-U. The bands at *ca*. 710 and 555 cm^{-1} for the three HTs can be assigned to lattice vibrations in brucite-like layers (viz., Mg–O–Al and Mg–O–Mg stretching). Finally, the solid obtained in the presence of Pluronic P123 exhibited the typical bands for C–H bond stretching in hydrocarbon groups at 2986, 2941 and 2933 cm^{-1}.

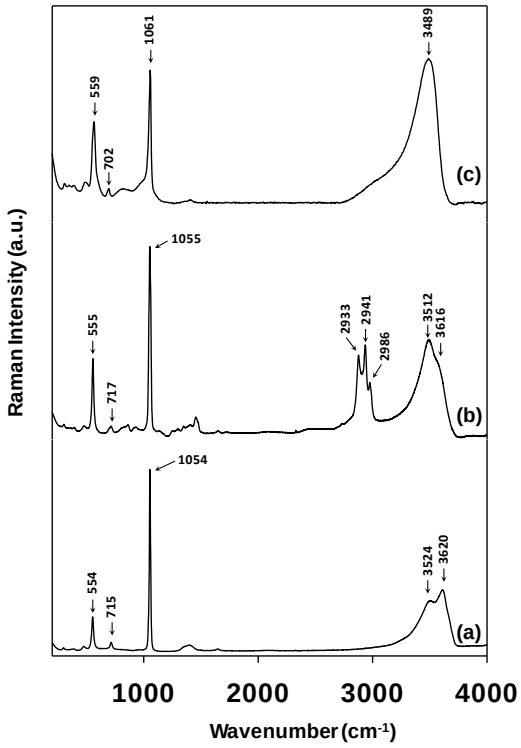

Figure 3. Raman spectra of (a) HT-C; (b) HT-P123; and (c) HT-U

V.3.1.3. Textural properties

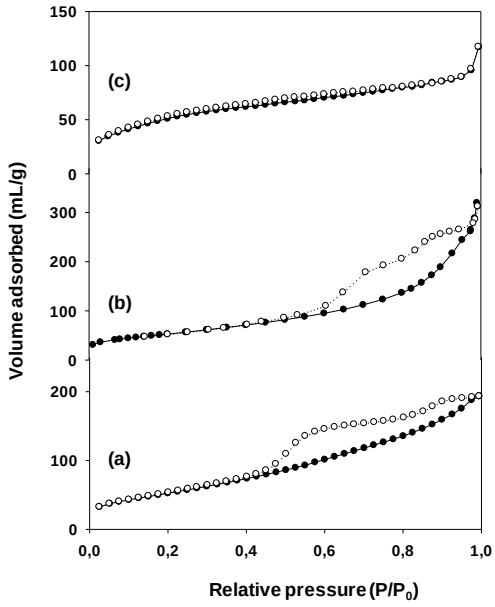

Figure 4. Nitrogen adsorption-desorption isotherms for HT-C-450 (a); HT-P123-450 (b); and HT-U-450 (c).

Nitrogen adsorption isotherms for catalysts are shown in figure 4. For HT-C-450 and HT-P123-450 are isotherms of type-IV with a large step in the adsorption at P/P_0 between 0,20-0,45 due to the capillary condensation of nitrogen in the mesopores, indicating a highly mesopore structure (figure 5). The nitrogen adsorption step is shifted to higher relative pressure for HT-P123-450 by the effect of the increase in the pore size when a block copolymer was used as template [38].

Table 2. Textural properties of the hydrotalcites and the catalysts obtained from them.

Catalyst	S_{BET}[a] (m^2/g)	S_{micro}[b] (m^2/g)	V_p[c] (mL/g)	V_{micro}[b] (mL/g)	D_p[d] (nm)
HT-C-450	201	-	0.30	-	4.2
HT-P123-450	183	-	0.41	-	8.4
HT-U-450	125	67	0.10	0.03	3.7

[a]BET specific surface area determined in the range of relative pressures from 0,05 to 0,2.
[b]Micropore area and micropore volume, calculated by t-Plot method.
[c]Single-point pore volume.
[d]Diameter pore average size, calculated according to DFT method.

Table 2 shows the estimated values for surface area, pore volume and pore diameter of the different catalysts, the catalyst HT-C-450 shows a higher surface area (201 m^2/g) in comparison with the catalyst obtained in the presence of Pluronic (183 m^2/g). However, the latter exhibits larger pore size (8.4 nm) and total pore volume (0.41 mL/g). Catalyst HT-P123-450 exhibits a hysteresis loop of type H1, which is indicative of the uniformity in the size of mesopores. In HT-U-450 catalyst, the adsorption and desorption curves are overlapped, which indicate that this solid has less mesopores. This result is further confirmed by the pore size distribution in figure 5c. Also, this solid has a wider distribution (2-10 nm, maximum between 2.5-3.0 nm) of pore size than other samples, and its average pore diameter (3.7 nm) is also smaller than that of others.

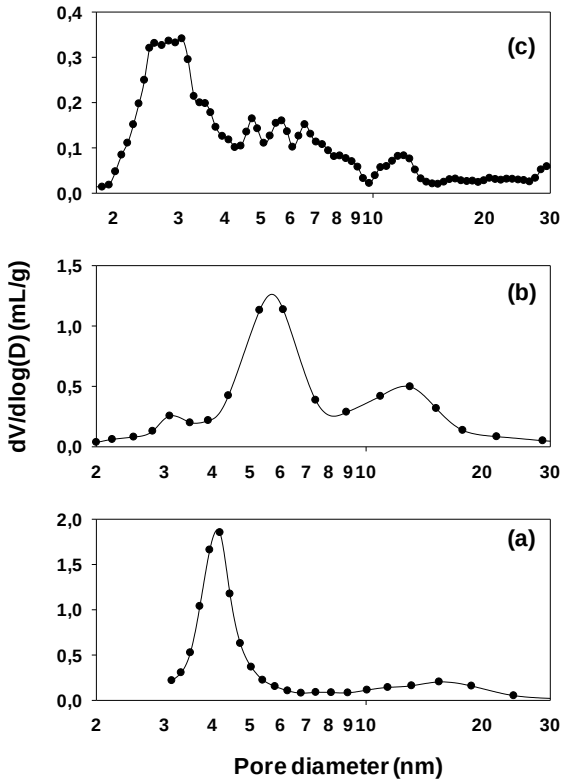

Figure 5. DFT pore size distribution and cumulative pore volume of the synthetized catalysts: HT-C-450 (a); HT-P123-450 (b); and HT-U-450 (c).

V.3.1.4. Basic properties.

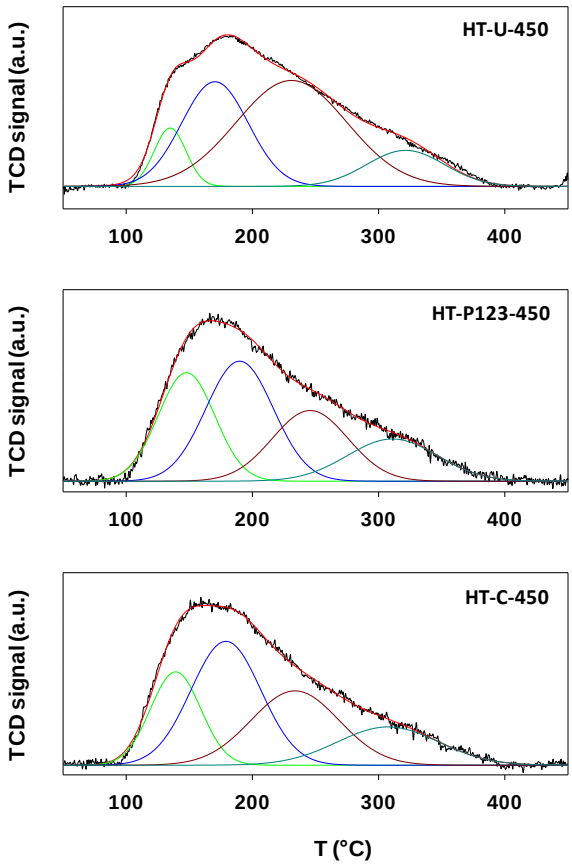

Figure 6. TPD profiles for CO_2 adsorption for the catalyst used in this work.

Figure 6 shows the carbon dioxide TPD profiles recorded with a view to determining the basic properties of the catalysts. In catalysis, this method is commonly used to determine both the number of basic centres and their strength. [39-41]. Such strength can be calculated in terms of the desorption temperature of previously adsorbed CO_2 molecules; thus, the higher the temperature is, the higher is the strength of basic sites in the sorbent. Usually, mixed oxides obtained by calcining hydrotalcites contain three types of basic sites reflecting the three ways in which CO_2 can be adsorbed at them depending on their strength.

As can be seen in figure 6, the desorption curves for the three catalysts were similar and their deconvolution provided four signals. The two peaks at the lowest desorption temperature (below 200 ºC) can be assigned to weak basic sites, and the other two, in the regions 230–240 and 310–320 ºC, to medium and strong sites, respectively. Table 3 shows the total number of basic sites, the proportion of each type and its density (*viz*., the number of sites per unit surface area) in the solids. The weak basic sites in the catalysts were provided by surface hydroxyl groups. On the other hand, the sites of medium basic strength were due to metal-bound oxygen atoms [Mg(II)–O^{2-} and Al(III)–O^{2-}] and strong sites to coordinatively unsaturated O^{2-} ions, these results are similar to those observed in the literature [42-44].

The desorption curves for catalysts HT-C-450 and HT-P123-450 were similar. The greatest difference between the two was that the curve for the former was slightly higher. As can be seen from table 3, the similarity between these two solids resulted in also similar populations of basic sites. The desorption curve for catalyst HT-U-450 was similar to those for the other two but much lower; consistent with this result, the solid contained nearly twice as many basic sites. The curve for HT-U-450 additionally included a shoulder at ca. 140 ºC and its deconvolution revealed that the population of basic sites was rather different from those of the other two solids (see table 3).

Table 3. Basic properties of the catalyst.

Catalyst	n_b[a]	D_b[b]	Proportion of basic sites (%)[c]			D_b[c]		
			W	M	S	W	M	S
HT-C-450	880	4.3	53.2	27.5	19.3	2.3	1.2	0.8
HT-P123-450	775	4.2	60.8	22.9	16.3	2.5	1.0	0.7
HT-U-450	1408	7.3	37.8	50.2	12.0	2.8	3.7	0.8

[a]Total number of basic sites (μmol CO_2/g_{cat}).
[b]Density of basic sites (μmol CO_2/m^2).
[c]S: Strong; M: Medium; W: Weak.

V.3.2. Meerwein-Ponndorf-Verley reaction.

The MPV reaction studied here is the reduction of benzaldehyde with 2-butanol. The catalytic hydrogen transfer process oxidized 2-butanol to butanone and released hydrogen that was used to reduce benzaldehyde to benzyl alcohol. Table 4 shows the initial catalytic activity of the three solids. Conversion after 24 h of reaction exceeded 95% and selectivity was also higher than 95% with the three catalysts. Based on these results, HT-U-450 was the most efficient catalyst, its activity virtually doubling that of the other two. The activity values were quite consistent with the number of basic sites in the solids; thus, the solid possessing the greatest number of sites was the most active in the MPV reaction. The specific catalytic activity (*viz*. the activity per unit surface area) was also greatest for the oxide obtained by calcining the hydrotalcite prepared by homogeneous precipitation.

Table. 4. Catalytic activity of the catalysts studied in the reaction of benzaldehyde with 2-butanol.[a]

Catalyst	r_a[b] (x 10^3)	r[c]	Conversion (%)[d]	Selectivity (%)[d]
HT-C-450	1.19	1,35	94	99
HT-P123-450	0.96	1,24	96	95
HT-U-450	2.05	1.46	94	97

[a]Reaction conditions: 3 mmol of benzaldehyde; 20 mmol of 2-butanol; T = 100 °C; 0,5 g of catalyst.
[b]Catalytic activity (mmol of benzyl alcohol/g_{cat}·min).
[c]Specific catalytic activity (mmol of benzyl alcohol/m^2·min)
[d]Conversion of benzaldehyde (24 h).
[e]Selectivity to benzyl alcohol (24 h).

The above-described results can be explained in terms of the reaction mechanism. In previous work [21,29], our group proposed a mechanism for the catalytic hydrogen transfer reaction of aldehydes and ketones with isopropanol in the liquid phase in the presence of mixed oxides acting as basic catalysts. The hydrogen transfer is a concerted process involving a six-link cyclic intermediate formed by the reactants (2-butanol and benzaldehyde) adsorbed at an acid–base pair on the surface of the magnesium–aluminium double oxide (see scheme 1). The rate-determining step of the reaction is the interaction of 2-butanol with an acid–base site, which causes the alcohol to dissociate to the corresponding alkoxide.

Therefore, the rate-determining step is adsorption of the alcohol at an acid–base pair (i.e., at a moderately to strongly acidic site). Consequently, the most active catalyst will be that with the highest density of moderate to strong basic sites (i.e., solid HT-U-450). Also, solids HT-P123-450 and HT-C-450, which possess a similar density of basic sites, will be similar in terms of catalytic activity.

Scheme 1. Proposed mechanism for the MPV reduction of benzaldehyde with 2-butanol.

This most active catalyst (HT-U-450) was used in the MPV reaction of other carbonyl compounds (see table 5). The reduction of pyridine-carboxaldehydes was strongly influenced by the position of the nitrogen atom in the aromatic ring. In any case, the introduction of this heteroatom in the ring produced a significant decrease in conversion (table 6, entries 1, 2 and 3). On the other hand, we have also carried out the MPV reaction of cyclohexanones and some compounds related to it. Cyclohexanone, 4-methylcyclohexanone have excellent conversion values, similar to those of benzaldehyde. However, when the methyl substituent changes from position 4 to 3 and 2, there was a significant decrease in conversion. As we described in a previous work [45], this decrease in the conversion can be explained by the steric hindrance of the methyl group on the proposed adsorbed complex showed in scheme 1.

Table. 5. Conversion and selectivity of catalyst HT-U-450 in the MPV reaction of various carbonyl compounds.

Entry	Carbonyl compound	Conversion (%)[a]	Selectivity (%)[b]
1	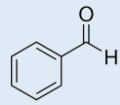	96	99
2	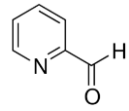	18	90
3	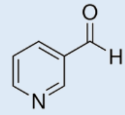	41	75
4	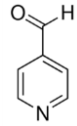	26	94
5	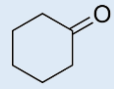	93	99
6	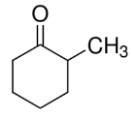	12	94
7	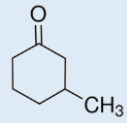	39	100
8	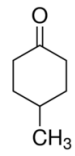	87	100

[a]Conversion of carbonyl compound (24 h).
[e]Selectivity to alcohol (24 h).

Finally, we have made the reuse of the catalyst. For this purpose, when MPV reaction between cyclohexanone and 2-butanol was finished, the catalyst was separated by filtration and washed several times with methanol, followed by calcination in the air at 450 °C. After three reuses the conversion and selectivity values are similar to the reaction with the fresh catalysts.

V.4. CONCLUSIONS

Mixed oxides obtained by calcining hydrotalcites prepared under microwave irradiation were used as catalysts in the Meerwein–Ponndorf–Verley (MPV) reaction between benzaldehyde and 2-butanol. The oxide obtained by homogeneous coprecipitation with urea possessed a high microporosity and a surface basicity almost doubling that of the two oxides obtained by coprecipitation in the absence or presence of Pluronic P123 as template. All oxides contained three types of basic sites, namely: weak, medium and strong. The most active oxide in the target MPV reaction was that possessing the largest population of moderately to strongly basic sites, which is consistent with the proposed reaction mechanism.

ACKNOWLEDGEMENTS

The authors gratefully acknowledge funding by Spain's Ministerio de Educación y Ciencia, Ramon Areces Foundation, Feder Funds and to the Consejería de Innovación, Ciencia y Empresa de la Junta de Andalucía.

REFERENCES

[1] D. Evans, R. Slade, Structural Aspects of Layered Double Hydroxides, in: Struct. Bond., Springer-Verlag, Berlin/Heidelberg, 2005: pp. 1–87.

[2] F. Cavani, F. Trifirò, A. Vaccari, Hydrotalcite-type anionic clays: Preparation, properties and applications., Catal. Today. 11 (1991) 173–301.

[3] R.P. Bontchev, S. Liu, J.L. Krumhansl, J. Voigt, T.M. Nenoff, Synthesis, Characterization, and Ion Exchange Properties of Hydrotalcite $Mg_6Al_2(OH)_{16}(A)_x(A')_{2-x} \cdot 4H_2O$ (A, A' = Cl^- , Br^- , I^- , and NO_3^- , $2 \geq x \geq 0$) Derivatives, Chem. Mater. 15 (2003) 3669–3675.

[4] J.T. Kloprogge, L. Hickey, R.L. Frost, The effects of synthesis pH and hydrothermal treatment on the formation of zinc aluminum hydrotalcites, J. Solid State Chem. 177 (2004) 4047–4057.

[5] D. Tichit, A. Rolland, F. Prinetto, G. Fetter, M. de Jesus Martinez-Ortiz, M.A. Valenzuela, P. Bosch, Comparison of the structural and acid–base properties of Ga- and Al-containing layered double hydroxides obtained by microwave

irradiation and conventional ageing of synthesis gels, J. Mater. Chem. 12 (2002) 3832–3838.

[6] J.A. Rivera, G. Fetter, P. Bosch, Microwave power effect on hydrotalcite synthesis, Microporous Mesoporous Mater. 89 (2006) 306–314.

[7] P. Benito, F.M. Labajos, J. Rocha, V. Rives, Influence of microwave radiation on the textural properties of layered double hydroxides, Microporous Mesoporous Mater. 94 (2006) 148–158.

[8] P. Benito, I. Guinea, F.M. Labajos, J. Rocha, V. Rives, Microwave-hydrothermally aged Zn,Al hydrotalcite-like compounds: Influence of the composition and the irradiation conditions, Microporous Mesoporous Mater. 110 (2008) 292–302.

[9] P. Benito, F.M. Labajos, V. Rives, Microwaves and layered double hydroxides: A smooth understanding, Pure Appl. Chem. 81 (2009) 1459–1471.

[10] X. Xu, D. Li, J. Song, Y. Lin, Z. Lv, M. Wei, X. Duan, Synthesis of Mg–Al–carbonate layered double hydroxide by an atom-economic reaction, Particuology. 8 (2010) 198–201.

[11] Y. Oka, Y. Kuroda, T. Matsuno, K. Kamata, H. Wada, A. Shimojima, K. Kuroda, Preparation of Mesoporous Basic Oxides through Assembly of Monodispersed Mg–Al Layered Double Hydroxide Nanoparticles, Chem. - A Eur. J. 23 (2017) 9362–9368.

[12] M.N. Pahalagedara, L.R. Pahalagedara, C.-H. Kuo, S. Dharmarathna, S.L. Suib, Ordered Mesoporous Mixed Metal Oxides: Remarkable Effect of Pore Size on Catalytic Activity, Langmuir. 30 (2014) 8228–8237.

[13] J. Wang, J. Zhou, Z. Li, Y. He, S. Lin, Q. Liu, M. Zhang, Z. Jiang, Mesoporous mixed metal oxides derived from P123-templated Mg-Al layered double hydroxides, J. Solid State Chem. 183 (2010) 2511–2515. http://dx.doi.org/10.1016/j.jssc.2010.08.027.

[14] J. Ruiz, C. Jimenez-Sanchidrian, Heterogeneous Catalysis in the Meerwein-Ponndorf-Verley Reduction of Carbonyl Compounds, Curr. Org. Chem. 11 (2007) 1113–1125.

[15] H. Meerwein, R. Schmidt, Ein neues Verfahren zur Reduktion von Aldehyden und Ketonen, Justus Liebig's Ann. Der Chemie. 444 (1925) 221–238.

[16] A. Verley, The exchange of functional groups between two molecules: The passage of ketones to alcohols and the reverse, Bull. Soc. Chim. Fr. 37 (1925) 871–874.

[17] G. Chuah, S. Jaenicke, Y. Zhu, S. Liu, Meerwein-Ponndorf-Verley Reduction over Heterogeneous Catalysts, Curr. Org. Chem. 10 (2006) 1639–1654.

[18] P.S. Kumbhar, J. Sanchez-valente, J. Lopez, F. Figueras, Meerwein – Ponndorf – Verley reduction of carbonyl compounds catalysed by Mg – Al hydrotalcite, Chem. Commun. 5 (1998) 535–536.

[19] J. Lopez, J.S. Valente, J.-M. Clacens, F. Figueras, Hydrogen Transfer Reduction of 4-tert-Butylcyclohexanone and Aldol Condensation of Benzaldehyde with Acetophenone on Basic Solids, J. Catal. 208 (2002) 30–37.

[20] Z. Xiao, Insight into the Meerwein-Ponndorf-Verley reduction of cinnamaldehyde over MgAl oxides catalysts, Mol. Catal. 436 (2017) 1–9.

[21] M.A. Aramendía, V. Borau, C. Jiménez, J.M. Marinas, J.R. Ruiz, F.J. Urbano, Catalytic transfer hydrogenation of citral on calcined layered double hydroxides, Appl. Catal. A Gen. 206 (2001) 95–101.

[22] M.A. Aramendía, V. Borau, C. Jiménez, J.M. Marinas, J.R. Ruiz, F.J. Urbano, Catalytic hydrogen transfer from 2-propanol to cyclohexanone over basic Mg–Al oxides, Appl. Catal. A Gen. 255 (2003) 301–308.

[23] C. Jiménez-Sanchidrián, J.M. Hidalgo, J.R. Ruiz, Reduction of heterocyclic carboxaldehydes via Meerwein–Ponndorf–Verley reaction, Appl. Catal. A Gen. 303 (2006) 23–28.

[24] J.R. Ruiz, C. Jiménez-Sanchidrián, J.M. Hidalgo, Meerwein–Ponndorf–Verley reaction of acetophenones with 2-propanol over MgAl mixed oxide: The substituent effect, Catal. Commun. 8 (2007) 1036–1040.

[25] M. Mora, M.I. López, C. Jiménez-Sanchidrián, J.R. Ruiz, Ca/Al Mixed Oxides as Catalysts for the Meerwein–Ponndorf–Verley Reaction, Catal. Letters. 136 (2010) 192–198.

[26] J.M. Hidalgo, C. Jiménez-Sanchidrián, J.R. Ruiz, Delaminated layered double hydroxides as catalysts for the Meerwein–Ponndorf–Verley reaction, Appl. Catal. A Gen. 470 (2014) 311–317.

[27] C. Jiménez-Sanchidrián, J.R. Ruiz, Tin-containing hydrotalcite-like compounds as catalysts for the Meerwein–Ponndorf–Verley reaction, Appl. Catal. A Gen. 469 (2014) 367–372.

[28] U. Costantino, F. Marmottini, M. Nocchetti, R. Vivani, New Synthetic Routes to Hydrotalcite-Like Compounds – Characterisation and Properties of the Obtained Materials, Eur. J. Inorg. Chem. 1998 (1998) 1439–1446.

[29] M.A. Aramendía, V. Borau, C. Jiménez, J.M. Marinas, J.R. Ruiz, F. Urbano, Reduction of α,β-unsaturated aldehydes with basic MgO/M2O3 catalysts (M=Al, Ga, In), Appl. Catal. A Gen. 249 (2003) 1–9.

[30] M. Mora, M.I. López, C. Jiménez-Sanchidrián, J.R. Ruiz, Near- and mid-infrared spectroscopy study of synthetic hydrocalumites, Solid State Sci. 13 (2011) 101–105.

[31] S. Nagendran, G. Periyasamy, P.V. Kamath, Hydration-induced interpolytype transformations in the bayerite-derived nitrate-intercalated layered double hydroxide of Li and Al, J. Solid State Chem. 266 (2018) 226–232.

[32] G. Pérez-Sánchez, T.L.P. Galvão, J. Tedim, J.R.B. Gomes, A molecular dynamics framework to explore the structure and dynamics of layered double hydroxides, Appl. Clay Sci. 163 (2018) 164–177.

[33] M.A. Aramendía, Y. Avilés, V. Borau, J.M. Luque, J.M. Marinas, J.R. Ruiz, F.J. Urbano, Thermal decomposition of Mg/Al and Mg/Ga layered-double hydroxides: a spectroscopic study, J. Mater. Chem. 9 (1999) 1603–1607.

[34] D. Arcos, A. López-Noriega, E. Ruiz-Hernández, O. Terasaki, M. Vallet-Regí, Ordered Mesoporous Microspheres for Bone Grafting and Drug Delivery, Chem. Mater. 21 (2009) 1000–1009.

[35] D. Cosano, C. Esquinas, C. Jiménez-Sanchidrián, J.R. Ruiz, Use of Raman spectroscopy to assess the efficiency of MgAl mixed oxides in removing cyanide from aqueous solutions, Appl. Surf. Sci. 364 (2016) 428–433.

[36] M. Mora, C. Jiménez-Sanchidrián, J.R. Ruiz, Raman spectroscopy study of layered-double hydroxides containing magnesium and trivalent metals, Mater. Lett. 120 (2014) 193–195.

[37] D. Cosano, C. Jiménez-Sanchidrián, J.R. Ruiz, Vibrational spectroscopic study of sol–gel layered double hydroxides containing different tri- and tetravalent cations, J. Sol-Gel Sci. Technol. 76 (2015) 614–620.

[38] E.-B. Cho, D. Kim, Multifunctional periodic mesoporous organosilicas prepared with block copolymer: Composition effect on morphology, Microporous Mesoporous Mater. 113 (2008) 530–537.

[39] H. Tsuji, A. Okamura-Yoshida, T. Shishido, H. Hattori, Dynamic Behavior of Carbonate Species on Metal Oxide Surface: Oxygen Scrambling between Adsorbed Carbon Dioxide and Oxide Surface, Langmuir. 19 (2003) 8793–8800.

[40] T. Seki, M. Onaka, Elucidation of basic properties of mesoporous alumina through the temperature-programmed desorption of carbon dioxide and heterogeneous basic catalysis of mesoporous alumina for the Knoevenagel reaction in supercritical CO2, J. Mol. Catal. A Chem. 263 (2007) 115–120.

[41] Y. Zhang, Z. Liu, S. Ren, W. Wang, B. Shen, Study on the basic centers and active oxygen species of solid-base catalysts for oxidation of iso-mercaptans, Appl. Catal. A Gen. 473 (2014) 125–131.

[42] A. Parejas, D. Cosano, J. Hidalgo-carrillo, R. Ruiz, A. Marinas, F.J. Urbano, Aldol Condensation of Furfural with Acetone Over, Catalysts. 9 (2019) 203.

[43] F. Wang, N. Ta, W. Shen, MgO nanosheets, nanodisks, and nanofibers for the Meerwein–Ponndorf–Verley reaction, Appl. Catal. A Gen. 475 (2014) 76–81.

[44] O.D. Pavel, D. Tichit, I.C. Marcu, Acido-basic and catalytic properties of transition-metal containing Mg-Al hydrotalcites and their corresponding mixed oxides, Appl. Clay Sci. 61 (2012) 52–58.

[45] M. a. Aramendía, V. Borau, C. Jiménez, J.M. Marinas, J.R. Ruiz, F.J. Urbano, Meerwein–Ponndorf–Verley reduction of cycloalkanones over magnesium–aluminium oxide, J. Chem. Soc. Perkin Trans. 2. 2 (2002) 1122–1125.

CONCLUSIONES/ CONCLUSIONS

CONCLUSIONES

Como conclusión general se puede decir que se han sintetizado con éxito diferentes hidróxidos dobles laminares, los cuales presentaban una estructura de tipo brucita. Algunos de estos HDLs y óxidos mixtos obtenidos por calcinación fueron utilizados en procesos de adsorción y catálisis, mostrando buenas propiedades adsortivas y catalíticas.

A continuación, se detallará las conclusiones específicas obtenidas en cada uno de los trabajos que han dado como resultado la presente Memoria de Tesis Doctoral.

Artículo 1: ***"Vibrational spectroscopic study of sol-gel layered double hydroxides containing different tri-and tetravalent cations"***

- Se sintetizaron HDLs de Mg/Al, Mg/Ga, Mg/In, Mg/Al/Sn y Mg/Al/Zr en una relación metálica de 3 [(Mg/M(III) + M(IV)] utilizando el método de sol-gel.

- Los patrones de DRX revelaron que los cinco sólidos poseen una estructura de HDL y el análisis elemental mostró una relación metálica muy cercana a la teórica.

- El entorno de los grupos hidroxilos fue estudiado en detalle utilizando la espectroscopia IR. La región IR de 2800-3900 cm^{-1} dio señales similares para los cinco sólidos, confirmando la presencia de unidades Mg_3OH y Mg_2Al-OH en los HDLs.

- La presencia de un catión trivalente distinto del aluminio o la incorporación de un metal tetravalente en la red cristalina del HDL generó variaciones poco significativas en los espectros de FT-IR de los sólidos.

- La espectroscopia Raman fue utilizada para examinar los aniones de la región interlaminar y los enlaces metal-oxigeno de los HDLs sintetizados.

- Los espectros Raman se registraron en dos zonas diferentes. La región entre 1000-1100 cm^{-1} del espectro contenía señales asignadas a la vibración del anión carbonato, cuya posición varía al variar el tamaño del catión trivalente; sin

embargo, la inserción de un catión tetravalente no provocó ningún efecto. La segunda región entre 135-700 cm^{-1}, presentó grandes diferencias entre los HDLs sintetizados. En esta región aparecen las vibraciones de los enlaces M(III)-O.

Artículo 2: ***"Use of Raman spectroscopy to assess the efficiency of MgAl mixed oxides in removing cyanide from aqueous solutions"***

- Se estudió la capacidad de eliminación de CN^- en disolución acuosa de un HDL de Mg/Al calcinado a 450 °C.

- La espectroscopía Raman demostró ser una técnica eficaz, precia y expedita para monitorizar y cuantificar la adsorción del ion cianuro en el óxido mixto obtenido tras la calcinación de un HDL.

- El cianuro se adsorbe mediante un proceso de rehidratación basado en el "efecto memoria" que restaura la estructura inicial del HDL. La adsorción decrecía con el aumento de la relación metálica de Mg/Al del HDL utilizado como precursor para el óxido mixto empleado, siendo el mejor el óxido mixto con relación Mg/Al=2.

- La cinética del proceso se ajustó a un modelo de Lagergren de primer orden. La adsorción de cianuro aumentaba al aumentar la temperatura, lo que sugiere que el proceso era endotérmico. Basándonos en la energía de activación del proceso, la adsorción del cianuro se rige por una reacción con el óxido mixto y no por difusión.

- Finalmente, se observó como la calcinación del HDL después de la adsorción del cianuro restaura el óxido mixto original haciendo posible la reutilización del material.

Artículo 3: ***"Microwave-assisted synthesis of hybrid organo-layered double hydroxides containing cholate and deoxycholate"***

- Se sintetizaron órgano-HDLs mediante un método asistido por microondas suponiendo un considerable ahorro de tiempo en la obtención de estos compuestos al ser comparados con los sintetizados por otros métodos de síntesis.

- La cristalinidad que se obtiene para los mismos es elevada, produciéndose una sustitución total del anión nitrato del HDL de partida por los aniones orgánicos.

- El aumento de tiempo del tratamiento con microondas más allá de una hora redunda negativamente en la cristalinidad del HDL sintetizado. Por primera vez se describe en la literatura el HDL intercalado con colato, cuyas características son similares a las del HDL conteniendo desoxicolato.

- En ambos casos, la distancia interlaminar, determinada experimentalmente por difracción de rayos X y confirmada por HR-TEM, tiene un valor cercano al doble de la longitud de las cadenas de colato o desoxicolato, lo que determina que las cadenas orgánicas se sitúan en el interior del HDL sin entrecruzamiento.

- Finalmente, se ha aplicado, también por primera vez, la espectroscopia Raman al seguimiento de la descomposición térmica del órgano-HDL. Monitorizando las bandas de tensión de los enlaces C-H de las moléculas de colato o desoxicolato se puede establecer la temperatura a la cual se produce la descomposición del mismo, produciéndose el colapso de la estructura del HDL, para transformarse en un óxido mixto de magnesio y aluminio. Este seguimiento nos ha permitido establecer que al intercalar el anión orgánico en el HDL se produce un aumento considerable de su temperatura de descomposición.

Artículo 4: ***"Microwave-assisted synthesis of basic mixed from hydrotalcites"***

- Los óxidos mixtos obtenidos por calcinación de hidróxidos dobles laminares sintetizados empleando distintos métodos de irradiación con microondas se han empleado como catalizadores en la reacción de Meerwein-Ponndorf-Verley de benzaldehído con 2-butanol.

- De los tres óxidos mixtos, el obtenido empleando un método de precipitación homogénea con urea presenta un elevado carácter microporoso y una basicidad superficial casi el doble de la de los dos óxidos mixtos obtenidos por el método coprecipitación (uno de ellos en presencia de Pluronic P-123).

- Todos los óxidos mixtos presentan tres tipos de centros básicos: débiles, medios y fuertes.

- El más activo en la reacción MPV estudiada es el que posee una mayor población de centros básicos de fortaleza moderada a media, como se ha puede justificar por el mecanismo propuesto para la reacción.

- También se realizó la reacción de MPV de ciclohexanonas y algunos derivados, obteniendo excelentes valores de conversión. En la metilciclohexanona, cuando el sustituyente metilo cambia de posición 4 a 3 y 2, se produjo una disminución significativa de la conversión, la cual pudo ser explicada por el impedimento estérico generado por el grupo metilo en el complejo adsorbido.

- Finalmente, se realizaron varias reutilizaciones del catalizador en la reacción de MPV entre ciclohexanona y 2-butanol obteniendo valores de conversión y selectividad similares a la reacción inicial.

CONCLUSIONS

As a general conclusion, it can be said that several layered double hydroxides (LDHs) have been synthesized successfully, exhibiting a brucite-type structure. Some of these LDHs and mixed oxides obtained by calcination, were used in adsorption processes and catalysis, most of them showing good adsorptive and catalytic properties.

Coming up next, the specific conclusions of each of the articles published that have resulted from this Doctoral Thesis are detailed.

Paper 1: ***"Vibrational spectroscopic study of sol-gel layered double hydroxides containing different tri-and tetravalent cations"***

- We prepared Mg/Al, Mg/Ga, Mg/In, Mg/Al/Sn and Mg/Al/Zr LDHs in a metal ratio of 3 [(Mg/*M*(III) + *M*(IV)] by using the sol–gel method.

- XRD patterns revealed that the five solids possess a layered double hydroxide structure and a metal ratio very close to the theoretical one.

- The environment of hydroxyl groups was studied in detail by using IR spectroscopy. The IR zone from 2800 to 3900 cm^{-1} was quite similar for the five solids and seemingly confirms the presence of Mg_3OH and Mg_2Al-OH environments in the LDHs.

- The presence of a trivalent cation other than aluminium or the insertion of a small amount of a tetravalent ion in the LDH crystal network had little effect on the FT-IR spectra for the solids in this zone.

- Raman spectra were recorded in two different zones. One spanned the wavenumber range 1000–1100 cm^{-1} and contained the signal for stretching vibrations in carbonate, its position changing with the size of the trivalent cation — inserting a tetravalent cation had no effect on it, however. The other zone, 135–700 cm^{-1}, was that exhibiting the greatest differences between LDHs. In this region the stretching vibration of *M*(III)–OH bonds was also present.

Paper 2: ***"Use of Raman spectroscopy to assess the efficiency of MgAl mixed oxides in removing cyanide from aqueous solutions"***

- the removal capacity of CN^- in aqueous solution of an LDH of Mg / Al calcined at 450 ° C was studied.

- Raman spectroscopy is an effective, accurate, expeditious technique for monitoring and quantifying the adsorption of cyanide ion on a mixed oxide obtained by calcining a layered double hydroxide (LDH).

- Cyanide is adsorbed by a rehydration process based on a "memory effect" that restores the initial structure of the LDH. The adsorption rate was found to decrease with increase in metal (Mg/Al) ratio of the LDH used as precursor for the mixed oxide, being optimum for the oxide with Mg/Al = 2.

- The kinetics of the process conformed to a first-order Lagergren model. The fact that the cyanide adsorption rate increased with increasing temperature suggests that the process is endothermic. Based on the activation energy for the process, the adsorption of cyanide is governed by its reaction with the mixed oxide rather than by diffusion.

- Finally, calcination of the LDH after adsorption of cyanide restores the original mixed oxide, which can thus be reused as a cyanide sorbent

Paper 3: ***"Microwave-assisted synthesis of hybrid organo-layered double hydroxides containing cholate and deoxycholate"***

- Microwave-assisted anion-exchange provides substantial time savings in synthesizing organo-LDHs when compared with those synthesized by other methods of synthesis.

- The resulting solids possess a high crystallinity by effect of the starting nitrate anion being completely substituted by the organic anions.

- More than 1 h of microwave treatment was found to have an adverse impact on crystallinity, however. A cholate-containing LDH was for the first time prepared here whose properties were similar to those of the deoxycholate-containing solid.

- In both, the interlayer distance as determined by XRD spectroscopy and confirmed by HR-TEM measurements was almost twice the length of a cholate or deoxycholate chain; there was thus no cross-over of organic chains in the LDHs.

- Finally, Raman spectroscopy was also for the first time used to monitor the thermal decomposition of the organo-LDHs through the stretching vibrations of C–H bonds in cholate and deoxycholate. This allowed the temperature at which the LDHs collapsed by decomposition into an Mg/Al mixed oxide to be precisely established. As shown by the results, intercalating an organic anion into an inorganic LDH considerably raises its decomposition temperature.

Paper 4: ***"Microwave-assisted synthesis of basic mixed oxides from hydrotalcites"***

- Mixed oxides obtained by calcining hydrotalcites prepared under microwave irradiation were used as catalysts in the Meerwein–Ponndorf–Verley (MPV) reaction between benzaldehyde and 2-butanol.

- Of the three mixed oxides, the oxide obtained by homogeneous coprecipitation with urea possessed a high microporosity and a surface basicity almost doubling that of the two oxides obtained by coprecipitation both in the absence or presence of Pluronic P123 as template.

- All oxides contained three types of basic sites, namely: weak, medium and strong.

- The most active oxide in the target MPV reaction was that possessing the largest population of moderately to strongly basic sites, which is consistent with the proposed reaction mechanism.

- Also, the MPV reaction of cyclohexanones and some compounds related to it were carried out obtaining excellent conversion values. In the methylcyclohexanone, when the methyl substituent changes from position 4 to 3 and 2, there was a significant decrease in conversion. This can be explained by the steric hindrance of the methyl group on the proposed adsorbed complex.

- Finally, several reuses of the catalyst were carried out in the reaction of MPV between cyclohexanone and 2-butanol, obtaining similar conversion and selectivity values to the initial reaction.

INDICIOS DE CALIDAD

Clave	Artículo
Título	Vibrational spectroscopic study of sol–gel layered double hydroxides containing different tri- and tetravalent cations
Autores	Daniel Cosano, César Jiménez-Sanchidrián, José Rafael Ruiz
Nombre de la revista	Journal of Sol-Gel Science and Technology
Año, Volumen, páginas	2015, 76, 614-620
Editorial	Springer US
Revista incluida en Journal Citation Reports (JCR)	Si
Índice de impacto (2015)	1.473
Categoría	Materials science, ceramics
Lugar que ocupa la revista en la categoría	7 de 27
Cuartil	Q2

Clave	Artículo
Título	Use of Raman spectroscopy to assess the efficiency of MgAl mixed oxides in removing cyanide from aqueous solutions
Autores	Daniel Cosano, Carlos Esquinas, César Jiménez Sanchidrián, José Rafael Ruiz
Nombre de la revista	Applied Surface Science
Año, Volumen, páginas	2016, 364, 428-433
Editorial	ELSEVIER
Revista incluida en Journal Citation Reports (JCR)	Si
Índice de impacto (2015)	3.387
Categoría	Materials Science, Coatings & Films
Lugar que ocupa la revista en la categoría	1 de 18
Cuartil	Q1

Clave	Artículo
Título	Microwave-assisted synthesis of hybrid organo-layered double hydroxides containing cholate and deoxycholate
Autores	Daniel Cosano, Dolores Esquivel, Francisco J. Romero, César Jiménez-Sanchidrián, José Rafael Ruiz
Nombre de la revista	Materials Chemistry and Physics
Año, Volumen, páginas	2019, 225, 28-33
Editorial	ELSEVIER
Revista incluida en Journal Citation Reports (JCR)	Si
Índice de impacto (2017)	2.210
Categoría	Materials Science, Multidiciplinary
Lugar que ocupa la revista en la categoría	127 de 285
Cuartil	Q2

OTRAS APORTACIONES CIENTÍCAS

OTRAS PUBLICACIONES QUE NO FORMAN PARTE DE LA MEMORIA DE TESIS DOCTORAL

1. **Raman microspectroscopic analysis of decorative pigments from the Roman villa of El Ruedo (Almedinilla, Spain)**

L.D. Mateos, D. Cosano, M. Mora, I. Muñíz, R, Carmona, C. Jimenez-Sanchidrián, J.R. Ruiz. Spectrochimica Acta - Part A: Molecular and Biomolecular Spectroscopy, Volume 151, 26 June 2015, Pages 16-21

2. **Identification by Raman microspectroscopy of pigments in seated statues found in the Torreparedones Roman archaeological site (Baena, Spain)**

D. Cosano, L.D. Mateos, C. Jimenez-Sanchidrián, J.R. Ruiz. Microchemical Journal, Volume 130, 1 January 2017, Pages 191-197

3. **Use of Raman microspectroscopy to characterize wallpaintings in Cerro de las Cabezas and the Roman villa of Priego de Cordoba (Spain)**

L.D. Mateos, D. Cosano, D. Esquivel, S. Osuna, C. Jimenez-Sanchidrián, J.R. Ruiz. Vibrational Spectroscopy, Volume 96, May 2018, Pages 143-149

4. **Micro-Raman analysis of mortars and wallpaintings in the Roman villa of Fuente Alamo (Puente Genil, Spain) and identification of the application technique**

L.D. Mateos, D. Esquivel, D. Cosano, C. Jimenez-Sanchidrián, J.R. Ruiz. Sensors and Actuators, A: Physical. Volume 281, 1 October 2018, Pages 15-23.

5. **Spectroscopic analysis of corrosion products in a bronze cauldron from the Late Iberian Iron Age**

D. Cosano, D. Esquivel, L.D. Mateos, C. Jimenez-Sanchidrián, J.R. Ruiz. Spectrochimica Acta - Part A: Molecular and Biomolecular Spectroscopy. Volume 205, 5 December 2018, Pages 489-496

6. Aldol condensation of furfural with acetone over Mg/Al mixed oxides. Influence of water and synthesis method

A. Parejas, D. Cosano, J. Hidalgo-Carrillo, J.R. Ruiz, A. Marinas, C. Jiménez-Sanchidrián, F.J. Urbano. Catalysts. Volume 9, February 2019, 203

7. Characterization of Wallpaintings from the Caliphal Baths of Cordoba (Spain) by X-Ray Diffraction and Raman Microspectroscopy

D. Cosano, D. Esquivel, A. Pérez, C. Jimenez-Sanchidrián, C.M. Costa, J.R. Ruiz.. Analytical Letters. Volume 52, 11 February 2019, Pages 411-422

8. Identification of pigments in the Annunciation sculptural group (Cordoba, Spain) by micro-Raman spectroscopy

D. Cosano, D. Esquivel, A. Pérez, C. Jimenez-Sanchidrián, C.M. Costa, J.R. Ruiz.. Spectrochimica Acta - Part A: Molecular and Biomolecular Spectroscopy. Volume 215, 5 May2019, Pages 489-496

COMUNICACIONES A CONGRESOS

1.- Adsorción de profenos en hidróxidos dobles laminares intercalados con ciclodextrina (poster).

D. Cosano, M.J. Prieto, M.I. López, F.J. Romero-Salguero, C. Jiménez-Sanchidrián, J.R. Ruiz. Conference: Reunión de la Sociedad Española de Catálisis (SECAT ´15). Barcelona (Spain), 2015.

2.- Aplicación como catalizadores de organosílices periódicas mesoporosas con grupos ácido sulfónico integrados en sus puentes (poster).

M.I. López, D. Esquivel, D. Cosano, J.R. Ruiz, C. Jiménez-Sanchidrián, P. Van Der Voort, F.J. Romero-Salguero. Conference: Reunión de la Sociedad Española de Catálisis (SECAT ´15). Barcelona (Spain), 2015.

3.- Influencia del tiempo de envejecimiento de un HDL y sus productos de calcinación sobre sus propiedades estructurales y químico-texturales (poster).

D. Cosano, M.I. López, V. Montes, F.J. Romero-Salguero, C. Jiménez-Sanchidrián, J.R. Ruiz. Conference: Reunión de la Sociedad Española de Catálisis (SECAT ´15). Barcelona (Spain), 2015.

4.- Estudio de reacciones de esterificación usando como catalizadores materiales híbridos orgánico-inorgánicos funcionalizados con grupos ácido sulfónico (poster).

M.I. López, D. Esquivel, D. Cosano, M. Mora, J.R. Ruiz, C. Jiménez-Sanchidrián, F.J. Romero-Salguero. Conference: Encuentro sobre Nanociencia y Nanotecnología de investigadores y tecnólogos andaluces (NANOUCO V). Córdoba (Spain), 2015.

5.- Influencia del tiempo de envejecimiento sobre las propiedades texturales y químico-superficiales de un HDL y sus productos de calcinación (poster).

D. Cosano, M.I. López, M. Mora, V. Montes, C. Jiménez-Sanchidrián, F.J. Romero-Salguero, J.R. Ruiz. Conference: Encuentro sobre Nanociencia y Nanotecnología de investigadores y tecnólogos andaluces (NANOUCO V). Córdoba (Spain), 2015.

6.- Síntesis por microondas de materiales híbridos orgánico-inorgánicos quirales (poster).

D. Cosano, M.I. López, M. D. Esquivel, F.J. Romero-Salguero , C. Jiménez-Sanchidrián, J.R. Ruiz. Conference: II Encuentro de Jóvenes Investigadores de la Secat. Ciudad Real (Spain), 2016.

7.- Uso de materiales periódicos mesoporosos organosilícicos (PMOs) funcionalizados con grupos tioles como soportes para la reacción de acoplamiento cruzado de Suzuki (poster).

M.I. López, M. D. Esquivel, M. Mora, D. Cosano, J. Amaro, J.R. Ruiz., C. Jiménez-Sanchidrián, F.J. Romero-Salguero. Conference: II Encuentro de Jóvenes Investigadores de la Secat. Ciudad Real (Spain), 2016.

8.- In situ SO3H-etano PMO: un eficaz catalizador reciclable para catálisis ácida (oral).

M. D. Esquivel, M.I. López, D. Cosano, J. Amaro, J.R. Ruiz., C. Jiménez-Sanchidrián, F.J. Romero-Salguero. Conference: II Encuentro de Jóvenes Investigadores de la Secat. Ciudad Real (Spain), 2016.

9.- Preparación de nanomateriales híbridos quirales y su aplicación a la resolución de mezclas racémicas. (poster).

J. Amaro-Gahete, D. Cosano, M.I. López, M. D. Esquivel, J.R. Ruiz., C. Jiménez-Sanchidrián, F.J. Romero-Salguero. I Congreso Científico de Investigadores Noveles. Córdoba (Spain), 2016.

10.- Síntesis de materiales híbridos orgánico-inorgánicos laminares con capacidad quiral. (poster).

D. Cosano, J. Amaro-Gahete, M.I. López, M. D. Esquivel, F.J. Romero-Salguero. C. Jiménez-Sanchidrián, J.R. Ruiz. V Congreso Científico de Investigadores en formación. Córdoba (Spain), 2016.

11.- Designing functionalized periodic mesoporous organilicas to be used in catalysis and adsorption (oral).

D. Esquivel, M. I. López, D. Cosano, J. Amaro, J. R. Ruiz, C. Jiménez-Sanchidrián, F. J. Romero-Salguero. Conference: 6th EuCheMS. 11-15 Septiembre 2016, Sevilla

12.- Optimización de la intercalación de materiales con capacidad quiral en sólidos híbridos orgánico-inorgánicos laminares. (oral).

D. Cosano, M.I. López, Mora-Márquez, Manuel J. Amaro-Gahete, C. Jiménez-Sanchidrián, F.J. Romero-Salguero. J.R. Ruiz. NANOUCO VI (Spain), 2017.

13.- Materiales híbridos orgánico-inorgánicos y su empleo en adsorción y catálisis. (poster).

J. Amaro-Gahete, D. Cosano, M.I. López, M. D. Esquivel, J.R. Ruiz., C. Jiménez-Sanchidrián, F.J. Romero-Salguero. NANOUCO VI. Córdoba (Spain), 2017.

14.- Síntesis de materiales periódicos mesoporosos organosilícicos (PMOS) funcionalizados con grupos tioles para su uso como soportes catalíticos en la reacción de acoplamiento cruzado de Suzuki (poster).

M.I. López, J. Amaro-Gahete, D. Cosano, M, Mora-Márquez, M. D. Esquivel, J.R. Ruiz, F.J. Romero-Salguero, C. Jiménez-Sanchidrián. NANOUCO VI. Córdoba (Spain), 2017.

15.- Aplicación de organosílices periódicas mesoporosas con grupos sulfónicos en catálisis ácida (poster).

M. D. Esquivel-Merino, M.I. López, D. Cosano, J. Amaro-Gahete, J.R. Ruiz, C. Jiménez-Sanchidrián, F.J. Romero-Salguero. NANOUCO VI. Córdoba (Spain), 2017.

16.- PMOs funcionalizados con grupos tioles como soportes catalíticos en la reacción de acoplamiento cruzado de Suzuki (poster).

M.I. López, M. D. Esquivel-Merino, D. Cosano, J. Amaro-Gahete, J.R. Ruiz, F.J. Romero-Salguero, C. Jiménez-Sanchidrián. SECAT`17. Oviedo (Spain), 2017.

17.- Estudio de la actividad catalítica de diferentes catalizadores ácidos en la reacción de Pechmann entre fenol y acetoacetato de etilo (poster).

M. D. Esquivel-Merino, D. Cosano, J. Amaro-Gahete, M.I. López, M, Mora-Márquez, J.R. Ruiz, C. Jiménez-Sanchidrián, F.J. Romero-Salguero. SECAT`17. Oviedo (Spain), 2017.

18.- Síntesis de polímeros de coordinación de zirconio con conectores quirales para su aplicación como catalizadores heterogéneos. (poster).

J. Amaro-Gahete, M. D. Esquivel-Merino, D. Cosano, M.I. López, M. D. Esquivel, J.R. Ruiz., C. Jiménez-Sanchidrián, F.J. Romero-Salguero. SECAT´17. Oviedo (Spain), 2017.

19.- Estudio de la adsorción de nitratos en LDHs calcinadas mediante espectroscopia Raman. (poster).

D. Cosano, M. D. Esquivel-Merino, M.I. López, J. Amaro-Gahete, F.J. Romero-Salguero, C. Jiménez-Sanchidrián, J.R. Ruiz. SECAT´17. Oviedo (Spain), 2017.

20.- Optimización de la intercalación del Sulfato de ß-Ciclodextrina en Hidróxidos Dobles Laminares. (poster).

D. Cosano, M. D. Esquivel-Merino, M.I. López-Martínez, M, Mora-Márquez J, Amaro-Gahete, C. Jiménez-Sanchidrián, F.J. Romero-Salguero, J.R. Ruiz. SECAT´17. Oviedo (Spain), 2017.

21.- Síntesis de polímeros de coordinación de zirconio con conectores quirales: Caracterización y aplicación como catalizadores heterogéneos en reacciones de cianosililación. (oral).

J Amaro-Gahete, M. D. Esquivel-Merino, C. Jiménez-Sanchidrián, F.J. Romero-Salguero, D. Cosano, J.R. Ruiz. II Congreso de Investigadores Noveles. Córdoba (Spain), 2017.

22.- Transferencia catalítica de hidrógeno empleando óxidos mesoporosos obtenidos a partir de hidrotalcitas. (poster).

D. Cosano, M. D. Esquivel-Merino, J, Amaro-Gahete, C. Jiménez-Sanchidrián, F.J. Romero-Salguero, J.R. Ruiz. III Encuentro de Jóvenes Investigadores de la SECAT. Valencia (Spain), 2018.

23.- Síntesis de nuevos materiales organo-LDHs asistidos por microondas. (poster).

D. Cosano, M. D. Esquivel-Merino, J, Amaro-Gahete, C. Jiménez-Sanchidrián, F.J. Romero-Salguero, J.R. Ruiz. III Encuentro de Jóvenes Investigadores de la SECAT. Valencia (Spain), 2018.

24.- Aplicación de polímeros de coordinación quirales en reacciones de cianosililación. (oral).

J Amaro-Gahete, M. D. Esquivel-Merino, M.I. López-Martínez, D. Cosano, R. Klee, J.R. Ruiz, C. Jiménez-Sanchidrián, F.J. Romero-Salguero. II Congreso de Investigadores Noveles. Córdoba (Spain), 2018.

25.- Aplicación de catalizadores de Pd soportado en organosílices periódicas mesoporosas funcionalizadas con grupos tioles en la reacción de acoplamiento cruzado de Suzuki. (oral).

M.I. López-Martínez, M. D. Esquivel-Merino, J Amaro-Gahete, D. Cosano, R. Klee, J.R. Ruiz, C. Jiménez-Sanchidrián, F.J. Romero-Salguero. XXVI Congreso Ibero-Americano de Catálisis. Coímbra (Portugal), 2018.

26.- Influencia del método de síntesis de las hidrotalcitas en la condensación aldólica del furfural con acetona para producir diésel. (poster).

J. Hidalgo-Carrillo, D. Cosano, A. Parejas, J.R. Ruiz, A. Marinas-Aramendia, C. Jiménez-Sanchidrián, F.J. Urbano-Navarro. XXVI Congreso Ibero-Americano de Catálisis. Coímbra (Portugal), 2018.

27.- Adsorción de etileno en diferentes MOFs de tipo MIL-88A. (oral).

J Amaro-Gahete, R. Klee, D. Cosano, M. D. Esquivel-Merino, J.R. Ruiz, C. Jiménez-Sanchidrián, F.J. Romero-Salguero. NANOUCO VII. Córdoba (Spain), 2019

28.- Síntesis de hidrotalcitas por irradiación con microondas. Aplicaciones en procesos de reducción (oral).

D. Cosano, M. D. Esquivel-Merino, J, Amaro-Gahete, J. Hidalgo-Carrillo, C. Jiménez-Sanchidrián, F.J. Romero-Salguero, J.R. Ruiz. NANOUCO VII. Córdoba (Spain), 2019.

29.- Análisis de los morteros de la Torre del Homenaje del Castillo de Priego de Córdoba (Spain) (oral).

D. Cosano, M. D. Esquivel-Merino, J, Amaro-Gahete, F.J. Romero-Salguero, C. Jiménez-Sanchidrián, J.R. Ruiz. VII Congreso Científico de Investigadores en Formación de la Universidad de Córdoba. Córdoba (Spain), 2019.

30.- Síntesis de MOF MIL-88A asistida por ultrasonidos y su aplicación como adsorbente de etileno. (oral).

J Amaro-Gahete, R. Klee, D. Cosano, M. D. Esquivel-Merino, J.R. Ruiz, C. Jiménez-Sanchidrián, F.J. Romero-Salguero. VII Congreso Científico de Investigadores en Formación de la Universidad de Córdoba. Córdoba (Spain), 2019

CAPÍTULOS DE LIBRO

1.- Título del capítulo: Preparación de nanomateriales híbridos quirales y su aplicación a la resolución de mezclas racémicas (capítulo 22)
Autores del capítulo: Amaro-Gahete, Juan; Esquivel-Merino, María Dolores; López-Martínez, María Isabel; Ruiz-Arrebola, Jose Rafael; Jimenez-Sanchidrian, Cesar; Romero-Salguero, Francisco José; Cosano, Daniel
Título del libro: Investigando por un futuro mejor
Autores del libro: Marinas-Aramendía, Alberto
Página inicial: 101
Página final: 104
Lugar: Córdoba
Editorial: UCOPress, Editorial Universidad de Córdoba
ISBN: 978-84-9927-291-7
Año: 2016

2.- Título del capítulo: Eliminación de nitratos de aguas por adsorción

Autores del capítulo: Cosano, Daniel; Esquivel-Merino, Maria Dolores; Amaro-Gahete, Juan; Jimenez-Sanchidrian, Cesar; Romero-Salguero, Francisco Jose; Ruiz-Arrebola, Jose Rafael

Título del libro: Creando redes doctorales. Vol. VI: ¿La generación del conocimiento?.

Autores del libro:

Página inicial: 113

Página final: 117

Lugar:

Editorial: UCOPress. Ediciones Universidad de Córdoba. Campus Universitario de Rabanales. Carretera Nacional IV, km. 396. 14071, Córdoba, España.

ISBN: 978-84-9927-239-9

Año: 2018

3.- Título del capítulo: Síntesis de polímeros de coordinación de zirconio con conectores quirales. Caracterización y aplicación como catalizadores heterogéneos en reacciones de cianosililación.

Autores del capítulo: Amaro-Gahete, Juan; Esquivel-Merino, Maria Dolores; Cosano, Daniel; Ruiz-Arrebola, Jose Rafael; Jimenez-Sanchidrian, Cesar; Romero-Salguero, Francisco Jose

Título del libro: Investigadores de hoy para los retos del mañana

Autores del libro: Marinas-Aramendía, Alberto

Página inicial: 39

Página final: 42

Lugar: Córdoba, España

Editorial: UCOPress

ISBN: 978-84-9927-386-0

Año: 2018

4.- Título del capítulo: Síntesis de MOF MIL-88A asistida por ultrasonidos y su aplicación como adsorbente de etileno
Autores del capítulo: Amaro-Gahete, Juan; Klee, Rafael Orlando; Cosano, Daniel; Esquivel-Merino, Maria Dolores; Ruiz-Arrebola, Jose Rafael; Jimenez-Sanchidrian, Cesar; Romero-Salguero, Francisco Jose
Título del libro: Creando redes doctorales. Vol. VII: "Investiga y comunica"
Autores del libro:
Página inicial: 251
Página final: 255
Lugar: Campus Universitario de Rabanales
Editorial: UCOpress. Editorial Universidad de Córdoba
ISBN: 978-84-9927-341-9
Año: 2019

5.- Título del capítulo: Análisis de los morteros de la Torre del Homenaje del Castillo de Priego de Córdoba (Spain)
Autores del capítulo: Cosano, Daniel; Esquivel-Merino, Maria Dolores; Amaro-Gahete, Juan; Romero-Salguero, Francisco Jose; Jimenez-Sanchidrian, Cesar; Ruiz-Arrebola, Jose Rafael
Título del libro: Creando redes doctorales. Vol. VII: "Investiga y comunica"
Autores del libro:
Página inicial: 279
Página final: 283
Lugar: Campus Universitario de Rabanales
Editorial: UCOpress. Editorial Universidad de Córdoba
ISBN: 978-84-9927-341-9
Año: 2019

PUBLICACIONES

J Sol-Gel Sci Technol (2015) 76:614–620
DOI 10.1007/s10971-015-3812-3

ORIGINAL PAPER

Vibrational spectroscopic study of sol–gel layered double hydroxides containing different tri- and tetravalent cations

Daniel Cosano[1] · **César Jiménez-Sanchidrián**[1] · **José Rafael Ruiz**[1]

Received: 29 April 2015 / Accepted: 15 July 2015 / Published online: 26 July 2015

Abstract Five different layered double hydroxides were synthesized from magnesium ethoxide in the presence of aluminium, gallium, indium, tin and zirconium acetylacetonates by using the sol–gel technique. The colloid suspensions initially obtained were gelled and separated by centrifugation. XRD patterns confirmed that the five solids thus obtained possessed a layered double hydroxide structure. Also, IR and Raman spectra revealed differences between the solids.

Graphical Abstract

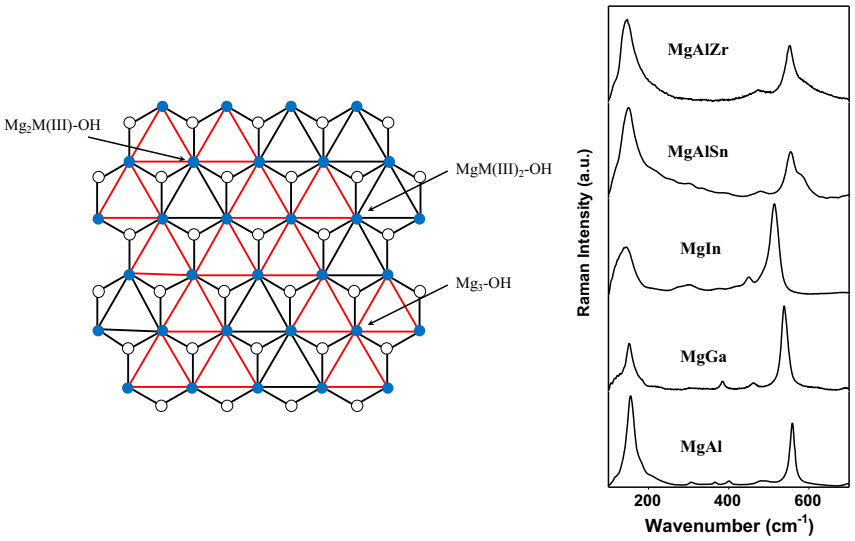

✉ José Rafael Ruiz
qo1ruarj@uco.es

[1] Departamento de Química Orgánica, Universidad de Córdoba, Campus de Rabanales, Edificio Marie Curie, Carretera Nnal. IV-A km. 396, 14071 Córdoba, Spain

Keywords Sn-layered double hydroxide · Zr-layered double hydroxide · FT-IR spectroscopy · Raman spectroscopy · Sol–gel method

SPRINGER NATURE LICENSE
TERMS AND CONDITIONS

Jun 13, 2019

This Agreement between University of Cordoba ("You") and Springer Nature ("Springer Nature") consists of your license details and the terms and conditions provided by Springer Nature and Copyright Clearance Center.

License Number	4607020528287
License date	Jun 13, 2019
Licensed Content Publisher	Springer Nature
Licensed Content Publication	Journal of Sol-Gel Science and Technology
Licensed Content Title	Vibrational spectroscopic study of sol–gel layered double hydroxides containing different tri- and tetravalent cations
Licensed Content Author	Daniel Cosano, César Jiménez-Sanchidrián, José Rafael Ruiz
Licensed Content Date	Jan 1, 2015
Licensed Content Volume	76
Licensed Content Issue	3
Type of Use	Thesis/Dissertation
Requestor type	academic/university or research institute
Format	print and electronic
Portion	full article/chapter
Will you be translating?	no
Circulation/distribution	<501
Author of this Springer Nature content	yes
Title	Vibrational spectroscopic study of sol–gel layered double hydroxides containing different tri- and tetravalent cations
Institution name	University of Cordoba
Expected presentation date	Jul 2019
Requestor Location	University of Cordoba Campus de Rabanales, Ed. Marie Curie Crta. Nacional IV-A, km. 396 Córdoba, Córdoba 14014 Spain Attn: University of Cordoba
Total	0.00 EUR

Terms and Conditions

Springer Nature Terms and Conditions for RightsLink Permissions

Springer Nature Customer Service Centre GmbH (the Licensor) hereby grants you a non-exclusive, world-wide licence to reproduce the material and for the purpose and requirements specified in the attached copy of your order form, and for no other use, subject to the conditions below:

1. The Licensor warrants that it has, to the best of its knowledge, the rights to license reuse of this material. However, you should ensure that the material you are requesting is original to the Licensor and does not carry the copyright of another entity (as credited in the published version).

   If the credit line on any part of the material you have requested indicates that it was

Applied Surface Science 364 (2016) 428–433

Contents lists available at ScienceDirect

Applied Surface Science

journal homepage: www.elsevier.com/locate/apsusc

Use of Raman spectroscopy to assess the efficiency of MgAl mixed oxides in removing cyanide from aqueous solutions

Daniel Cosano, Carlos Esquinas, César Jiménez-Sanchidrián, José Rafael Ruiz*

Departamento de Química Orgánica, Universidad de Córdoba, Campus de Rabanales, Edificio Marie Curie, Carretera Nacional IV-A, km. 396, 14014 Córdoba, Spain

ARTICLE INFO

Article history:
Received 16 September 2015
Received in revised form
21 December 2015
Accepted 22 December 2015
Available online 24 December 2015

Keywords:
Layered double hydroxides
Cyanide removal
Raman spectroscopy
Memory effect

ABSTRACT

Calcining magnesium/aluminium layered double hydroxides (Mg/Al LDHs) at 450 °C provides excellent sorbents for removing cyanide from aqueous solutions. The process is based on the "memory effect" of LDHs; thus, rehydrating a calcined LDH in an aqueous solution restores its initial structure. The process, which conforms to a first-order kinetics, was examined by Raman spectroscopy. The metal ratio of the LDH was found to have a crucial influence on the adsorption capacity of the resulting mixed oxide. In this work, Raman spectroscopy was for the first time use to monitor the adsorption process. Based on the results, this technique is an effective, expeditious choice for the intended purpose and affords *in situ* monitoring of the adsorption process. The target solids were characterized by using various instrumental techniques including X-ray diffraction spectroscopy, which confirmed the layered structure of the LDHs and the periclase-like structure of the mixed oxides obtained by calcination.

1. Introduction

Cyanide is an anion easily bonding to metals such as gold, silver, copper, zinc or mercury to form chelates that are usually highly water-soluble but differ markedly in stability. This key property of cyanide has been used to extract metals such as gold or silver from mineral ores. Cyanide is also used for other purposes such as plastic, agrochemical, dye and pharmaceutical production [1]. This anion is present in virtually negligible amounts in uncontaminated natural waters [2] but can reach levels millions of times higher in wastewater from the previous production processes. The gold mining industry is the greatest source of water contamination with cyanide, which poses serious hazards owing to the high toxicity of the anion. Cyanide is typically removed from water by alkaline chlorination but can also be eliminated by using other chemical oxidants such as hydrogen peroxide, sulphur dioxide or ozone, as well as alternative techniques such as osmosis, acidification/volatilization or even photolysis. Most of these techniques, however, are energy-consuming or use environmentally unfriendly reagents.

Adsorption methods are being increasingly used lately to purify aqueous solutions containing anionic or cationic contaminants. Some use layered double hydroxides (LDHs) or mixed oxides obtained by calcining LDHs to adsorb anions such as nitrate [3,4], fluoride [5] phosphate [6,7], radioactive species [8,9], herbicides [10,11] or humic acid [12]. However, mixed oxides from LDHs have never to the authors' knowledge been used to adsorb cyanide. Some authors have successfully removed hydrogen cyanide by using nickel-based LDHs to form cyanide complexes of formula $[Ni(CN)_4]^{2-}$ [13]. Also, cyanide can be removed from aqueous solutions using activated carbon as adsorbent [14].

Layered double hydroxides (LDHs) are a class of anionic clays structurally similar to brucite, $Mg(OH)_2$, except that some Mg^{2+} ions are replaced by trivalent metals of a similar ionic radius [15,16]. This introduces a charge deficiency which causes brucite-like layers to be positively charged. Restoring electroneutrality requires inserting an appropriate anion [17] in addition to crystallization water in the interlayer region (Fig. 1).

The general formula of LDHs is $[M(II)_{1-x}M(III)_x(OH)_2]^{x+}[A_{x/m}]^{m-}\cdot nH_2O$, where M(II) and M(III) are a divalent and trivalent metal, respectively, at octahedral positions of Mg^{2+} in brucite-like layers and *A* is the interlayer anion — which can vary widely in nature and be either inorganic or organic. *x*, which represents the ratio M(II)/[M(II)+M(III)], typically ranges from 0.17 to 0.33, which corresponds to an *M*(II)/*M*(III) ratio of 2–4 [15]. Calcination at 400–700 °C of an LDH containing magnesium and aluminium as metals, and carbonate as interlayer anion, gives a mixed oxide of the same cations via the following reaction:

$$Mg_{1-x}Al_x(CO_3)_{x/2}(OH)_2 \xrightarrow{400-700\,^{\circ}C} Mg_{1-x}Al_xO_{1+x/2} + x/2CO_2$$

* Corresponding author. Tel.: +34 957218638; fax: +34 957212066.
E-mail address: qo1ruarj@uco.es (J.R. Ruiz).

http://dx.doi.org/10.1016/j.apsusc.2015.12.181
0169-4332/

Materials Chemistry and Physics 225 (2019) 28–33

Contents lists available at ScienceDirect

Materials Chemistry and Physics

journal homepage: www.elsevier.com/locate/matchemphys

Microwave-assisted synthesis of hybrid organo-layered double hydroxides containing cholate and deoxycholate

Daniel Cosano, Dolores Esquivel, Francisco J. Romero, César Jiménez-Sanchidrián, José Rafael Ruiz*

Departamento de Química Orgánica, Universidad de Córdoba, Campus de Rabanales, Edificio Marie Curie, Carretera Nal. IV-A km. 396, 14071, Córdoba, Spain

HIGHLIGHTS

- First synthesis of LDH containing cholate anions.
- Synthetic method more expeditious than existing alternatives for the same purpose.
- The resulting solids possess a high crystallinity.
- More than 1 h of MW treatment have an adverse impact on crystallinity.

GRAPHICAL ABSTRACT

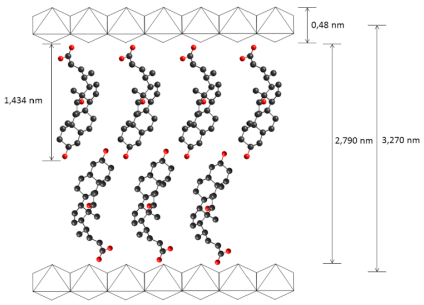

ARTICLE INFO

Keywords:
Organo-LDHs
Cholate
Deoxycholate
Raman spectroscopy

ABSTRACT

Organic–inorganic layered double hydroxides (LDHs) were obtained by using a microwave-assisted method to intercalate cholate or deoxycholate ion into an Mg, Al mixed LDH. Based on the X-ray diffraction and Raman spectra for the resulting LDHs, a treatment time of only 1 h sufficed to ensure complete intercalation of the organic anions. This makes the proposed synthetic method more expeditious than existing alternatives for the same purpose. Based on the baseline spacing for the organo-LDHs, the organic anions were intercalated with no cross-over between their molecular chains. The interlayer distance of the solids was confirmed by high-resolution transmission electron micrographs (HR-TEM). As revealed by thermogravimetric monitoring measurements, and confirmed by Raman spectra, the decomposition temperature for the LDHs increased considerably upon intercalation of the organic anion.

1. Introduction

Layered double hydroxides (LDHs), also known as “anionic clays” or “hydrotalcite-like compounds”, are a family of naturally occurring compounds of general formula $[M(II)_{1-x}\ M(III)_x\ (OH)_2]^{x+}[A_{x/n}]^{n-}\cdot mH_2O$, where A denotes a charge-neutralizing anion and x, which usually ranges from 0.20 to 0.36, is the fraction of trivalent metal substituting the divalent metal in hydroxide layers [1–3]. LDHs are assumed to come from the natural compound hydrotalcite $[Mg_6Al_2CO_3(OH)_{16}\cdot 4H_2O]$, which is structurally similar to brucite $[Mg(OH)_2]$. Brucite has a layered structure consisting of an infinite number of stacked $Mg(OH)_6$ octahedra connected by hydrogen bonds. A variable number of Mg^{2+} ions in an LDH can be substituted by a trivalent ion, the resulting charge deficiency being neutralized by anions

* Corresponding author.
E-mail address: qo1ruarj@uco.es (J.R. Ruiz).

https://doi.org/10.1016/j.matchemphys.2018.12.060
Received 10 October 2018; Received in revised form 4 December 2018; Accepted 21 December 2018
Available online 23 December 2018
0254-0584/